Mixed Polyelectrolyte Brush Modified Adsorbents for the Separation of Proteins

by

Thantawat Theeranan

A thesis submitted to

The University of Birmingham for the degree of

DOCTOR OF PHILOSOPHY

School of Chemical Engineering

College of Engineering and Physical Sciences

The University of Birmingham

January 2020

Abstract

Bioprocess chromatography plays key roles in the manufacture of biotherapeutic proteins and guarantees the safe removal of critical impurities, but in its present guise future sustainability is questionable. The past decade has seen a conspicuous rise in the application of ‘smart’ or ‘stimuli responsive’ polymers in downstream processing, and especially in adsorption chromatography. This interest is largely driven by the realization that smart polymer based separation systems might afford lean green solutions to endemic defects of conventional chromatographic systems. Temperature and pH responsive varieties are the most obvious candidates for bioprocess application. Effective use of temperature sensitive chromatography media materials in bioprocessing requires the development of specialized equipment. No such requirement affects the application of chromatography media embellished with pH responsive polymers, which have been used extensively, for example in the manufacture of high capacity tentacular ion exchange resins featuring single types of polyelectrolyte (PEL) chains.By sequentially tethering two weak oppositely charged PEL chains, poly(2-vinylpyridine) (P2VP) and poly(methacrylic acid) (PMAA), side-by-side within the pores of beaded meso-macroporous chromatography matrices (Tresyl activated Toyopearl HW65 and Praesto 45) mixed PEL brush adsorbents displaying the 'Chameleon-like' ability to reversibly transform between anion exchange (AEX), and cation exchange (CEX) binding modes, have been created in this study. This involved: (i) prior activation with tresyl chloride (for the Praesto 45 starting material only); (ii) patterning the pores of tresyl-activated media with two amine-terminated weak PELs, i.e. poly(2-vinylpyridine), P2VP (DP = 126) and poly(*t*-butyl methacrylate), P*t*BMA (DP = 204) or poly(methyl methacrylate), PMMA (DP = 98) used sequentially for creating mixed PEL adsorbents (grafting P*t*BMA or PMMA first, P2VP second), and singly for homo PEL supports; (iii) blocking unreacted tresyl functions; and (iv) deprotecting P*t*BMA and

PMMA modified media to remove tertiary butyl protecting groups, thereby liberating the poly(methacrylic acid), PMAA chains.

PEL adsorbents and intermediates in their manufacture were subjected to a battery of physico-chemical and functional characterisation tests, which included: (i) FTIR (for composition and loading of each PEL type); (ii) gravimetry (for polymer loadings); (iii) fluorescence imaging with fluorophore-tagged proteins (to assess uniformity of PEL brush distribution within supports); (iv) zeta potential measurements (to measure points of zero charge and examine pH switching behaviour); and (v) functional protein binding and elution tests using model acidic, neutral and basic proteins.

Loading calibration studies with each PEL chain type provided a simple framework for creating of mixed PEL fimbriated supports with different 'PMAA:P2VP' contents and inter-chain spacings in two sequential grafting steps. Successful manufacture of 'functional' mixed PEL supports was gauged from the following observations: (i) Smooth reversible charge switching of mixed PEL brush layers on modified Toyopearl supports demonstrated from measurements of zeta potential as the pH was swung back and forth across the point of zero charge; (ii) The point of zero charge of mixed PEL adsorbents strongly correlated with brush composition; (iii) mixed PEL supports displayed 'chameleon-like' pH switchable AEX-CEX protein binding-desorption behaviour; (iv) Protein binding and elution performance of mixed PEL brush supports correlated with composition and individual PEL loadings, the balance of AEX-CEX character being clearly determined by the relative populations of the two oppositely charged PELs rooted 'side-by-side' in the same surface, and the loading of each type correlates with the support binding and elution performance; (v) The mixed PEL supports also displayed similar and in some cases superior pH mediated elution behaviour to homo PEL supports (e.g. when shifted by 1 or 2 pH units); and (vi) predictable pH mediated chromatographic separation of a

model mixture of acidic, basic and neutral proteins under low-salt conditions.Attempts to improve the low operational binding capacity of mixed PEL porous adsorbents for lysozyme, involving utilisation of a shorter chained of PMAA, and a different base matrix (Praesto 45), met with some success, but necessary further increases in binding capacity will likely require a ‘grafting from’ manufacturing approach.

Dedication

To my family and my friends for all the love, support, and encouragement

To myself for my brave to step outside my comfort zone

Acknowledgements

I would like to express my gratitude to numerous individuals for their help and supports during my PhD study;

Firstly, Professor Owen Thomas, my supervisor, for his continued advice and encouragement throughout my PhD. It was a pleasure to work under your supervision and I learnt a lot from you, not only about this project, but also work style and attitude from your experience. Also, Dr. Zhenyu Jason Zhang for his useful suggestion and guidance.

The Royal Thai Government for granting my scholarship for my master and PhD studies. It does not only provide me an academic knowledge, but also the opportunities to get many valuable experiences which I have never got before.

Our technician staff, Elaine Mitchell for technical supports in the laboratories and enthusiasm in helping me always. Also, Dr Mark Taylor for helping me about zeta potential measurements.

My lovely colleagues in our Downstream Process group, Stephan Joseph, Hong Li, Charles Moore-Kelly, for offering any support in my PhD, especially help me to find my way in our laboratories and get through any experiment. Also, everybody else for helping in one way or another.

Finally, my parents for always believing in me and raising me with such a positive attitude that leads me pass through any tough time. Also, my friends in Thailand for mentally support and encouragement and making my life here less stressful.

Table of contents

List of figures

List of tables

List of Abbreviations

AINB	2,2’-azoisobutyronitrile
AEX	Anion exchange chromatography
AFM	Atomic force microscopy
APTES	(3-Aminopropyl)triethoxysilane
ATR-FTIR	Attenuated total reflectance-Fourier transform infrared spectroscopy
ATRP	Atom transfer radical polymerisation
BCA	Bicinchoninic acid
BMA-*co*-DMAPAAM	Butyl methacrylate-*co*-*N*,*N*-dimethylaminopropyl acrylamide
BSA	Bovine serum albumin
CEX	Cation exchange chromatography
CLSM	Confocal laser scanning microscopy
CM	Carboxymethyl
CNBr	Cyanogen bromide
CV	Column volume
DEAE	Diethylaminoethyl
DMAE	Dimethylaminoethyl
DMF	Dimethylformamide
DMSO	Dimethyl sulfoxide
DOPA	3,4-dihydroxyphenylalanine
DP	Degree of polymerisation
E-SEM	Environmental scanning electron microscopy
EPEI	Ethoxylated polyethylenimine
FTIR	Fourier-transform infrared spectroscopy
GPS	Glycidoxypropyltrimethoxy-silane

HIC	Hydrophobic interaction chromatography
HPLC	High performance liquid chromatography
HSA	Human serum albumin
ICP-OES	Inductively coupled plasma - optical emission spectrometry
IgG	Immunoglobulin G
IMAC	Immobilised metal ion affinity chromatography
IRSE	Infrared spectroscopic ellipsometry
LCST	lower critical solution temperature
LDS	Lithium dodecyl sulphate
mAb	Monoclonal antibody
MEO_2MA	2-(2-methoxyethoxy)ethyl methacrylate
MES	2-(*N*-morpholino)ethanesulphonic acid
MW	Molecular weight
NHS	*N*-hydroxysuccinimide
NMP	Nitroxide-mediated polymerisation
OEGMA	Oligo(ethylene glycol) methacrylate
P2VP	Poly(2-vinylpyridine)
PAA	poly(acrylic acid)
PAGE	Polyacrylamide gel electrophoresis
PBA	Poly(butyl acrylate)
PCBMA	Poly(carboxybetaine methacrylate)
PCL	Poly(ε-caprolactone)
PCMS	Poly(chloromethylstyrene)
PDMAEMA	Poly(2-(dimethylamino)ethyl methacrylate)
PDMAM	Poly(*N*,*N*-dimethylacrylamide)
PDMAPAA	Poly(*N*,*N*-dimethylaminoproplacrylamide)

PDMC	Poly (methacryloxyethyltrimethyl ammonium chloride)
PDMS	Poly(dimethylsiloxane)
PEDMA	Poly ethylene glycol dimethacrylate
PEG	Polyethylene glycol
PEL	Polyelectrolyte
PEO	Polyethyleneoxide
PGMA	Poly(glycidyl methacrylate)
PHEMA	Poly(2-hydroxyethyl methacrylate)
pI	Isoelectric point
PLA	Poly(lactic acid)
PMA	Poly(methyl acrylate)
PMAA	Poly(methacrylic acid)
PMEDSAH	Poly [2-(methacryloyloxy) ethyl dimethyl-(3-sulphopropyl) ammonium hydroxide]
PMETAC	Poly(2-methacrylolyloxyethyltrimethylammonium chloride)
P(MEO_2MA-*co*-OEGMA)	Poly(2-(2-methoxyethoxy) ethyl methacrylate-*co*-oligo(ethylene glycol) methacrylate
PMMA	Poly(methyl methacrylate)
P*N*IPAAm	Poly(*N*-isopropylacrylamide)
POEGMA	Poly(oligoethylene glycol methacrylate)
P(*N*IPAAm-*co*-AAc)	Poly(*N*-isopropylacrylamide-*co*-acrylic acid)
P(*N*IPAAm-*co*-BMA)	Poly(*N*-isopropylacrylamide- *co*-*n*-butyl methacrylate)
PPEI	Poly(*N*-propionylethyleneimine)
PS	Polystyrene
PSBMA	Poly(sulphobetaine methacrylate)
PSF	Poly(styrene-co-2,3,4,5,6-pentafluorostyrene)
PSPM	Poly(3-Sulfopropyl Methacrylate)

P*t*BMA	Poly(*t*-butyl methacrylate)
PVA	Poly(vinyl alcohol)
PVBIm-PF_6	Poly[1-(4-vinylbenzyl)-3-butyl imidazolium hexafluorophosphate]
PZC	Point of zero charge
Q	Quarternary ammonium
QCM-D	Spectroscopic ellipsometry-quartz crystal microbalance with dissipation
RAFT	Reversible addition-fragmentation chain transfer
R_F	Flory radius
R_g	Radius of gyration
ROP	Ring opening polymerisation
RPC	Reversed phase chromatography
S	Methyl sulphonate
SAM	Self-assembled monolayer
SDS	Sodium dodecyl sulphate
SEC	Size exclusion (or gel filtration) chromatography
SP	Sulphopropyl
TEMPO	Nitroxide radical
TFA	Trifluoroacetic acid
THF	Tetrahydrofuran
TNBS	2,4,6-trintrobenzene sulphonic acid
UCST	Upper critical solution temperature
XPS	X-ray photoelectron spectroscopy

Chapter 1 Introduction

1.1 Chromatography

Chromatography is one of the most widely used techniques for protein separation, especially in biopharmaceutical processes. This separation technique is based on an affinity of different molecules toward a stationary phase and a mobile phase. This affinity determines the various travel rates of these molecules through the system and the molecules can be separated by that. With a solid stationary phase (a porous matrix) packed in a column and a liquid mobile phase (mostly an aqueous buffer) pass through it, this is called 'Column chromatography', which has been the most extensive used technique in protein purification processes. There are various types of column chromatography based on different principles in separation as summarised in Table 1-1.

Table 1-1 Chromatography techniques based on their fundamentals (Janson and Jonsson, 2011).

Chromatography Technique	Separation Principle
Ion exchange chromatography	Net charge
Hydrophobic interaction chromatography (HIC) and Reversed phase chromatography (RPC)	Hydrophobicity
Size exclusion (or gel filtration) chromatography (SEC)	Size and shape
Affinity chromatography	Biological function
Immobilised metal ion affinity chromatography (IMAC)	Metal binding

1.1.1 Ion exchange chromatography

The principle of ion exchange chromatography is charge interaction between charged biomolecules and a stationary phase containing opposite charges. Adsorption and desorption can be manipulated by changing environmental pH or ionic strength which has an impact on net charges of biomolecules and/or a stationary phase. Ion exchange chromatography has been widely employed in industrially separating and purification different biomolecules, including

proteins, antibodies, and nucleic acids because of its high capacity, resolving power, and mild conditions of binding and eluting steps (Desai *et al.*, 2000).

Ion exchange chromatography has been mainly classified in two subtypes according to a stationary phase's charges. Anion exchange matrix expresses positive charges and can bind with negatively charged molecules. Another one is cation exchange matrix containing negative charges which can capture positively charged molecules (Karlsson, 2011). These supports display either positive or negative charges depending on functional groups on the support that possesses different pK values (Table 1-2). With these different numbers, protonation and ionisation can be performed in different pH and/or ionic strength.

Table 1-2 Functional groups in ion exchangers with structures and pK values (Desai *et al.*, 2000).

Functional group	Chemical structure	pK
Anion exchangers		
Quarternary ammonium (Q)	-O-CH_2-CHOH-CH_2-O-CH_2-CHOH-CH_2-$N_+(CH_3)_3$	>9.5
Dimethylaminoethyl (DMAE)	-O-CH_2-CH_2-$N^+H(CH_3)_2$	8-9
Diethylaminoethyl (DEAE)	-O-CH_2-CH_2-$N^+H(CH_2CH_3)_2$	9-9.5
Cation exchangers		
Methyl sulphonate (S)	-O-CH_2-CHOH-CH_2-O-CH_2-CHOH-$CH_2SO_3^-$	2
Sulphopropyl (SP)	-O-CH_2-CHOH-CH_2-O-CH_2-CH_2-$CH_2SO_3^-$	<1
Carboxymethyl (CM)	-O-CH_2-COO-	3-5

Different functional groups also provide two subtypes for each exchanger type, including strong and weak ion exchangers. These do not indicate strength of interaction, but they refer to influence of pH on the group. As weak exchangers, such as, DEAE and CM, their charges are affected by changing pH and can be expressed only above the dissociation constant, while, the

charges are maintained along a wide pH range for strong exchangers, such as, Q and S (Desai *et al.*, 2000).

1.1.2 Hydrophobic interaction chromatography

Hydrophobic interaction chromatography is based on the interaction between hydrophobic region of protein and non-polar ligand, which alternates the order of water around their molecules and generate thermodynamically favourable binding (Figure 1-1).

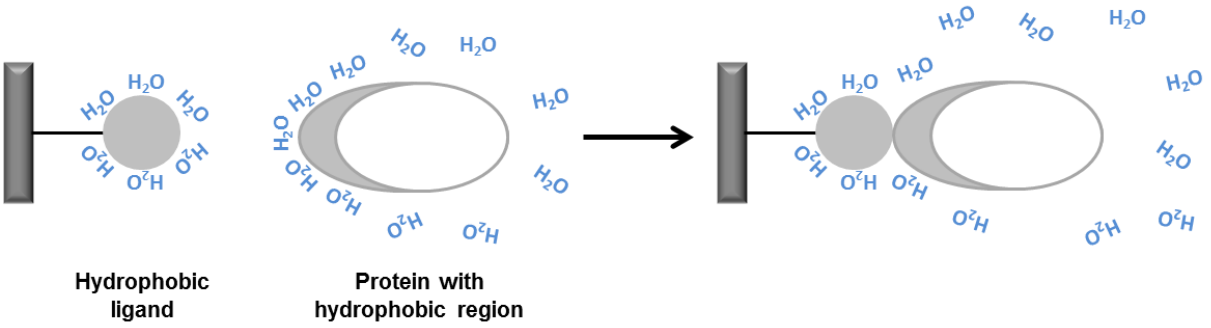

Figure 1-1 Schematic of interaction between HIC matrix and protein (Redrawn from Tomaz and Queiroz, 2013).

The strength of interaction is dependent on salt in mobile phase. High salt concentration or salts with high salting-out effect following the Hofmeister Series (Figure 1-2) in aqueous environment promotes strong interaction between protein and ligand. Desorption can be occurred by lower the salt concentration leading to reduction of surface tension in a liquid phase and subsequently dissociation of protein from the support (Desai *et al.*, 2000; Eriksson and Belew, 2011; Tomaz and Queiroz, 2013).

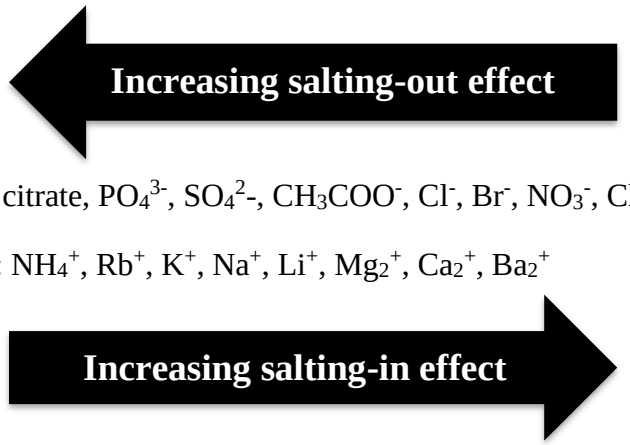

Figure 1-2 Diagram represents The Hofmeister Series of some ions ordered by the impacts on the protein solubility in aqueous solution. Salting-out refers to impact on protein precipitation, while salting-in refers to impact on protein stabilising (Redrawn from Tomaz and Queiroz, 2013).

1.1.3 Reversed phase chromatography

Reversed phase chromatography is closely related to HIC in term of the principle of separation molecules with different hydrophobicity. However, the techniques are practically different. Stronger interaction between ligands and hydrophobic regions of protein can be observed because of more hydrophobicity of ligands. Therefore, desorption process requires non-polar mobile phase, such as, methanol or acetonitrile. RPC absorbents are usually silicon materials with surface modification like n-Alkyl silanes on the surface of silica bead. Due to organic solvents are presented in the system, it is possible that protein denaturation or conformation changes will be occurred. Thus, RPC is less commonly used than HIC in large-scale purification of therapeutic proteins (Pettersson, 2011; GE Healthcare, 2012).

1.1.4 Size exclusion chromatography

Size exclusion chromatography is separating molecules based on their molecular size. Molecules with smaller size than the pore size of matrix tend to penetrate through the pore and travel for long time in a column. If the molecular size is larger, the travel time in the column

will be possibly shorter (Figure 1-3). Several SEC matrices have been commercially available and extensively used. These matrices are made of various materials including agarose, polyacrylamide, cross-linked dextran, silica, or highly cross-linked agarose which provide different characteristics, such as, bead size and pore size. Due to low capacity of SEC for processing samples, large amounts of SEC matrices would be required in industrial-scale production. However, SEC has been effectively exploited in polishing steps of purification process for buffer exchange or concentrating purpose (Desai *et al.*, 2000; Hagel, 2011).

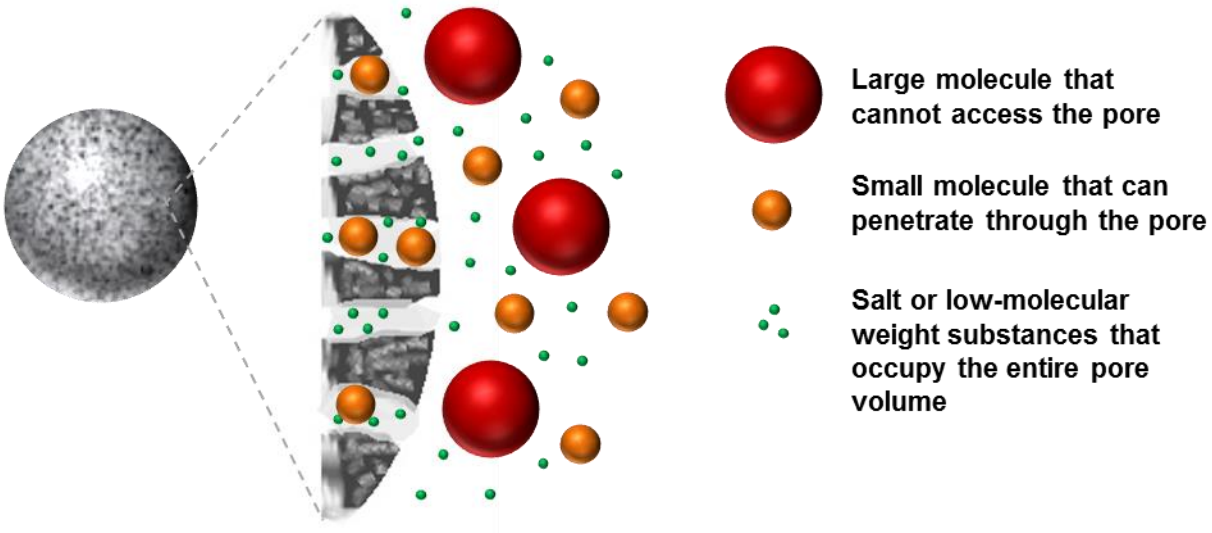

Figure 1-3 Principle of SEC (Redrawn from GE Healthcare, 2014).

1.1.5 Affinity chromatography

Affinity Chromatography is based on the specific interaction between target proteins and immobilised ligands which is reversible. Typically, the specific interaction refers to biological specificity. However, affinity chromatography also actually includes separations related to non-biological interaction, such as, group-specific, synthetic affinity, and pseudo-biospecific ligands, as long as, the highly selective bindings between target proteins and ligands are presented. These bindings could originate from electrostatic forces, hydrophobic interactions, Van der Waals forces, hydrogen bonding, or a combination of these. Since specificity of

biorecognition is achieved, affinity chromatography has advantages over other techniques including high selectivity, high capacity, and high resolution. However, the affinity ligands are very expensive and could be vulnerable to harsh conditions. Several affinity ligands have been developed and some of them are commercially available including the well-known one, Protein A, which industrially used for monoclonal antibody (mAb) production (Batista-Viera *et al.*, 2011; Rowe *et al.*, 2012).

1.1.6 Immobilised metal ion affinity chromatography

Immobilised metal ion affinity chromatography is based on the interaction between transitional metal ions, which are mostly Cu(II), Ni(II), Zn(II), Co(II), and Fe(III), and electron donor groups in the amino side chains of the protein, such as, cysteine, histidine, and methionine. Metal ions can be immobilised by using chelating compounds which are attached to the base matrix. Metal chelates can be formed as bidentate to pentadentate compounds which depend on the amount of occupied coordination bonds, while the available coordination sites, which commonly contain buffer or water molecule, can be bonded with electron donor groups on the surface of protein. The base matrix can be made of agarose, polysaccharides, or inorganic materials, such as, silica. High degree of metal chelating ligands, including tetradentate and pentadentate, tend to exhibit low capacity of protein binding due to the major loss of coordination sites. Therefore, the chosen metal ion has a direct impact on the protein affinity. IMAC has been evolved for various applications in protein purification. One common example is utilisation of histidine-tagged protein which is the target protein fused of histidine terminus and can be selectively separated in one step of IMAC (Kagedal, 2011; Cheung *et al.*, 2012).

1.1.7 Challenges from conventional chromatography

As the chromatography has been the blueprint in downstream process in biopharmaceutical industry for many decades, it is still the bottleneck and cannot be matched with the advance of upstream process that can produce higher capacities and larger titres (De Palma, 2017; *GEN-Genetic Engineering & Biotechnology News*, 2018). The conventional chromatography is expensive which was mainly linked with low productivity. One of the contribution factors is limitation of the technique for some specific biomolecules, for example, plasmid DNA which has as remarkably similar properties as the host cell's impurities leading to technical challenges in applying suitable chromatography. Moreover, a regulatory requirement of high purity of supercoiled plasmid DNA (>90%) made it more challenging because the supercoiled structure can be changed by ionic strength alteration (Prazeres *et al.*, 1999; Ferreira, 2005; Sousa *et al.*, 2012). Another factor influencing low productivity is requirement of several-steps operation and long process time which can be found in downstream processing of some high value therapeutic biomolecules, such as, virus particles (Nestola *et al.*, 2015; Silva *et al.*, 2015; Lagoutte *et al.*, 2016; Mochao Zhao *et al.*, 2019) and monoclonal antibody (mAb) (Thömmes and Etzel, 2007; Farid, 2008). Among all chromatography techniques, ion exchange chromatography is one of the most extensively used in bioprocessing due to its versatility and high capacity (Karlsson and Rydén, 1989; Jungbauer and Hahn, 2009; Cramer and Holstein, 2011; Lenhoff, 2016). Although it has provided the advantages in bioprocess purification, high amount of salt is still required to achieved high product recovery, for example, in mAb (Levy *et al.*, 2016; Großhans *et al.*, 2018) and protein purifications (Faraji *et al.*, 2017). This will consequently create considerable amount of salt that need to be managed, leading to a non-economic and non-environmental-friendly process. Hence, development of a new

chromatography media by adapting smart polymer concept is an attractive way to overcome these issues.

Applying smart polymer with thermo-responsive behaviour created the chromatography supports that can perform protein binding and elution in low salt condition by switching temperature (Maharjan *et al.*, 2009; Müller *et al.*, 2013; Cao *et al.*, 2015). However, modification of equipment for controlling temperature is required which can cause an engineering constraint in development of large-scale process. With pH-responsive polymer, there is no such requirement for achieving protein adsorption and desorption in low salt buffers (Willett, 2009).

1.2 Polymer brush

Polymer brush is the term used to explain when polymer chains are attached to a surface with sufficiently high density. These chains are subsequently overlapped and stretched out from the surface like a brush (De Gennes, 1976; Milner, 1991; Halperin *et al.*, 1992). The Alexander model (Alexander, 1977) is simply way to describe behaviour of polymer chains tethered on an interface and polymer brushes arrangement. Monodisperse polymer chains attached to a flat and non-adsorbing surface are considered in this model. The free energy of each polymer chain consists of two contributions, the interaction energy (F_{int}) and the elastic energy (F_{el}), as follow equation:

$$F = F_{int} + F_{el} \qquad (1\text{-}1)$$

The lowest overall free energy is favourable for the stable polymer conformation. When high density of tethered polymer chains on a surface is presented, the coils are strongly overlapping. This leads to increase of monomer-monomer contact, and subsequently high interaction energy. Thus, the polymer chains are enforced to stretch away causing increase of the layer thickness

and decrease of the interaction energy, whereas the elastic free energy is higher as a consequence. Therefore, the interplay of both two terms affects the thickness of layer and the formation of polymer brushes (Zhao and Brittain, 2000).

Polymer chains tethered on a surface can possibly be established as three different regimes depending on the grafting density and the interaction between the chains (Figure 1-4). If the grafting density is insufficient and no interaction with neighboured chains can be expected, a flat ‘pancake’ or a ‘mushroom’ conformation can be observed. Pancake regime is formed in case of a high affinity between the polymer chains and the substrate is presented, whereas, mushroom regime is occurred from the non-adsorbed polymer chains. In a situation that the grafting density of polymer chains is adequately high, ‘brush’ conformation can be likely created (Fleer *et al.*, 1998; Das *et al.*, 2015).

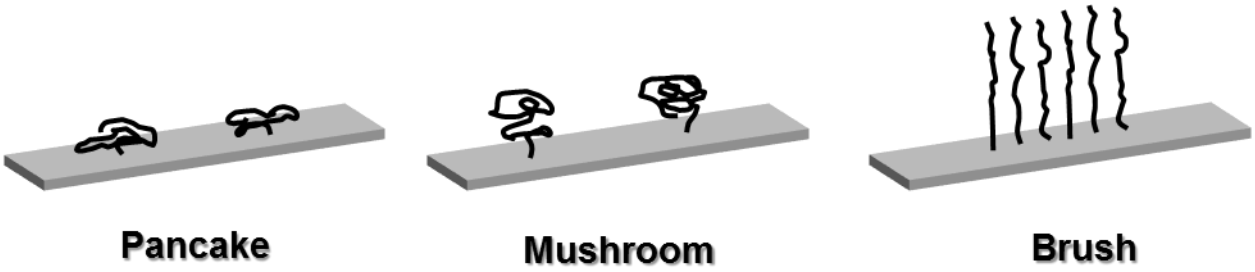

Figure 1-4 Schematic of the tethered polymer chains on the substrate surface.

The brush formation can be predicted by two parameters, one is the distance between each grafted chain (D) and another one is the Flory radius (R_F). The Flory radius or the radius of gyration (R_g) is defined by the expected ‘random walk’ of the tethered polymer chain which can roughly indicate the polymer chain dimension (Bartucci *et al.*, 2002). The Flory radius can be simply calculated by the following equation;

$$R_F \approx AL^{v} \qquad (1\text{-}2)$$

where A is the monomer size (nm), L is the polymer length in term of monomer units (degree of polymerisation), and v is the Flory exponential, which is influenced from the interaction between polymer and solvent.

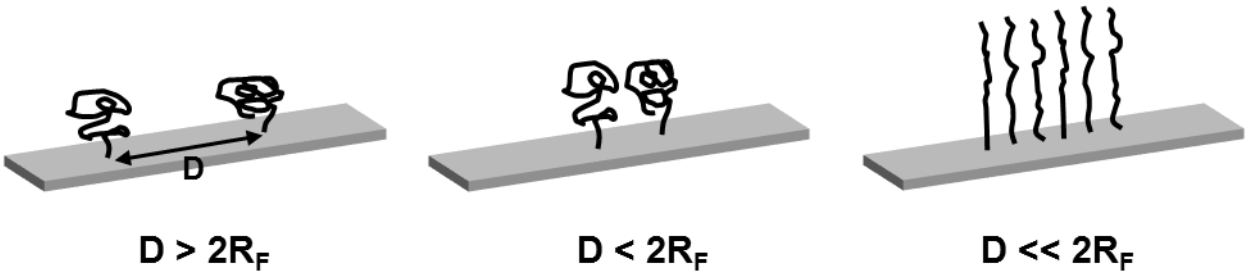

Figure 1-5 Illustration of polymer chains conformation related to the inter-graft space (D) and the Flory radius (R_F) (Adapted from Unsworth *et al.*, 2005).

The relation between the inter-graft space (D) and the Flory radius (R_F) with polymer brush formation is shown in Figure 1-5. If D value is larger than $2R_F$, the mushroom regime will be likely occurred. After increasing grafting density, the distance between each polymer chain is smaller and weak overlapping is possibly observed if D is less than $2R_F$. If the grafting density is sufficiently high and reaches the point, where D is a lot less than 2 R_F, the polymer brush can be expected (Unsworth *et al.*, 2005; Zhu *et al.*, 2007).

1.3 Smart polymer brush

Polymer brushes can change their height or morphology when exposed to different environment, such as, solvent (Sidorenko *et al.*, 1999; Minko *et al.*, 2002a). It shows a potential to create a smart polymer brush which can characteristically controllable by switching environmental conditions. With two different polymer chains grafted on the surface, mixed polymer brush can be obtained and can get an advantage from different properties from two polymers.

1.3.1 Solvent-responsive polymer brushes

The different polymer chains can act differently in the solvent depending on several factors, including their chemical structures, molecular weights, solubilities, compositions, and preferences to the substrate. Therefore, the surface morphology of mixed polymer brush can be changed by exposing to selective or non-selective solvent for the grafted polymer chains (Minko *et al.*, 2002; Draper *et al.*, 2004)

Mixed brush of polystyrene (PS) and poly(2-vinylpyridine) (P2VP), for example, exhibit different wettability, evaluated by the contact angle measurement, when they are treated with toluene, ethanol, or acidic water. The PS-P2VP brushes are hydrophobic by exposing to toluene, whereas less hydrophobic and highly hydrophilic surfaces are observed when treating with ethanol and acidic water, respectively. These could be the effect of morphology and composition alteration of the top layer, which was proved by the images from atomic force microscopy (AFM). It is possible that when the mixed brushes are exposed with toluene, which is prefer to PS, PS chains are swollen and stretched away from grafting point and occupy the top layer, while P2VP chains collapse on the surfaces. On the other hand, expectedly opposite results could be observed when the PS-P2VP brushes were treated with ethanol or acidic water, which are the selective solvents for P2VP (Figure 1-6). This was confirmed by detecting the chemically difference using X-ray photoelectron spectroscopy (XPS) (Sidorenko *et al.*, 1999; Minko *et al.*, 2002; Draper *et al.*, 2004; Vyas *et al.*, 2008).

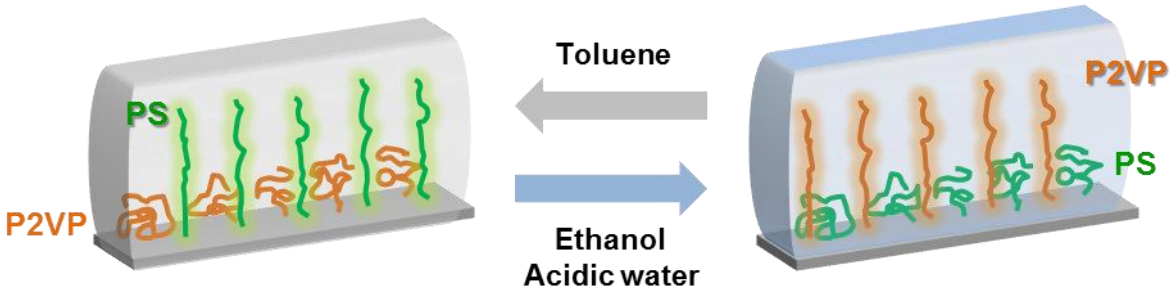

Figure 1-6 Diagram demonstrating solvent-responsive behaviour of mixed PS-P2VP brushes when exposing with different selective solvents (Redrawn from Vyas *et al.*, 2008).

The solvent-responsive behaviour was also observed in the substrate grafted with poly(methyl acrylate) (PMA) and poly(styrene-co-2,3,4,5,6-pentafluorostyrene) (PSF). After characterising by contact angle measurement and AFM, it suggested that PMA was swelled and dominated the surface when exposing to acetone, while, PSF was dominant on the surface after exposure to toluene (Minko *et al.*, 2002a; Lemieux *et al.*, 2003).

The mixed brushes composed of poly(dimethylsiloxane) (PDMS) and ethoxylated polyethylenimine (EPEI) can be rapidly changed from hydrophilic to hydrophobic surface when immersed in water and dried in air, respectively. Thus, they can perform adhesion or reactivity in aqueous environment, while exhibiting non-fouling surface in the air (Motornov *et al.*, 2007). The non-adhesive surface has been also observed in the mixed brushes of PDMS and polyethyleneoxide (PEO). Due to quickly spontaneous changing in constitutions of the top layer from PEO chains in water to PDMS chains in air, the mixed brush can display non-sticky surface in both environment (Sheparovych *et al.*, 2008).

1.3.2 Temperature-responsive polymer brushes

Thermo-responsive polymers are mainly classified in two types, one has a lower critical solution temperature (LCST) and another one has an upper critical solution temperature (UCST). A polymer presenting LCST becomes insoluble in solvent at the temperature above

LCST, while a polymer with UCST is insoluble in solvent below the UCST. These behaviours result from a balance between the entropy of the system, especially the entropy of water, and the enthalpy effects in order to reach energetically favourable state (Ward and Georgiou, 2011). Since these polymers have different preferences to water depending on temperature, they can change hydrophilicity/hydrophobicity of surface when grafting to the surface.

Poly(*N*-isopropylacrylamide) (P*N*IPAAm) has been extensively studied as a thermo-responsive polymer for biomedical application because its LCST, of approximately 32 ºC, is close to the human body temperature. P*N*IPAAm brushes can be switched from hydrophilic to hydrophobic surface when the temperature increase from below 32 ºC to above 32 ºC (Jonas *et al.*, 2007; Mizutani *et al.*, 2008). The P*N*IPAAm brush with functionalised terminal demonstrated thermos-responsive cell adsorption/desorption. Cells were adhered to the brush at high temperature, where the brush collapsed at the surface. When decreasing temperature below the critical temperature, the brush was rehydrated and cell detachment was observed (Matsuzaka *et al.*, 2013). The P*N*IPAAm brush was not only tested with cells, but also proteins. There have been studies about using this brush as a protein resistance layer. The brush reaction with proteins was similar to the reaction with the cells. Briefly, bovine serum albumin (BSA) and human serum albumin (HSA) were highly adsorbed on the P*N*IPAAm brush at high temperature, while very low adsorption was shown at low temperature (Burkert *et al.*, 2009; Xue *et al.*, 2011).

Poly [2-(methacryloyloxy) ethyl dimethyl-(3-sulphopropyl) ammonium hydroxide] (PMEDSAH) brushes exploiting the UCST properties have been studied and perform reversible change of wettability by altering temperature. This is influenced by molecular weight of PMEDSAH and grafting density (Azzaroni *et al.*, 2006; Cheng *et al.*, 2008).

1.3.3 Ion and pH-responsive polymer brushes

This type of polymer brushes is alternatively named as “Polyelectrolyte (PEL) brushes”. This refers to polymer chains grafted on surface which contain charged monomers. Consequently, change in conformation or properties of polymer chains could be presented when exposing different pH or ionic strength. These changes are dependent on the interplay of three main factors; electrostatic interaction, solvation, and excluded volume effects. Poly(2-methacrylolyloxyethyltrimethylammonium chloride) (PMETAC), for example, express hydrophilic surface in the solution without electrolytes because of significant impact from charge repulsion and excluded volume effect, whereas in the presence of electrolytes, electrostatic interaction dominantly affect collapse of the polymer chains (Azzaroni *et al.*, 2005). This behaviour was also seen in another polymer brush. Poly[1-(4-vinylbenzyl)-3-butyl imidazolium hexafluorophosphate] (PVBIm-PF_6) brush tethered on silicon surface exhibiting hydrophobic nature switch to more hydrophilic surface after being exposed to 0.2 M NaCl aqueous solution for 1 h. This resulted from anion exchange between PF_6^- and Cl^- (He *et al.*, 2008).

Polymers containing acidic or basic groups, especially weak acid or base groups, such as carboxylic acids, amines, and phosphoric acids are possible to perform pH-responsive properties due to their ability to be ionised by variation of pH. Polymer brushes containing phosphate groups, which possess $pK_1 \sim 1$ to 2 and $pK_2 \sim 6$ to 7 (Wazer, 1958), can display three different wettability properties depending on pH of the solution. In high pH (more than 12) solution, they were fully ionised leading to hydrophilic surface. In low pH (less than 1), they were fully protonated resulting in hydrophobic surface, supposedly, due to the hydrogen bond between protonated groups. In pH around 4, they were partly protonated causing intermediate hydrophilicity (Figure 1-7) (Zhou and Huck, 2005).

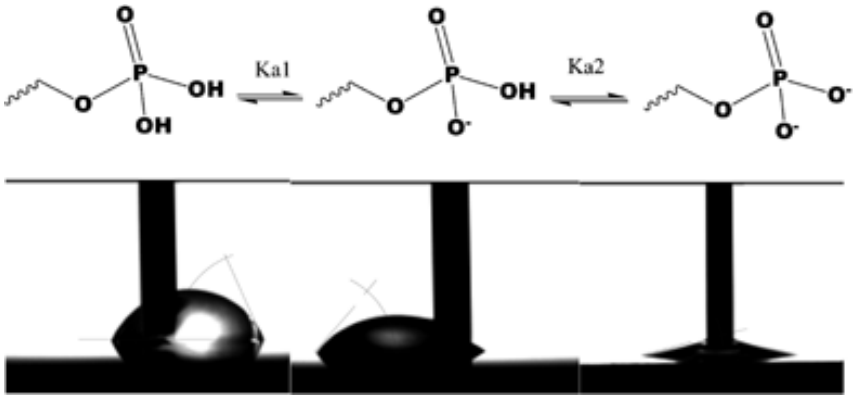

Figure 1-7 Schematic of ionisation of phosphate group in different pH (Top) resulting in different wettability demonstrated by contact angle of water droplet (Bottom) (Zhou & Huck 2005).

Mixed PEL brushes consisting of two oppositely charged polymer chains are highly attractive, since they could be potentially developed for a number of useful applications including non-fouling surfaces, adjustment of surface wettability, and regulation of protein adsorption. An extension of mixed PEL brushes is influenced by the intra- and inter-chain Coulomb repulsion and the compensation of repulsion which depends on charge ratio (Shusharina and Linse, 2001).

Several mixed PEL brushes have been extensively studied and developed. The interesting one is the brush composed of an acidic polymer, poly(acrylic acid) (PAA) and a basic polymer, poly(2-vinyl pyridine) (P2VP). Homopolymer PAA, P2VP, and mixed PAA-P2VP brushes grafted on silicon wafer have been studied. Isoelectric points of these brushes determined by zeta potential measurements were at pH 3.2, 6.7, and 4.9 for PAA, P2VP, and mixed PEL brush, respectively. These isoelectric points indicate charged or uncharged state of these polymer chains. The mixed PAA-P2VP brush could be switched surface charge by exposing to different pH solutions according to contact angle measurements, zeta potential measurements, and the brush thickness analysed by ellipsometer (Houbenov *et al.*, 2003). At pH below 6.7 (isoelectric point of P2VP), P2VP chains were protonated, whereas at pH above 3.2 (isoelectric point of PAA), PAA chains were ionised. Thus, at low pH (< 3.2), P2VP chains were highly positively

charged and stretched away from the surface, subsequently occupying the top layer, while PAA chains collapsed at the bottom. At high pH (> 6.7), the reversed behaviour was observed. Ionised PAA chains were stretched to the top layer, while P2VP chains were packed at the bottom. These switchable conformations of P2VP chains agreed with the conformation of adsorbed P2VP chains detected by AFM which demonstrated the extended P2VP chains in low pH solution, whereas, compact coils of P2VP was found at high pH solution (Roiter and Minko, 2005). In the pH ranging from 3.2 to 6.7 (around isoelectric point of the mixed brushes), the neutral surface was possibly formed because of the compensation of the charges between those polymer chains. This led to complex and compact conformation of the mixed brush, which was confirmed by the film thickness that was close to the thickness of dry state film. Besides, the hydrophobic surfaces were presented when the pH was around isoelectric point of the mixed brush, whereas at low (pH 2) or high (pH 10) pH, the surfaces were hydrophilic which indicated charged surfaces (Houbenov *et al.*, 2003; Ionov *et al.*, 2004). The mixed PAA-P2VP has been also investigated using infrared spectroscopic ellipsometry (IRSE), which can detect chemical changes in different pH solutions. At high pH, carboxylic groups were detected on the mixed brush surface indicating PAA chains were ionised and dominated the surface. In contrast, at low pH, protonation of pyridine ring was observed from the IR spectrum suggesting P2VP chains were extended. No obvious peak was detected at around neutral pH indicating both polymer chains formed complex possibly promoting charge compensation. From these findings, the proposed schematic model was reported (Figure 1-8) (Mikhaylova *et al.*, 2007; Hinrichs *et al.*, 2009).

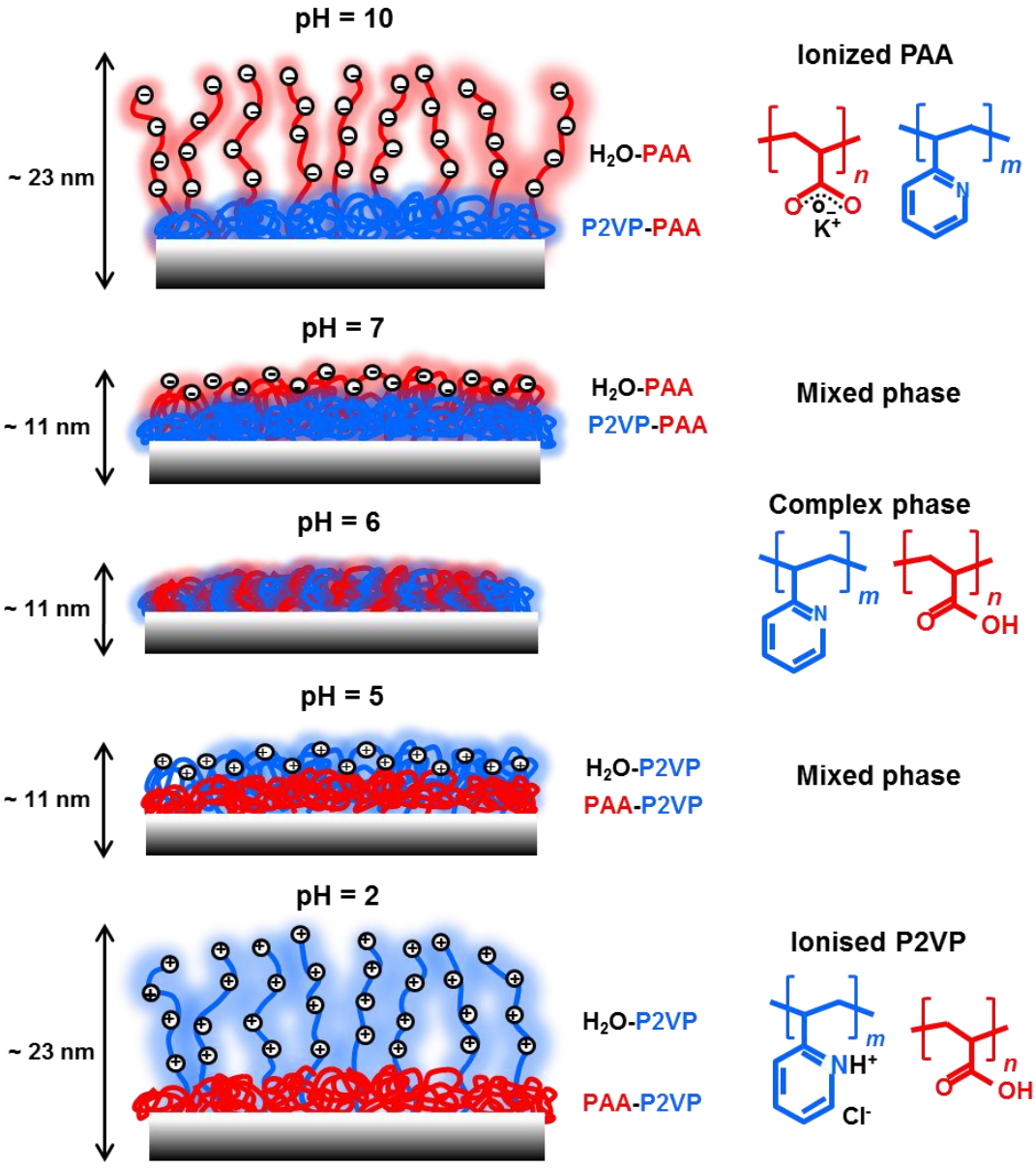

Figure 1-8 Model of pH-responsive morphology of the mixed PAA-P2VP brush (Redrawn from Hinrichs *et al*. 2009).

Due to the capability of reversibly switching surface charges of these PEL brushes, they are promising for regulating adsorption and desorption of proteins, cells, and other biomolecules by controlling environmental ionic strength or pH. The PAA brush has been investigated in term of protein adsorption. The PAA brush grafted on the flat surface was presented with BSA solutions in different pHs and the adsorption was analysed by fixed-angle optical refractometry

(De Vos *et al.*, 2008). BSA bound to the ionised PAA brush at pH 3 to 5 as expected because charge interaction between the negatively charged brush and positively charged BSA. However, at pH 6, binding of BSA was still observed even though both brush and protein had negative charges. This could be possibly explained by charge regulation, which infers that the protein change its charge following the high negative electrostatic potential in the brush (De Vos *et al.*, 2008). The binding on the PAA brush at the "wrong side" of isoelectric point (pI) of BSA has been further explored by employing spectroscopic ellipsometry-quartz crystal microbalance with dissipation (QCM-D). The results showed that excess buffer molecules were incorporated in the polymer-protein layer, suggesting an adjustment of protein charges, which supports the previous argument (Bittrich *et al.*, 2010). It is interesting that the PAA brush could display pH-switchable protein adsorption/desorption due to changing in brush configuration and shifting in protein charges. This PAA brush bound BSA and HSA at pH 5 and released proteins out after changing pH to 7 (De Vos *et al.*, 2008; Kroning *et al.*, 2015).

Ionov *et al*. (2009) fabricated mixed PEL brushes with various compositions of PAA and P2VP and used these as platforms for investigating protein adsorption as a function of pH. The adsorption was performed using BSA as a model protein. As pI of BSA is 4.9, negatively charged BSA was expected at pH above 4.9, whereas, positively charged BSA was expected at pH below 4.9. At pH 4, high adsorption of BSA was observed for the mixed PEL brush with high ratio of PAA, which contained weak negative charges, while low adsorption was obtained for the mixed brush with high ratio of P2VP. These can be explained by electrostatic attraction and repulsion which appears to be a similar situation at high pH, where low adsorption was found in the high PAA mixed brush, whereas, high adsorption was detected in the high P2VP mixed brush. This finding shows promising pH-responsive behaviour of the mixed PEL brush for protein binding (Ionov *et al.*, 2009).

Protein adsorption of the mixed PAA-P2VP brush has been studied using two globular proteins, α-chymotrypsin (a basic protein, pI=8.1) and α-lactalbumin (an acidic protein, pI=4.3), as a model. The expected net charges of proteins and the mixed brushes at different pH are demonstrated in Figure 1-9 (Uhlmann *et al.*, 2007).

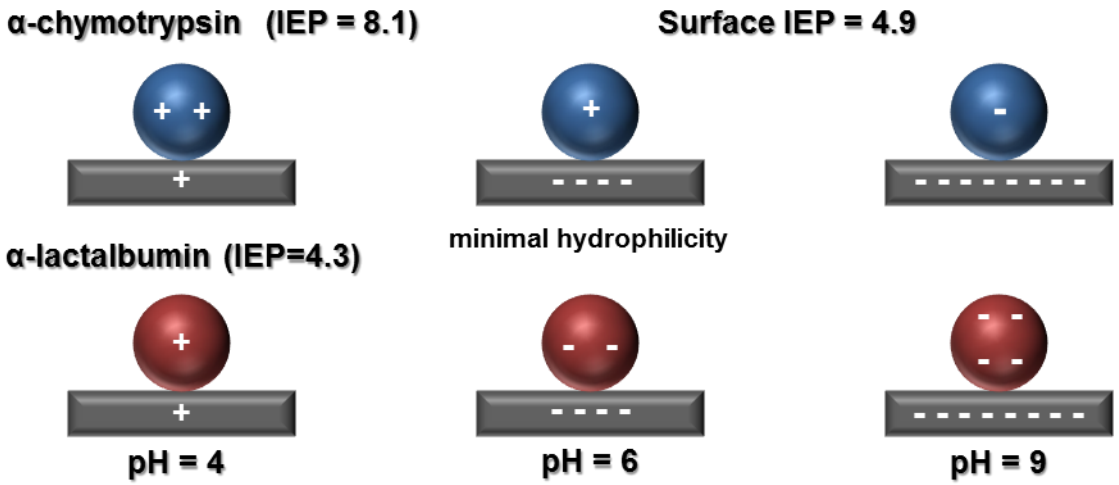

Figure 1-9 Illustration of the expected net charge of α-chymotrypsin, α-lactalbumin, and brush surfaces influenced by IEP and pH buffer (Redrawn from Uhlmann et al. 2007).

The protein adsorption profiles, however, are not as expected, especially in low salt condition, high amount of α-chymotrypsin bind with the mixed brushes at pH 9. Additionally, protein desorption processes are not significantly achieved by changing pH from 4 to 9 or by inversed order. These indicate that the interaction between proteins and the PAA-P2VP mixed brushes is quite complicated and not only influence by electrostatic or hydrophobic interactions, but also other factors such as salt concentration and confined counter-ions in the brush (Uhlmann *et al.*, 2007). The binding on the "wrong side", previously mentioned above, might also explain this scenario.

1.4 Fabrication of polymer brush

Fabrication of polymer brush can be conducted by two common approaches, 'grafting from' and 'grafting to' (Figure 1-10). The 'grafting from' method refers to synthesis of polymer chains from initiators, which are previously bonded with the substrate surface, by providing monomers and allows polymerisation on the surface. On the other hand, the 'grafting to' strategy exploits 'ready-made' polymer chains containing functionalised end groups that can stably form bond to the substrate surface via 'click-chemistry'.

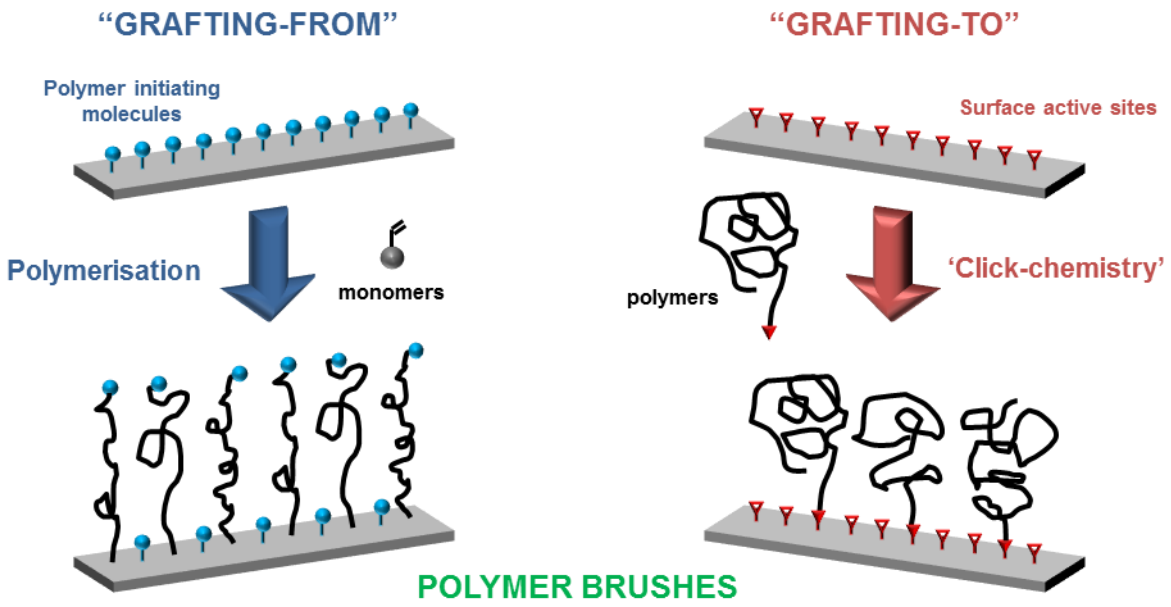

Figure 1-10 Diagram represents two approaches for polymer brush synthesis (Adapted from Azzaroni, 2012).

1.4.1 'Grafting from' method

This method has been widely used because it allows controllability of grafting density and composition. Thus, dense polymer brushes can be accomplished. In addition, block polymer brushes can be formed with this method. There are a lot of polymerisation techniques which can be exploited including ring opening polymerisation (ROP), nitroxide-mediated

polymerisation (NMP), atom transfer radical polymerisation (ATRP), and reversible addition-fragmentation chain transfer (RAFT) polymerisation.

1.4.1.1 Ring opening polymerisation (ROP)

Several polymers are produced by polymerising cyclic monomers, such as polylactide and polycaprolactone. Some of polymer brushes are created by ROP. Poly(*N*-propionylethyleneimine) (PPEI) can be grafted on a glass slide coated with gold by employing the ROP of 2-ethylene-2-oxazoline. Trifluoromethane sulphonate groups are deposited on the slide as a self-assembled monolayer (SAM) before reacting with 2-ethylene-2-oxazoline (Jordan and Ulman, 1998). ROP is also used for grafting poly(ε-caprolactone) (PCL) (Husemann *et al.*, 1999) and poly(lactic acid) (PLA) (Choi and Langer, 2001) on gold surfaces with the aid of catalysts, aluminium alkoxide and tin(II) octoate, respectively. SAMs presenting OH groups were used for initiating ROP of both polymers.

1.4.1.2 Nitroxide-mediated polymerisation (NMP)

This technique is based on the ability of a nitroxide leaving group to reversibly couple with an active chain-end radical, subsequently causing deactivation of reaction. This method was applied to polystyrene brushes formation. Alkoxylamine initiators were first attached to silicon wafers. The alkoxylamine moiety was then transformed into an alkly radical and the nitroxide radical (TEMPO) after heating. Polymerisation is controlled by the TEMPO radical to achieve polystyrene brushes (Husseman *et al.*, 1999).

1.4.1.3 Reversible addition-fragmentation chain transfer (RAFT) polymerisation

RAFT method is based on the process of transferring chains which require a RAFT chain transfer agent (or called RAFT agent). RAFT polymerisation can be accomplished by two ways

which use different surface-immobilised moieties. One is free radical initiators, while another one is RAFT agents. Poly(methyl methacrylate) (PMMA), poly(*N*,*N*-dimethylacrylamide) (PDMAM), and polystyrene brushes were achieved by using RAFT (Baum and Brittain, 2002). The polymer chains were formed on silicon wafers, which were activated with azo groups, with addition of RAFT agent, 2-phenylprop-2-yl dithiobenzoate, and free initiator, 2,2'-azoisobutyronitrile (AIBN). AIBN played an important role in removing some impurities and increasing the quantity of radicals that help promoting brush growth. A number of polymer brushes, which can also be prepared by the same technique, such as poly(chloromethylstyrene) (PCMS) (Yu *et al.*, 2004), poly(sulphobetaine methacrylate) (PSBMA) (Zhai *et al.*, 2004), and poly(2-(dimethylamino)ethyl methacrylate) (PDMAEMA) (Chen *et al.*, 2006). Another way of RAFT polymerization is exploiting RAFT agent as initiators which are immobilised on the surface. RAFT agent consists of "Z group" and "R group" (Figure 1-11). Either of these two groups can attach to the surface, and then initiating polymer chains (Tsujii *et al.*, 2001; Stenzel *et al.*, 2006).

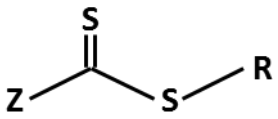

Figure 1-11 General structure of RAFT agent with a dithioester group and "Z" and "R" groups (Fairbanks *et al.*, 2015)

1.4.1.4 Atom transfer radical polymerisation (ATRP)

ATRP has been most widely used for preparing polymer brushes because of its chemical robustness and versatility. ATRP involves with the reversible redox reaction of the alkyl halide moiety in polymer chain end which requires single electron transfer process from the transition metal complex to the halogen atom. This process results in the cleavage of the alkyl-halogen

bond and subsequently, generating an active alkyl radical, which initiates polymerisation. The transition metal complex is concurrently oxidized to higher oxidation state, which fast reversibly transform the active radical to the corresponding alkyl-halide dormant chain (Patten and Matyjaszewski, 1998). The preparation of polymer brushes via ATRP is influenced by several factors including type of ligand, initiator, ratio of ligand to transition metal, or Cu^{II}/Cu^{I} ratio (Kim *et al.*, 2003; Cheng *et al.*, 2006; Tang and Matyjaszewski, 2006).

PMMA brushes grafted on 2-(4-chlorosulphonylphenyl)ethyl silane SAMs were achieved by ATRP with the Langmuir-Blodgett technique (Ejaz *et al.*, 1998). This preparation required addition of free initiator, *p*-toluenesulphonyl chloride, in order to avoid the low concentration of the initiator, which is related to the low concentration of the deactivating Cu^{II} species, leading to uncontrolled polymerisation. Direct addition of the deactivating Cu^{II} species can also be done to solve this problem. This was proven by the study of grafting PS brush on bromoisobutyrate-immobilised silicon wafers (Matyjaszewski *et al.*, 1999). However, utilization of the metal catalyst is not desirable in term of biological application. Therefore, the exploitation of reducing agent, such as ascorbic acid or Cu^{0}, has been successfully introduced to reduce the amount of copper used in polymerization (Zhao *et al.*, 2005).

1.4.2 'Grafting to' method

'Grafting to' method is based on the chemical interaction between functionalised-end group of polymer chains and reactive groups attached on the solid surface. Since polymerization is conducted prior to the grafting process, the polymer can be well prepared and thoroughly characterized in order to obtain suitable polymers with a narrow weight distribution. Additionally, this method avoids the difficulty of chemical optimization during grafting process. On top of that, 'grafting to' method possibly allows mixed two polymer species

simultaneously grafting on the surface in one step. The ‘grafting to’ approach is unlikely to create as dense brush as the ‘grafting from’ method because of steric hindrance effect. However, by supplying high concentration of polymer solution to the surface, high density polymer brush can be achieved as shown in grafting high density polyethylene oxide (PEO) (Taylor and Jones, 2010) and polyethylene glycol (PEG) brush (Emilsson *et al.*, 2015).

Coupling reaction between the polymer chains and the reactive groups on the surface is important and significantly influence the grafting density and the stability of the brushes. The coupling reaction between epoxy and carboxy groups (Luzinov and Tsukruk, 2002; Julthongpiput *et al.*, 2003; Lemieux *et al.*, 2004), carboxy and amino groups (Montagne *et al.*, 2009), and epoxy and amino groups (Penn *et al.*, 2002; Huang and Penn, 2005; Motornov *et al.*, 2008) have been exploited for polymer brushes formation. Surface modification is required if the surface does not exhibit the essential functionalities. The modification can be performed in several ways including plasma treatment, deposition of SAM, physisorption and chemisorption (Luzinov *et al.*, 2000; Iyer *et al.*, 2003; Burtovyy *et al.*, 2007). Surface functionalisation using chemical interaction typically displays a great performance and stability as a result of the formation of covalent bond. One of the most widely used methods for surface modification for flat silicon wafer is using silane chemistry. Glycidoxypropyltrimethoxy-silane (GPS)-deposited silicon wafer is employed for grafting mixed PAA-P2VP brushes which demonstrate a good performance of brush-like layer and pH-responsive behaviour (Houbenov *et al.*, 2003; Uhlmann *et al.*, 2007).

Poly(glycidyl methacrylate) (PGMA) has been promising to generate an anchoring layer on the surface for grafting mixed polymer brushes due to its relatively stable epoxy groups (Zdyrko *et al.*, 2003). Homo- and mixed polymer brushes of PEG and P2VP grafted on the PMGA layer are developed to regulate adhesion of bacteria (*Staphylococcus aureus*) (Zdyrko *et al.*, 2009).

Thin film of PGMA deposited on silicon wafer by spin-coating technique is also employed as the anchoring layer for mixed PAA-P2VP brushes (Ionov *et al.*, 2004; Mikhaylova *et al.*, 2007; Hinrichs *et al.*, 2009).

Apart from GPS and PGMA, there are other chemicals, which show promising for surface modification, including (3-Aminopropyl)triethoxysilane (APTES) (Kim, 2009; Acres *et al.*, 2012), poly(vinyl alcohol) (PVA) (Kozlov and McCarthy, 2004; Ammar *et al.*, 2009), and dextran (Ombelli *et al.*, 2003; Miksa *et al.*, 2005). However, regarding chromatography materials, the conventional approaches for functionalising chromatography adsorbents are worth exploring due to well-established methods and robustness. This includes using cyanogen bromide (CNBr) (March *et al.*, 1974), *N*-hydroxysuccinimide (NHS) ester (Cuatrecasas and Parikh, 1972), tresyl chloride (Nilsson and Mosbach, 1980) activations, etc., which commonly have been used for immobilising proteins, enzymes, or other biomolecules to create affinity chromatography (Acikara *et al.*, 2013). However, these reactions were also successfully adapted to create polymer brushes on adsorbents via 'grafting-to' approach. For example, copolymers of 2-(2-methoxyethoxy) ethyl methacrylate and oligo(ethylene glycol) methacrylate (P(MEO_2MA-*co*-OEGMA)) was stably attached to the functionalised silica monoliths using NHS ester reaction (Tan *et al.*, 2009). Another example of applying these reactions is grafting mixed PEL brushes containing PMAA and P2VP chains on the magnetic adsorbents via tresyl chloride activation (Willett, 2009).

Table 1-3 Summary of the advantages and disadvantages for 'graft from' and 'graft to' techniques

Grafting techniques	Advantages	Disadvantages
'Graft from'	- High grafting density - Different compositions in each polymer chains, such as, block polymer	- Difficulty in controlling polymerization process and degree of polymerization - Chemically-harsh polymerisation process
'Graft to'	- Simple process - Well-characterised polymer chain before grafting step	- Low grafting density (comparing to 'graft from')

1.5 Polymer brush in chromatography matrix

One of the advantages of polymer brushes is ability to alter properties or morphology regarding to surround environmental conditions. Another benefit is to boost binding capacity because of more active sites provided by polymer chains, for example, tentacular ion exchange chromatography (Bhambure *et al.*, 2016, 2017) and dendritic adsorbent (Qu *et al.*, 2018). As a result, recent trends have emerged to explore the application of polymer brush for chromatography matrix to improve separation of several target molecules, summarised in Table 1-4.

Table 1-4 Application of polymer brushes in chromatography supports.

Smart polymer brush	Polymer	Chromatography type	Base matrix	Target molecule	Reference
Thermo-responsive	Poly(*N*-isopropylacrylamide-*co*-*n*-butyl methacrylate) (P(*N*IPAAm-*co*-BMA))	HPLC	Silica bead	Benzoic acid family and phenol	Nagase *et al.*, 2010
	P*N*IPAAm	HPLC	Silica bead	Steroids	Nagase *et al.*, 2008
	P*N*IPAAm	HPLC	Silica bead	Hydrophobic steroids, insulin chain A, and insulin	Nagase *et al.*, 2007
	P*N*IPAAm	HPLC	Polystyrene bead	Insulin chain A, insulin chain B, insulin, pullulans	Mizutani *et al.*, 2010b
	P*N*IPAAm	HPLC	Polystyrene bead	Angiotensin I, angiotensin II, angiotensin III, bradykinin	Mizutani *et al.*, 2010a
	P*N*IPAAm	HPLC	Monolithic-silica-rod	Steroids	Nagase *et al.*, 2011
	P(MEO_2MA-*co*-OEGMA)	HPLC	Poly(ethylene glycol dimethacrylate) (PEDMA) monolith	Steroids	Li *et al.*, 2013
	P*N*IPAAm	HIC	Macroporous polystyrene bead	Small molecules, peptides, cytochrome c, chymotrypsinogen A, lysozyme, BSA, monoclonal antibodies	Lamprou *et al.*, 2015
	Poly(oligoethylene glycol methacrylate) (POEGMA)	SEC	Quaternary ammonium cationized agarose adsorbent	BSA, myoglobin, hepatitis B virus-like particle, hepatitis B core antigen, insulin aspart	Lee *et al.*, 2015
Ion/pH-responsive	Poly(*N*,*N*-dimethylaminoethyl methacrylate) (PDMAEMA)	AEX	Superporous polyacrylamide gel	BSA	Savina *et al.*, 2005
	Poly(2-hydroxyethyl methacrylate) (PHEMA)	SEC	Monolithic silica	Pullulans, thyroglobulin, IgG, BSA, myoglobin, aprotinin	Yoshikawa *et al.*, 2007

Table 1-4 (cont'd).

Smart polymer brush	Polymer	Chromatography type	Base matrix	Target molecule	Reference
Ion/pH-responsive	PHEMA	Affinity	porous alumina membrane	Polyhistidine-tagged ubiquitin	Jain *et al.*, 2007
	Poly(methyl methacrylate) (PMMA)	SEC	Monolithic silica	Nanoparticles	Arita, Yoshimura and Adschiri, 2010
	Polymer containing multiple sulphonate groups	CEX	Polystyrene-based macroporous latex	α-chymotrypsinogen, cytochrome c, and lysozyme	de Neuville *et al.*, 2014; Lamprou *et al.*, 2014
	Poly (methacryloxyethyltrimethyl ammonium chloride) (PDMC)	AEX	PGMA matrix	ϒ-globulin	Li *et al.*, 2015
	Poly(carboxybetaine methacrylate) (PCBMA)	AEX	polyacrylamide-based cryogel monolith	ϒ-globulin	Tao *et al.*, 2015
	Poly(3-Sulfopropyl Methacrylate) (PSPM)	CEX	Azide-Containing Macroporous microclusters from azide-containing polymeric core-shell nanoparticles	Lysozyme, chymotrypsinogen A, cytochrome C, monoclonal antibody	Lorenz *et al.*, 2019
	PSPM	CEX	Sepharose FF matrix	Lysozyme, ϒ-globulin	Wang *et al.*, 2016
	Poly(acrylonitrile) functionalised with tetrazole groups	CEX	Regenerated cellulose membrane	Lysozyme, ovotransferrin	Wang *et al.*, 2018

Table 1-4 (cont'd).

Smart polymer brush	Polymer	Chromatography type	Base matrix	Target molecule	Reference
Ion/pH-responsive	Poly(*N*,*N*-dimethylaminoproplacrylamide) (PDMAPAA)	AEX	Sepharose FF matrix	BSA	Wang *et al.*, 2019
	Poly(2-(dimethylamino)ethyl methacrylate) (PDMAEMA)	AEX	Macropore cryogel	β-glucosidase	Mól *et al.*, 2019
Ion/pH- and thermo-responsive	Poly(*N*-isopropylacrylamide-*co*-acrylic acid) (P(*N*IPAAm-*co*-AAc))	HIC/IEX	Silica bead	D, L- DOPA, adrenaline, dopamine hydrochloride, and tyramine	Kobayashi *et al.*, 2001
	Poly(*N*-isopropylacrylamide-*co*-butyl methacrylate-*co*-*N*,*N*-dimethylaminopropyl acrylamide) (P(*N*IPAAm-*co*-BMA-*co*-DMAPAAM))	HIC/IEX	Gigaporous polystyrene microsphere	BSA, myoglobin, and trypsin	Qu *et al.*, 2016
	Poly(*N*-isopropylacrylamide-*co*-*N*-*tert*-butylacrylamide-*co*-acrylic acid-*co*-*N*,*N*′-methylenebisacrylamide)	CEX	Sepharose CL-6B	Bovine whey lactoferrin	Müller *et al.*, 2013
	Poly(*N*-isopropylacrylamide-*co*-*N*-*tert*-butylacrylamide-*co*-acrylic acid-*co*-*N*,*N*′-methylenebisacrylamide)	CEX	Sepharose CL-6B	Bovine whey lactoferrin, BSA	Cao *et al.*, 2015

In summary, two main groups of polymers have been employed in chromatography supports, including thermo-responsive and ion/pH-responsive polymers. For the former, P*N*IPAAm is one of the most commonly used polymers in chromatography because it provides switchable surface properties from hydrophilic to hydrophobic by increasing temperature. The separation using the P*N*IPAAm-grafted supports involves small molecules, peptides, and proteins. In case of ion/pH responsive polymer grafted supports, they have been widely used in macro biomolecules, including antibodies and proteins. These supports are based on changing in electrostatic interaction influenced by ionic strength and/or pH of mobile phases. To extend these smart properties, there have been several studies using polymers with both thermos- and ion/pH-responsive behaviours in the chromatography supports. However, in term of developing large-scale chromatography, the thermo-responsive supports might have an engineering constraint which is a requirement of equipment modification. Thus, the ion/pH-responsive chromatography supports are promising for further development.

1.6 Outline of the work

In this research, smart polymers with pH-responsive property, P2VP and PMAA, were employed to fabricate homo and mixed PEL brushes on porous chromatography adsorbents to create a novel bi-functional chromatography matrix which can reversibly transform between anion exchanger and cation exchanger by pH alteration. This matrix can offer two modes of binding and elution of biomolecules, such as, proteins, DNA, and viruses in low-salt environment without the development of specialised equipment leading to greener and simpler purification processes.

Chapter 2 describes all materials and methods used in this thesis. ‘Graft to’ approach was employed for all homo and mixed PEL brushes grafted on the chromatography supports because

of simplicity of the method and controllability of polymer characteristics. Characterisations, analysis assays, and performance testing conducted in this research were also described in this chapter.

In Chapter 3, the optimisation and fabrication of homo and mixed PEL brushes modified porous methacrylate-based matrices were described. A series of characterisations and functionality tests, including protein binding and elution studies as a function of pH, have been conducted to explore the best option for the further column chromatography. Chapter 4 covers the dynamic protein binding and elution as a function of pH studies of the best selected adsorbent from Chapter 3 performed in the column chromatography using a model protein system, consisting of acidic, neutral, and basic proteins.

Chapter 5 covers improvement of the mixed PEL brush modified support by using alternative cation exchanger polymer and an alternative agarose-based adsorbent. The characterisations and performance tests of these supports were also investigated.

Finally, conclusion of this work and future work, based on the result of this work, are explained in Chapter 6.

Chapter 2 Materials and Methods

2.1 Materials

Toyopearl® AF-Tresyl-650M (mean particle size = 65 μm; specific surface area = 31 m^2/g (Heldt *et al.*, 2009)) purchased from Tosoh Bioscience (Griesheim, Germany) and Praesto® Pure 45 (mean particle size = 45 μm) acquired from Purolite Life Science (Llantrisant, UK), were employed as starting materials for the fabrication of homo and mixed PEL adsorbents. Amine-terminated poly(2-vinylpyridine) (P2VP) (molecular weight, MW = 13200; degree of polymerisation, DP = 126), amine-terminated poly(*t*-butyl methacrylate) (P*t*BMA) (MW = 29000, DP = 204) and thiol-terminated poly(methyl methacrylate) (PMMA) (MW = 9800, DP = 98), were supplied by Polymer Source Inc. (Montreal, Québec, Canada). The chemicals, 2,2,2,-trifluoroethanesulfonyl chloride (tresyl chloride) (99%, CAS: 1648-99-3), sodium hydroxide (≥98%, CAS: 1310-73-2), picric acid (1.3% in H_2O (saturated), CAS: 88-89-1), ethanolamine (≥98%, CAS: 141-43-5), potassium bromide (≥99.5%, CAS: 7758-02-3), 2,4,6-trintrobenzene sulphonic acid (TNBS) (1 M in H_2O, CAS: 2508-19-2), Orange II sodium salt (>85%, CAS: 633-96-5), sodium phosphate monobasic monohydrate (≥99.0%, CAS 10049-21-5), sodium phosphate dibasic dihydrate (≥99.0%, CAS: 10028-24-7), citric acid monohydrate (≥99.0%, CAS 5949-29-1), sodium citrate dehydrate (≥99.0%, CAS 6132-04-3), sodium bicarbonate (≥99.7%, CAS 144-55-8), sodium carbonate decahydrate (99.9%, CAS 6132-02-1), 1-butanol (99.8%, CAS: 71-36-3), *N*,*N*-dimethylformamide (DMF) (≥99.9%, CAS: 68-12-2), dimethyl sulfoxide (DMSO) (anhydrous, ≥99.9%, CAS: 67-68-5), tetrahydrofuran (anhydrous, ≥99.9%, CAS: 109-99-9), and ammonium hydroxide (28% NH_3 in H_2O, ≥99.99%, CAS: 1336-21-6) were all obtained from Sigma Aldrich (Poole, Dorset, UK). Acetone (≥99.9%, CAS: 67-64-1) was purchased from Argos Organics (Molinons, France), whereas ethanol (99.8%, CAS: 64-17-5), di-sodium-tetraborate (0.05M, CAS: 1330-43-4), trifluoroacetic acid (TFA) (≥99.9%, CAS: 76-05-1), and fluorescence dyes, Texas Red-X® succinimidyl ester

(CAS: T10244) and Cyanine 5 succinimidyl ester (Cy5™) (CAS: KIT0610), were obtained from Fischer Scientific (Loughborough, Leics, UK). The model proteins: pepsin from porcine gastric mucosa (CAS: 9001-75-6 647-008-00-6); lysozyme from chicken egg white (CAS: 12650-88-3); myoglobin from equine skeletal muscle (95-100%, CAS 100684-32-0); amyloglucosidase from *Aspergillus Niger* (120 U/mg, CAS: 9032-08-0); bovine serum albumin (≥98%, CAS: 9048-46-8); ribonuclease A from bovine pancreas (50-100 Kunitz units/mg protein, CAS: 9001-00-4) were purchased from Sigma Aldrich (Poole, Dorset. UK). For the preparation of buffers and aqueous solutions purified water from Sartorius Arium® Advanced EDI Pure Water System (Sartorius AG, Göttingen, Germany) was used. The buffers (10 mM citrate pH 3.5, 4 and 5; 10 mM phosphate pH 6 and 7; and 10 mM bicarbonate pH 8 and 9 buffers) were prepared freshly and adjusted to the desired pH using 1 M HCl or 1 M NaOH and Fisherbrand accumet XL200 pH and conductivity meter (Fischer Scientific, Loughborough, UK).

2.2 Support and liquid handling

At all stages during the preparation and use, supports were recovered from solution by gentle centrifugation in VWR Mini Star (Radnor, PA, USA) or MSE MicroCentaur (Scientific Laboratory Supplied Ltd., Salford, Manchester, UK) microfuges operated at 1000 g for 5 minutes. Room temperature mixing operations were done with a VM20 vortex mixer, or a Revolver™ Adjustable Lab Rotator (Labnet International Inc., Edison, NJ, USA) with attachments for 1.5 and 5 mL Eppendorf tubes, rotating at 20 rpm, and temperature-controlled mixing was carried out in an Eppendorf® Thermomixer Comfort heater (Sigma Aldrich, Poole, Dorset, UK) fitted with a shaker rack for 1.5 mL Eppendorf vials, and operated at 900 rpm.

2.3 Methods of polymer brush preparation

2.3.1 Tresyl activation of Praesto® 45

Praesto® Pure 45 beads (1 mL drained) were into dry acetone by sequential washing with 5 mL portions of deionised water (3×), 30% (v/v) acetone in water (1×), 70% (v/v) acetone in water (1×), and dry acetone (3×), before drying in a fume hood.

Subsequently portions of the dried supports (90 mg dry weight from 1 mL) were suspended in 1 mL aliquots of dry acetone, to which 0.5 mL of dry pyridine and (40 – 270 μL) of tresyl chloride were added. After mixing in the dark at room temperature for 2 h, the tresyl activated beads were separated from solution and washed three times with 1 mL volumes of dry acetone, and then air dried in a fume cupboard.

2.3.2 PEL grafting on Toyopearl® AF-Tresyl-650M and tresyl-activated Praesto® 45

Routinely 5 mg portions of dry tresylated-supports were swollen in 1 mL of deionised water for 1 h, and then exchanged into dry acetone by draining off the water, and washing 3× with 1 mL changes of dry acetone for 15 min. One millilitre portions of dry acetone containing various amounts of amine or thiol terminated polymers (2 – 15 mg) were then added to supports recovered from the third dry acetone wash and the reaction cocktails were mixed at room temperature for 48 h. At the end of the reactions the supernatants were removed and retained for analysis of residual polymer content, and the polymer grafted supports were washed 3 times with dry acetone to remove traces of unreacted polymers, and then air dried. In case of mixed PEL grafting, the second polymer solution (1 mL dry acetone containing 2 – 8 mg polymer) was added to supports just grafted with the first polymer chain, and the reaction mixtures were incubated for a further 48 h, at ambient temperature with shaking. The reaction supernatants

were kept for later analysis of remaining second polymer, and the mixed PEL grafted supports were rinsed 3× by resuspension in dry acetone and dried in a fume hood.

2.3.3 Blocking of unreacted tresyl chloride groups and de-protection of cation ion exchange polymer brushes

Unreacted tresyl functions on homo and mixed PEL brush grafted were blocked by reaction with ethanolamine. For this the supports were rehydrated in with 1 mL of 1 M ethanolamine pH 8.5 and incubated in thermomixer operated at 40 ºC and 900 rpm for 24 h, and then rinsed 5× with 1 mL portions of deionised water.

After blocking with ethanolamine homo and mixed PEL supports grafted with P*t*BMA were de-protected by hydrolysis in 1 mL 50% (v/v) of TFA in water for 24 h at 40 ºC (Willett, 2009), and then washed copiously with deionised water (5× 1 mL) at ambient temperature. In some experiments with P*t*BMA coupled supports de-protection was conducted before blocking with ethanolamine. The resulting PMAA-grafted supports were tested for lysozyme binding and no significant difference from the supports which was blocked before de-protecting, was observed (Appendix 7.1).

For homo and mixed PEL supports coupled with PMMA de-protection was only done after blocking with ethanolamine and a different procedure was used. The supports at 60 ºC for 6 h in 1 mL of solution of 0.5 M NaOH in 50% (v/v) ethanol (Patel *et al.*, 2006; Clarke, 2017). After cooling to room temperature, the supports were washed with deionised water (5× 1 mL).

2.4 Testing of supports

2.4.1 Static protein binding and elution

PEL modified supports (20 μL) were equilibrated in 10 mM strength binding buffers of the desired pH (citrate pH 3.5, 4 and 5; phosphate pH 6 and 7; and bicarbonate pH 8 and 9) for 1 h, then separated and mixed at room temperature with 1 mL of 1 mg/mL protein solutions (prepared in the same buffers) for 2 h. At the end of incubation, the adsorbents were separated and the supernatants analysed for residual protein content. The protein bound to the supports was determined from the difference between the protein concentration in the starting binding solution and the supernatant after binding. In some experiments, protein-loaded supports were washed once with 1 mL of binding buffer for 15 min, before performing elution with a new buffer with a pH one, two or three units away from that used in the binding step. The wash and elution fractions were subjected to analysis for protein content, and elution efficiencies were calculated.

2.4.2 Column chromatography

A fixed bed (0.94 mL, bed height = 4.8 cm) of a mixed PEL-Toyopearl adsorbent (B-Mix 10) contained in Tricorn 5/50 (GE Healthcare Bioscience, Uppsala, Sweden) (internal diameter = 5 mm and column height = 50 mm) chromatography column was prepared according to manufacturer's instructions. The packing quality of the bed was inspected after packing and a peak asymetry factor of 0.99 was recorded. Note, the acceptable range is 0.8 – 1.8 and a value of 1.0 indicates a perfectly symmetrical peak (see Appendix 7.2). The column was connected to an ÄKTA Explorer 100 system controlled by UNICORN 5.1 software (GE Healthcare Bioscience, Uppsala, Sweden) and was operated under downward flow throughout with a constant flow rate of 0.3 mL/min (~92 cm/h). The bed was equilibrated with 5 column volumes

(CVs) of either 10 mM sodium citrate pH 4 or 10 mM sodium phosphate pH 7, before loading 125 µL samples of protein in equilibration/loading buffer, and washing with 10 CVs of loading buffer. Elution was performed using pH step gradients across 3 units of pH. When loading and washing had been done at pH 4, elution was conducted of 10 mM phosphate pH 7, and regeneration with 10 mM NaOH. Conversely, after loading and washing had been performed at pH 7, 10 mM citrate pH 4 was employed for elution, and 10 mM citric acid was used for regenerating the bed. Flow exiting the column was continuously monitored in-line for UV absorbance at 280 nm and pH, and collected fractions were subjected to the BCA assay for protein content and reducing LDS-PAGE for protein identification.

2.5 Analysis and characterisation methods

2.5.1 Extent of tresylation detected by TNBS assay

Samples of tresyl activated-supports (5 mg for Toyopearl® AF-Tresyl-650M) were aminated by reacting with 30% NH_4OH in water (1 mL) for 1 h at room temperature (Figure 2-1).

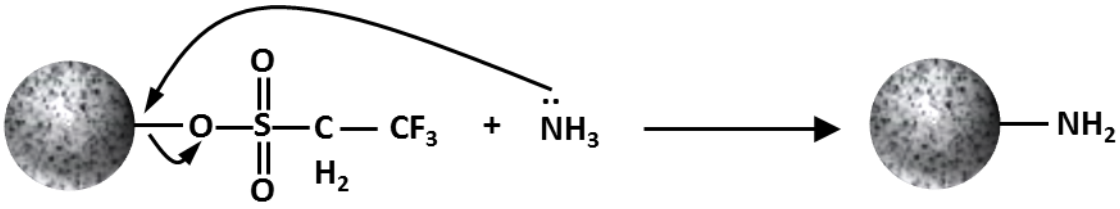

Figure 2-1 Amination of tresyl-activated support.

After rinsing 5× with deionised water aminated supports (5 mg) were mixed with 1.51 mL portions of a solution containing 0.33 mM $Na_2B_2O_7$ and 6.62 mM 2,4,6-trinitrobenzene sulphonic acid (TNBS) at 70 ºC for 1 h (Figure 2-2) as described by Halling and Dunnill (1979) before cooling to room temperature.

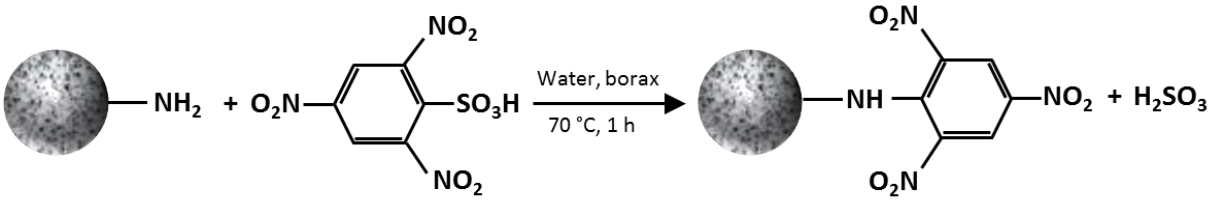

Figure 2-2 Coupling of TNBS to aminated support.

The supernatants were removed, and the supports were copiously washed with water (5×1 mL), before incubating in (1 mL) 1 M NaOH at 70ºC for 1 h to release picric acid into the bulk phase (Figure 2-3).

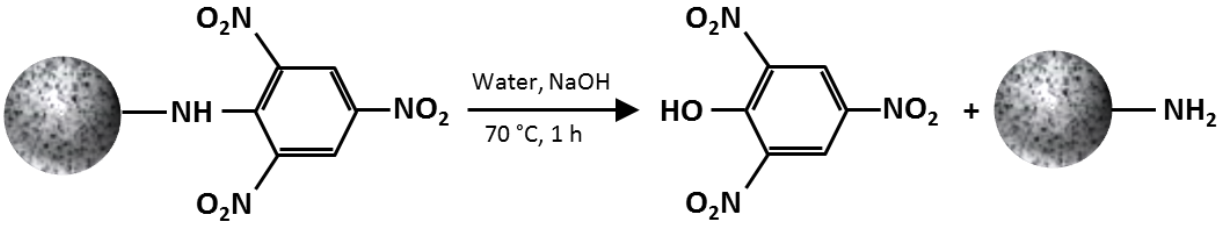

Figure 2-3 Release of picric acid.

After cooling to room temperature, the picric acid concentrations of supernatants were determined from the absorbance at 410 nm with reference to a calibration curve constructed using picric acid in 1 M NaOH (Appendix7.3). Tresyl activated-supports that had not been aminated were used as controls for non-specific reaction or binding, which was very low.

2.5.2 Orange II assay

At acidic pH values, Orange II is negatively charged and can interact electrostatically with positively charged groups (e.g. the protonated amine of aminated supports and protonated pyridines in P2VP chains). On switching to basic pH previously bound Orange II is released into the bulk phase (Noel *et al.*, 2011). Thus, in principle this assay can be employed to detect residual surface amine functions after grafting P*t*BMA or PMMA, or alternatively to assess P2VP loadings on supports. In the assay adapted from Noel *et al.* (2011), 5 mg of supports were

mixed with 1 mL of an acidic aqueous solution of Orange II (1.4 mg/mL, pH 3) and incubated at 40 °C for 1 h. After removing the excess Orange II solution, the supports were rinsed 5× with acidic solution (deionised water adjusted to pH 3) or until no colour was detected in the supernatants. One millilitre of alkaline solution (water adjusted to pH 12) was then added to each support sample and mixed at room temperature. After 15 min incubation, the supernatant absorbance at 484 nm was converted into Orange II concentration by reference to a standard calibration curve (Appendix7.4).

2.5.3 Elemental analysis for sulphur content

For determination of the extent of tresyl activation of Praesto® 45, the cross-linked beaded structure was dissolved by heating 100 μL samples of tresyl-activated Praesto® 45 with 2% (v/v) nitric acid in water at 90 ºC for 2 h, cooled, filtered through a 0.22 μm filter and then analysed for sulphur content by inductively coupled plasma - optical emission spectrometry (ICP-OES) in an Optima 8000 spectrometer (PerkinElmer, Inc., MA, USA) with reference to a standard curve constructed using 'Sulphur Standard for ICP TraceCERT®'solution (Appendix7.5).

2.5.4 Fourier-transform infrared spectroscopy (FTIR)

FT-IR analysis was employed quantitatively on liquid samples and qualitatively for direct detection of chemical changes introduced into Toyopearl® AF-Tresyl-650M and Praesto® 45 media at different points in the fabrication of homo and mixed PEL supports. Liquid samples (e.g. reaction supernatants after polymer coupling) were evaporated at 70 ºC for 15 min. The dry residues were then dissolved in 1-butanol for P2VP and P*t*BMA, and in DMSO for PMMA. The samples were subsequently analysed with a Nicolet 380 FT-IR fitted with Smart 53 Orbit diamond accessory. Samples (25 μL) were pipetted on to diamond plate and then scanned 64×

in Attenuated Total Reflection (ATR) mode and averaged at a resolution of 2 cm^{-1}. Spectra for 1-butanol and DMSO were recorded and subtracted from those of samples, and specific peaks for both P2VP and P*t*BMA were selected for quantification purposes. Individual standard curves were constructed for each polymer type and standards were prepared in the same way as samples (Appendix7.6). The amounts of polymers grafted on supports were computed from the differences in calculated concentrations before and after coupling reactions. For qualitative analysis of solid samples, supports were washed with acetone, and then were dried in a fume hood. Small amounts (~2 mg) were then combined with KBr (198 mg), ground to fine powders in agate mortar, dried overnight in a 60 ºC oven before compressing into FTIR suitable tablets using a Specac™ Atlas™ manual 15 T hydraulic press (Model GS15011, Specac Ltd, Orpington, Kent, UK). Each sample was scanned 64× at 2 cm^{-1} resolution, and the averaged spectra were compared with those of FTIR tablets made by combining the free polymers ('no support') with KBr.

2.5.5 Gravimetric analysis

Gravimetric measurements were employed routinely for determining the polymer loadings on chromatography supports following polymer grafting reactions. 30 – 50 mg quantities of dried supports (tresyl activated and those grafted with the first polymer) contained in Eppendorf tubes were accurately weighed in an Ohaus Pioneer PA114C analytical balance (Ohaus Inc., Parsippany, NJ, USA). After grafting reactions, extensive washing with dry acetone and drying to constant mass, the masses of grafted polymer on the same supports were calculated from the gains in mass; and in the case of mixed PEL supports, the masses of the two polymer chain types were used to calculate brush compositions. Gravimetry was also used to establish relationships between dry masses and suction drained bed volumes of unmodified and polymer grafted media.

2.5.6 Zeta potential measurements

Zeta potential measurements for each support sample were conducted using a Malvern Zetasizer Nano ZS (Malvern Instruments, Malvern, Worcs, UK). Five milligram samples of each support were equilibrated in 1 mL of different buffers ranging in pH from 3.5 to 9 for 1 h. Nine hundred microlitre aliquots of each support suspension were pipetted into a re-useable folded capillary zeta cell (DTS1061, Malvern Instruments) and measured for at least 8 runs for each measurement. Three consistent results were obtained from which mean zeta potentials ± standard deviations were calculated.

2.5.7 Sedimentation rate

Five milligram amounts of various supports were equilibrated in buffers of different pH for 1 h. Nine hundred microlitre portions of each suspension were then pipetted in disposable Sarstedt® semi-micro acrylic cuvettes (Sarsted Ltd, Leicester, Leics, UK) and immediately inserted in the light path of an Thermo Scientific™ Evolution™ 300 UV-vis spectrophotometer (Thermo Fischer Scientific, Waltham, MA, USA), and the absorbance at 400 nm was recorded every 5 s for 200 s. For each sample, three such measurements were made, and the averaged 'absorbance versus time' traces were plotted in each case.

2.5.8 Environmental scanning electron microscopy (E-SEM)

The modified adsorbents were visualised by E-SEM with the assistance of Theresa Morris from the School of Metallurgy & Materials, University of Birmingham. After polymer grafting, the adsorbents were exchanged and dehydrated by sequential resuspension in increasing concentrations of methanol in water (50%, 70%, 80% and 95% v/v) and then finally in pure anhydrous methanol. The adsorbent beads were mounted on aluminium stubs before critical point drying and sputter coating with a thin layer of platinum to reduce the effect of charging

and improve imaging contrast. The samples were imaged in a Philips XL-30 FEG Environmental Scanning Electron Microscope (FEI Company, OR, USA).

2.5.9 Fluorescence imaging of PEL modified adsorbents

Fluorophore-tagged proteins for use in fluorescence imaging of PEL modified chromatography adsorbents were prepared as described by Joseph (2019). The proteins, BSA and hen egg white lysozyme, were dissolved in 0.1 M sodium bicarbonate buffer pH 8.3, and the fluorescent dye probes, Texas Red-X® and Cy5™, were dissolved in DMSO to a concentration of 1 mg/mL. BSA and lysozyme were respectively conjugated with Texas Red-X® and Cy5™; in both cases, a molar dye/protein ratio of 1:50 was used. The solutions were mixed for 1 h at room temperature whilst protected from light. After reaction, dye conjugated proteins were purified using a gravity fed gel filtration protocol recommended by GE Healthcare employing PD-10 desalting columns packed with Sephadex™ G-25 'Medium' resin (GE Healthcare, Uppsala, Sweden). Aliquots of reaction mixtures (2.5 mL) were applied to columns previously equilibrated with 25 mL of an appropriate running buffer (i.e. 10 mM citrate pH 5 for BSA, 10 mM bicarbonate pH 9 for lysozyme). After sample application the columns were supplied with discrete 0.7 mL portions of running buffer. Collected fractions (0.7 mL) were analysed for absorbance at 280 nm (as a measure of protein), 595 nm (for Texas Red-X®) and 647 nm (for Cy5™), and those containing both dye and protein (elution volume, V_e = 0.7 – 3.5 mL) were pooled. Chromatograms were plotted and the degree of conjugation was determined (Appendix7.8).

PEL grafted supports (previously equilibrated for 1 h with binding buffer, i.e. 10 mM citrate pH 5 or 10 mM bicarbonate pH 9) were incubated with Texas Red-X® labelled BSA or Cy5™ labelled lysozyme for 2 h, and were then recovered from solution and washed 3× with the

binding buffer. The matrices were re-suspended in the same buffer, and 5 µL aliquots were pipetted onto microscope slides, before applying a coverslip and analysing at 40× magnification (oil immersion) in a confocal laser scanning microscope (CLSM) (Leica TCS SPE 102A, Leica Microsystems, GmbH, Mannheim, Germany) equipped with krypton/argon (λ = 488 nm and λ = 568 nm) and helium/neon lasers (λ = 633 nm). For experiments with Texas Red-X® ($\lambda_{excitation}$ = 596 nm, $\lambda_{emission}$ =615 nm) and Cy5™ ($\lambda_{excitation}$ = 646 nm, $\lambda_{emission}$ = 666 nm) support samples were respectively excited with the 568 nm and 633 nm lasers. Leica Application Suite (LAS X) software, Version 1.9 (Leica Microsystems, GmbH) was used to capture and process acquired images.

2.5.10 Determination of protein content

The bicinchoninic acid (BCA) assay was used for the determination of protein contents in samples, and the manufacturer's protocol was implemented. Briefly, 200 µL aliquots of BCA solution were mixed with 25 µL samples and then incubated at 37 ºC for 0.5 h, before measuring the absorbance at 562 nm in an Evolution™ 300 UV-vis spectrophotometer. The absorbance was converted into protein concentration by reference to a standard calibration curve (Appendix7.9) constructed using bovine serum albumin (BSA). Three measurements of each sample were taken to determine a mean concentration ± standard deviation in each case.

2.5.11 Polyacrylamide gel electrophoresis (PAGE)

Protein samples for reducing lithium dodecyl sulphate polyacrylamide gel electrophoresis (LDS–PAGE) were prepared by mixing 10 µL of each sample with NuPAGE® LDS sample buffer (5 µL), NuPAGE® reducing agent (2 µL), and deionised water (3 µL). The mixtures were heated at 70 ºC for 10 min, cooled down to room temperature and centrifuged.

Pre-cast NuPAGE Bis-Tris 4-12% gels (Life Technologies, CA, USA) were placed in a mini-gel tank, containing NuPAGE MES running buffer (after removing the comb and the white tape near the bottom of the gel cassette and rinsing the gel 3× with running buffer). Samples (typically 10 µL) and SeeBlue® Plus2 pre-stained protein markers (Life Technologies, CA, USA) were loaded in to individual wells of gels, before filling running buffer to the mark, adding 0.5 mL of antioxidant solution to the chamber, and connecting the mini-gel tank to the power supply. Electrophoresis was performed at 180 V constant voltages until the dye front left the gel. The tank was then disassembled, and the gel carefully transferred to a shallow container containing 50 mL of deionised water on a shaking platform. After three changes (5 min each), the water was replaced with 25 mL of SimpleBlue® SafeStain and gentle shaking was continued for 3 h. Thereafter, the recovered gels were rinsed briefly (3× 5 min each with shaking), before destaining overnight by shaking in 25 mL of deionised water. Immediately before scanning gels at 2400 dpi on a HP ScanJet C7716A flat bed scanner (Hewlett-Packard Company, Palo Alto, CA, USA) they were rinsed with deionised water one final time. Captured images were analysed using ImageJ software (Schneider *et al.*, 2012).

Chapter 3 Fabrication and characterisation of homo PEL brush modified Toyopearl

3.1 Introduction

Ion exchange chromatography has been regarded as the most widely used technique for bioseparation (Goheen and Gibbins, 2000; Asenjo and Andrews, 2009). This technique is based on charge interaction between oppositely charged protein and stationary phase, which can be varied by changing mobile phase's ionic strength or pH. This allows high loading capacity and high-resolution separations of molecules with differences in pI (Cummins *et al.*, 2011; Karlsson, 2011). However, to achieve high recovery of desired biomolecules, it requires high ionic strength of mobile phase to effectively elute the bound protein. Thus, this leads to low productivity, high cost from excessive waste generated from high salt solution, and non-environmental friendly (Durham *et al.*, 2004; Przybycien *et al.*, 2004; Maharjan *et al.*, 2008). To compensate these issues, improvement of ion exchange chromatography is required.

Polyelectrolyte (PEL) brush, one of smart polymer applications, has been extensively studied and applied in many fields, including bioseparation (Ballauff and Borisov, 2006; Minko, 2006; Ballauff, 2007). PEL brush can be formed by grafting high density of polymer chains, possessing ionisable groups, on a surface and is able to change its surface charges in response to environmental ionic strength or pH (Zhao and Zhang, 2014). If two oppositely charged polymer chains are grafted, mixed PEL brush can be formed. This mixed PEL brush can display both anion exchange and cation exchange properties, which is a great advantage to employ in an ion exchange chromatography for bioseparation applications.

Mixed PEL brush have been fabricated on a flat surface and extensively analysed by one research group. Poly(acrylic acid) (PAA) and poly(2-vinylpyridine) (P2VP) have been first fabricated on a silicon wafer to create mixed PEL brush surface (Houbenov *et al.*, 2003). The surface has been broadly investigated using different techniques, including zeta potential

measurement, contact angle measurement, infrared in situ ellipsometry, etc., as a function of pH (Houbenov *et al.*, 2003; Mikhaylova *et al.*, 2007; Hinrichs *et al.*, 2009). From these exclusive characterisations, they were all agreed that this mixed PEL brush have been exhibited pH-switchable behaviour and a schematic model was proposed: In a low-pH environment, P2VP chains were protonated and extended while PAA chains were collapsed. Conversely, in a high pH environment PAA chains were ionised and extended while P2VP chains were collapsed. In the intermediate 4-7 pH range, both components had partially ionised groups and as a result, a PEL complex was formed (Figure 1-8).

Mixed PEL brush has not only been fabricated on the flat surface, but it was also successfully grafted on a non-porous adsorbent (Willett, 2009). A series of mixed PEL brush has been fabricated on the magnetic nanoparticles, called M-PVA, using both 'grafting from' and 'grafting to' method. In this study, poly(methacrylic acid) (PMAA) (pK_a = 6.4) (Santonicola *et al.*, 2010) was applied, instead of PAA (pK_a = 4.5) (Wittemann *et al.*, 2003). The replacement with weaker polyacid PMAA aimed at narrowing the operational pH range into more neutral pH which is more practical to apply in protein separation. This research achieved fabricating the dense layer of mixed PEL brush onto the supports by both grafting techniques. These mixed PEL brush supports were attainable to selectively bind the proteins as a function of pH, elute the bound protein by pH shifting, and possess the reversible versatility of both anionic and cationic exchanger. This study shows promising results to apply this mixed PEL brush on a porous chromatography matrix.

In order to accomplish high density of PEL brush on surfaces, 'grafting from' method has been mostly used because it avoids steric hindrance limitation (Ejaz *et al.*, 2002; Liu and Liang, 2018). However, 'grafting to' has benefits over 'grafting from' methods due to its simplicity and controllability of polymer chain length before grafting process. Furthermore, there is a way

to overcome the steric limitation by supplying high concentration of polymer solution that can force polymer chains to pass through to surface's active sites (Taylor and Jones, 2010). The 'grafting to' approach involves reaction between terminal end groups of polymer chains and active sites on substrate surface, forming chemically covalent bond. This allows thermally and chemically stable bond which is suitable for further application.

One of conventional methods to couple ligands with base chromatography matrix is using sulphonyl chlorides, which are sulphonic acid derivatives consisting of a SO_2Cl group bonded to an aliphatic chain or an aromatic ring. The sulphonyl chlorides are reactive for nucleophilic functional groups, including amine and thiol groups. The most commonly used sulphonyl chlorides is 2,2,2-trifluoroethanesulphonyl chloride (tresyl chloride), which was reported in many studies for successful coupling with ligands via a nucleophilic substitution reaction (Nilsson and Mosbach, 1981; Scouten *et al.*, 1986; Demiroglou *et al.*, 1994). This approach can be applied in the 'grafting to' method by coupling tresyl chloride activated base matrix with amine or thiol terminated end groups of polymer chains (Figure 3-1).

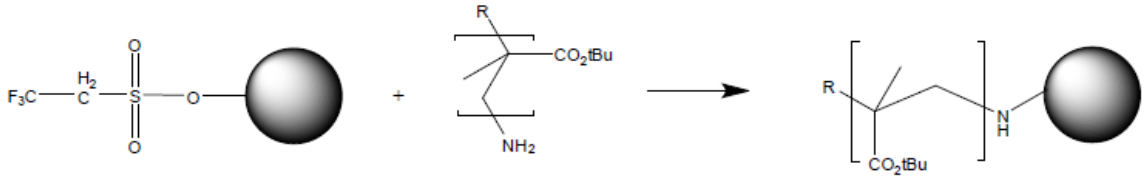

Tresylated support | Amine-terminated polymer | Polymer grafted support

Figure 3-1 Reaction of nucleophile terminated polymer with tresylated support.

In this chapter, we first optimise the grafting and de-protection process by applying the similar chemistry from the previous work, done in non-porous adsorbent, to a pre-activated porous methacrylate base matrix, Toyopearl. Second, we make homo PMAA and P2VP brush modified

porous supports and characterise these supports, in term of physicochemical test and functional test, to obtain constructive groundwork for fabrication of mixed PEL brush supports.

3.2 Results and discussion

3.2.1 Optimisation of polymer grafting reaction

To achieve suitable polymer grafting condition, P2VP was first used for testing. Acetone was used as a solvent of choice and reaction time was 24 hours according to previous study (Willett, 2009). The concentration of P2VP solution for grafting reaction was varied to find the effect of concentration to grafting density. TNBS and Orange II assays were performed to confirm grafting process. The TNBS reaction was used to detect surface amine groups after coupling with tresyl chloride groups. Thus, the TNBS assay indirectly determines degree of tresylation the support surface. The degree of tresylation of Toyopearl was 10.56 $\pm$ 0.38 μmol/mL support according to picric acid release. Reduction of picric acid release from TNBS assay shows that the higher the supplied P2VP, the higher the decrease in picric acid release (Figure 3-2). This indicates higher amount of P2VP attached to the support because less tresyl chloride groups were available for amination and subsequent TNBS reaction. This agreed with the result from Orange II assay that increase of Orange II release shows higher P2VP chains on the surface, which was based on charge interaction between Orange II and protonated amine groups (Figure 3-2). These emphasise importance of high polymer concentration to obtain high grafting density.

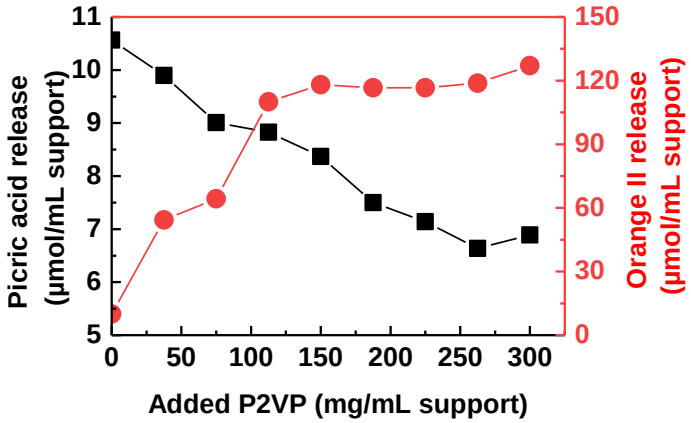

Figure 3-2 Influence of supplied P2VP in 'grafting to' reaction with tresylated Toyopearl supports on extent of surface reactive amine displayed as picric acid release (black squares) and amine content on the supports determined by Orange II release (red circles).

The optimal grafting time of 24 hours was previously employed for the non-porous magnetic adsorbent (Willett, 2009). However, with a porous polymethacrylate-based support, Toyopearl, polymer might require more reaction time to penetrate and diffuse to the active sites. The grafting time was optimised first by using constant P2VP concentration of 200 mg/mL support. The result shows that 48 hours was the best reaction time and improve grafting density approximately two times (Figure 3-3). Increasing reaction time to 72 hours has not had significant effect. Additionally, the plot of supplied P2VP vs reduction of picric acid release for 48 hours reaction time shows similar behaviour to that for 24 hours, but around twice higher grafting density was observed in all concentration points (Figure 3-3). From these results, the grafting time of 48 hours was applied throughout this research.

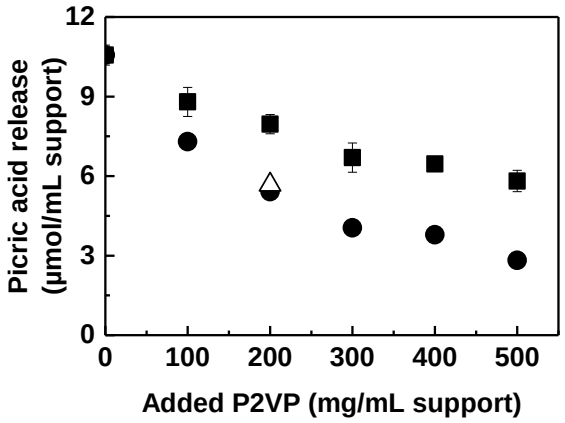

Figure 3-3 Effect of grafting time on surface amine content expressed as picric acid release. Key: 24 h (close squares); 48 h (close circles); and 72 h (open triangles).

The P2VP used in previous study and this research has molecular weight of 13,200 (DP = 126). The monomer size of P2VP is 0.67 nm (Seo *et al.*, 2004), so the actual length of P2VP chain is 84.42 nm. To match this length, P*t*BMA, a protected form of PMAA, has to possess approximately two times larger molecular weight (MW = 29000, DP = 204) because the monomer size of P*t*BMA is 0.33 nm (Hester *et al.*, 2002). Therefore, suitable solvent for P*t*BMA had been investigated. P*t*BMA in acetone, DMF, and THF with different concentrations was supplied to the support. The P*t*BMA solutions before and after grafting were analysed by ATR-FTIR and mass balance was applied to find the grafted amount of P*t*BMA on the support. The grafted P*t*BMA from DMF solutions showed fluctuation when increasing supply concentration (Figure 3-4). This indicates that DMF was not a good solvent for P*t*BMA. The grafted P*t*BMA from both THF and acetone were increased with higher added P*t*BMA concentrations. Thus, both solvents looked promising for P*t*BMA grafting. Since P*t*BMA in acetone performance was slightly better, acetone was selected as a solvent of choice for grafting P*t*BMA. Moreover, using acetone for both P2VP and P*t*BMA is for ease in manufacturing mixed PEL brush modified support.

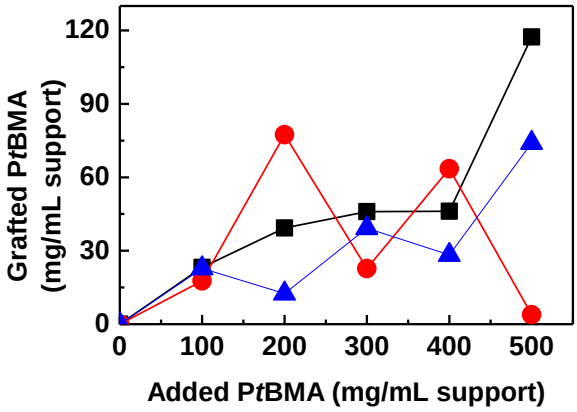

Figure 3-4 Influence of reaction solvent on P*t*BMA grafting to tresylated Toyopearl supports. Key: acetone (black squares); DMF (red circles); and THF (blue triangles). The tresylated Toyopearl supports were mixed with P*t*BMA in acetone (2, 4, 6, 8, and 10 mg/mL) at room temperature for 48 hs.

The grafting reaction with P*t*BMA in acetone was additionally tested by TNBS and Orange II assays. The reduction in picric acid and Orange II releases was observed with increasing P*t*BMA supplied concentrations (Figure 3-5). Low numbers in reduction of picric acid release were likely from interaction between tertiary butyl ester groups with ammonia during amination. This may create amide groups, which may interfere with the TNBS reaction (Willett, 2009). However, this reaction did not affect Orange II assay, which was based on charge interaction between free primary amine groups on surface and Orange II. This Orange II assay used in P*t*BMA was similar with that in P2VP, but it is for indirectly detecting remained tresyl sites on the support, not for the polymer itself. Despite detecting different parameters from the assay, the results similarly demonstrate that the higher the supplied concentration, the higher the grafted polymers. Thus, acetone was confirmed as the optimal solvent for grafting P*t*BMA.

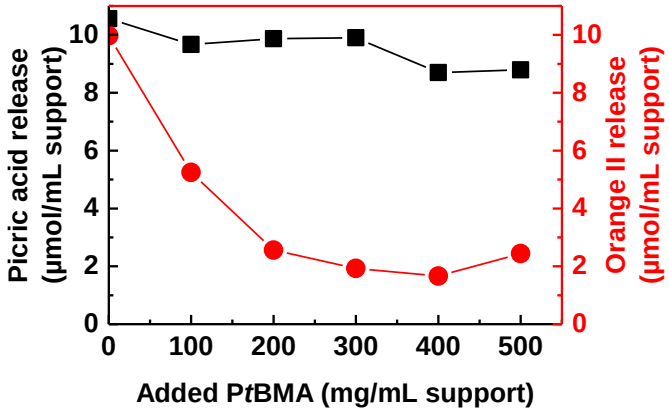

Figure 3-5 Influence of P*t*BMA supplied in 'grafting to' reaction with tresylated Toyopearl supports on immobilised reactive amine content determined by TNBS (black squares) and Orange II (red circles) assays.

3.2.2 Fabrication and characterisation of homo PEL brush grafted support

After grafting reaction was performed, the success of grafted P2VP and P*t*BMA on the tresylated support was confirmed by the FTIR spectrum (Figure 3-6). The peaks for tresylated Toyopearl support were assigned as following; 1728 cm^{-1} for carbonyl (ester) C=O, 1478 and 1255 cm^{-1} for methyl $–CH_3$, 1139 cm^{-1} for ester C-O, and 752 and 697 cm^{-1} for methylene $–(CH_2)_n-$ (Clayden *et al.*, 2012; Solomons *et al.*, 2017). In P*t*BMA grafted support, the additional peaks at 1450 and the doublet at 1399 and 1366 cm^{-1}, corresponding to the *tert*-butyl group, were observed (Iacono and Heise, 2015). The unique new peaks relating to P2VP was clearly visible at 877 cm^{-1} for aromatic C-C bonds, also 1450 and 1600 cm^{-1}, corresponding to aromatic C-H bonds (Coates, 2006; Nowak *et al.*, 2016). Additionally, the growth of peak heights at 752 and 697 cm^{-1} was detected in both P*t*BMA- and P2VP-grafted adsorbents due to increase in methylene $–(CH_2)_n-$ from the polymers backbone (Coates, 2006).

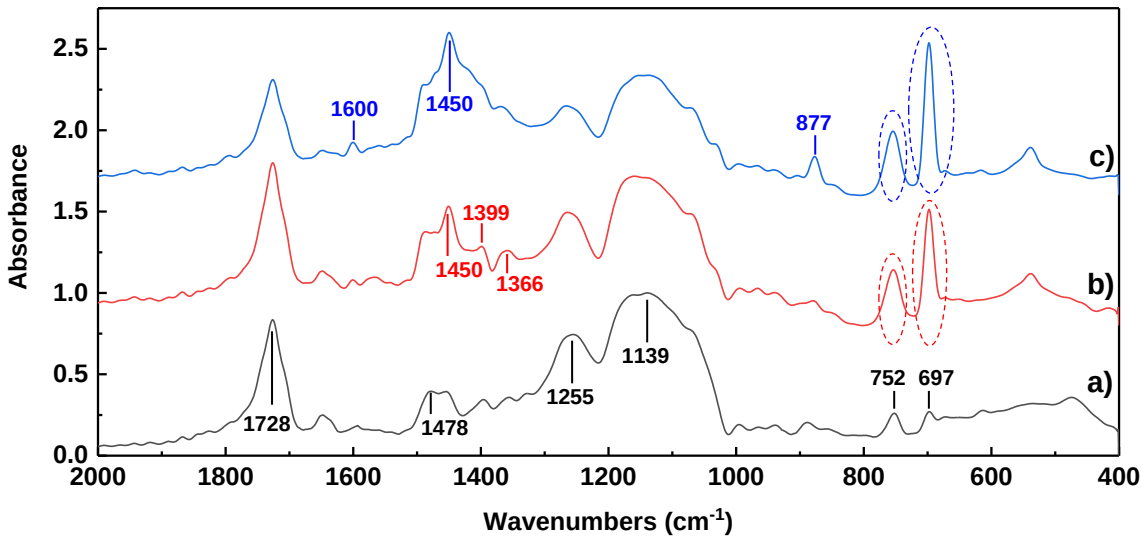

Figure 3-6 FTIR spectrum of a) Toyopearl, b) P*t*BMA-grafted Toyopearl, c) P2VP-grafted Toyopearl.

The polymer grafted supports were imaged by E-SEM to investigate surface morphology (Figure 3-7). The images obtained from E-SEM show differences between the surfaces of tresylated Toyopearl support, P2VP-grafted Toyopearl support, and P*t*BMA-grafted Toyopearl support. The grafted supports had thicker structures than the un-grafted support that indicates attached polymers on the supports. Slightly thicker grafted P*t*BMA support was observed comparing to the P2VP one because of larger molecular weight of P*t*BMA.

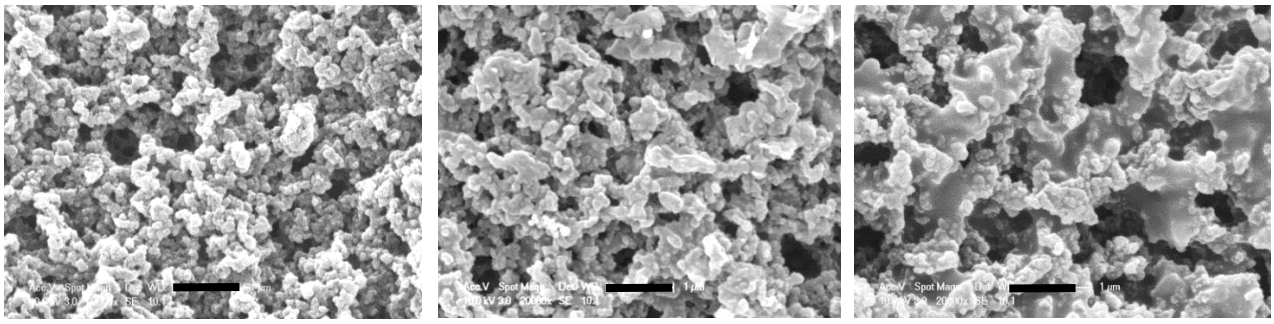

Figure 3-7 SEM images of Toyopearl (left), P2VP-grafted Toyopearl (middle), and P*t*BMA-grafted Toyopearl (right). Each scale bar represents 1 μm.

The grafted P*t*BMA must be de-protected to liberate PMAA brush. De-protection by 50% aqueous TFA was tested by solid FTIR. The spectrum of de-protected P*t*BMA (Figure 3-8) showed loss or reduction of the specific peaks for P*t*BMA, including 1399 and 1366 cm^{-1} for the *tert*-butyl group; 1255 cm^{-1} for methyl $–CH_3$; 1147 cm^{-1} for ester C-O, suggesting formation of PMAA. The peak at 1728 cm^{-1}, corresponding to carbonyl (ester) C=O, was remain, but smaller and broader, indicating a shift to the delocalised (carboxylic acid) C=O (Akkahat and Hoven, 2011; Lei *et al.*, 2014; Banerjee *et al.*, 2016).

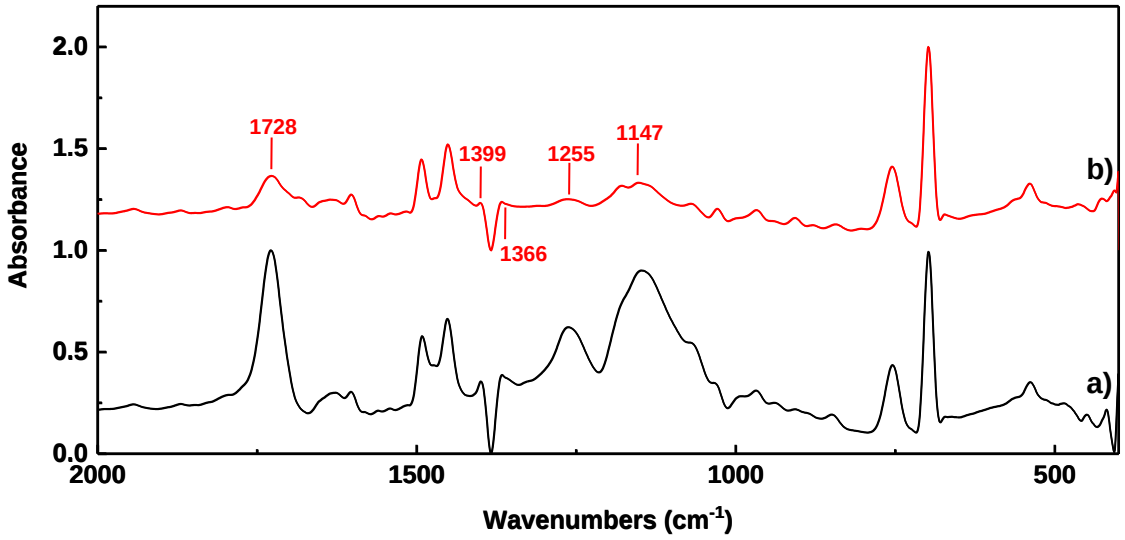

Figure 3-8 FTIR spectrum of a) P*t*BMA-grafted Toyopearl, and b) P*t*BMA-grafted Toyopearl after de-protection by 50% TFA at 40 °C for 24 h.

After de-protection, lysozyme binding of P*t*BMA- and hydrolysed P*t*BMA-grafted adsorbents was performed at pH 9, where PMAA is expected to ionise and lysozyme possesses positive charges, to confirm degree of hydrolysis. The result showed that lysozyme bound of the hydrolysed support was approximately 6 times higher than the non-hydrolysed one (Figure 3-9). This result was quite comparable to the one from the binding study between α-chymotrypsin, a basic protein, with PAA and non-hydrolysed form, PBA, grafted substrate (Uhlmann *et al.*,

2007). This suggests the good de-protection process, reflected from ionised PMAA bound with lysozyme.

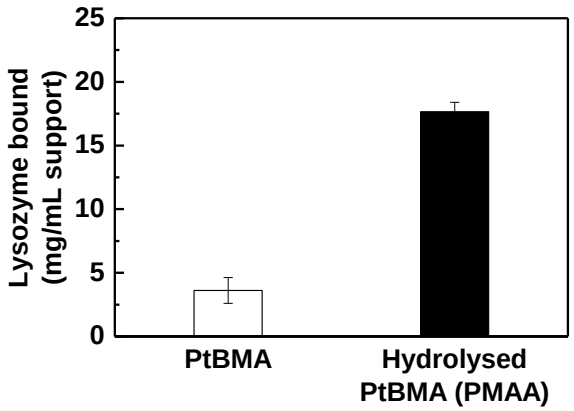

Figure 3-9 Static lysozyme binding of P*t*BMA- and hydrolysed P*t*BMA-grafted supports.

To quantify amount of polymer grafted on the support, gravimetric analysis was used. Supplied polymer amount was varied to find the maximum grafted amount. Due to limited solubility of polymers, two different percentages of slurry in grafting reaction were employed to achieve higher ratio of mg polymers per mL support. The result showed that both P*t*BMA and P2VP grafted matrices shared similar trend in grafting. Plateau phases were observed in both materials indicating the maximum grafting had been reached (Figure 3-10). However, grafting densities were different. Higher grafting densities were noted for P2VP. A possible explanation for this might be that smaller molecular weight, P2VP, is more soluble than larger molecular weight, P*t*BMA. For P*t*BMA chains, the maximum grafted amount of 17.5 mg/mL support was initially observed at 75 mg/mL support of supply concentration and was quite constant until the maximum supply, whereas 35 mg/mL support of P2VP grafted was obtained at supply of 300 mg/mL support. The later plateau phase from the P2VP grafted support also suggests the advantage of higher solubility and smaller sizes. This small size polymer was more likely to penetrate between grafted polymer chains and reach the active sites. It was also reported that

P2VP chains had high affinity to the substrate comparing to PAA chains, which is quite similar chemistry to PMAA (Houbenov, 2005).

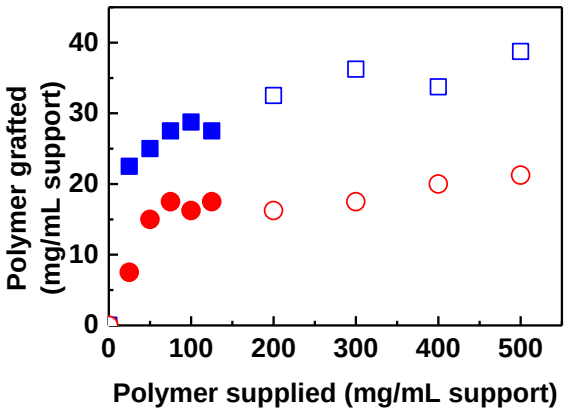

Figure 3-10 Calibration curve of PEL loading for P2VP-grafted support (close and open squares), and P*t*BMA-grafted support (close and open circles). Close squares and circles represent 8% slurry, whereas open squares and circles represent 2% slurry.

Static protein binding studies were subsequently conducted using both homo PEL brush modified adsorbents to investigate relationship between loading PEL and protein binding. Model proteins applied in these studies were selected by its isoelectric point (pI). The pIs of proteins were screened by zeta potential measurement as a function of pH (Appendix 7.7) and the summarised net charge as a function of pH for each protein shown in Table 3-1. According to the studies of the mixed PEL brush on silicon wafers (Houbenov *et al.*, 2003), the pI of P2VP was 6.7. Thus, P2VP brush should be extended and protonated at pH below 6.7. In case of PAA brush, the pI is 3.2. However, PAA was replaced by PMAA in this research to shift the pI of the brush to more neutral. Thus, the pI is likely expected to be more than 4.9. From this expected pI, PMAA should be stretched and ionised at pH above 6. Based on the pIs of brushes and proteins, the protein binding study of P2VP brush was performed at pH 4 using pepsin as a model protein, whereas that of PMAA brush was conducted at pH 9 using lysozyme. Therefore, charge interaction between ion exchange supports, both AEX and CEX, and proteins can be expected.

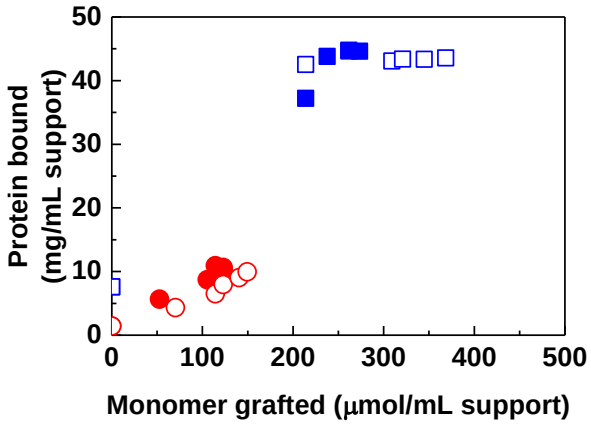

Figure 3-11 Protein bound against monomer grafted on the supports, P2VP-grafted support (close and open squares), and PMAA-grafted support (close and open circles). Close squares and circles represent 8% slurry, whereas open squares and circles represent 2% slurry.

The proteins bound was illustrated against monomer units grafted, calculated from degree of polymerisation for P2VP and PMAA, which is 126 and 204, respectively. As previously mentioned about lower solubility of P*t*BMA, this reflected in lower grafted monomers, further translated to lower protein binding capacity comparing to P2VP grafted support (figure 3-11). Despite higher loading of P2VP brush was achieved when increasing polymer supply, pepsin bound was not much different in each point even at the lowest point of monomer grafted. Regarding PMAA grafted support, there was not much influence of monomer grafted on lysozyme bound. These results offer a simple framework for manufacturing mixed PEL modified supports with varied PMAA: P2VP contents. These additionally provide the optimal P2VP and P*t*BMA supply of 100 and 75 mg/mL support, respectively, to obtain the maximum protein binding capacities with cost-effectiveness.

To assess distribution of PEL brush in the adsorbent, fluorescence images from confocal laser scanning microscopy (CLSM) were obtained by using fluorophore-tagged proteins as a probe. Due to protein conjugation with fluorescence dye must be done at basic pH, pepsin was replaced by BSA as a model protein and binding pH was adjusted to pH 5 to get maximum binding with

BSA. The images from Figure 3-12 suggest uniform binding of tagged proteins in both P2VP- and PMAA-grafted beads (Zhu *et al.*, 2018). This indicates good distribution of PEL chains throughout the beads.

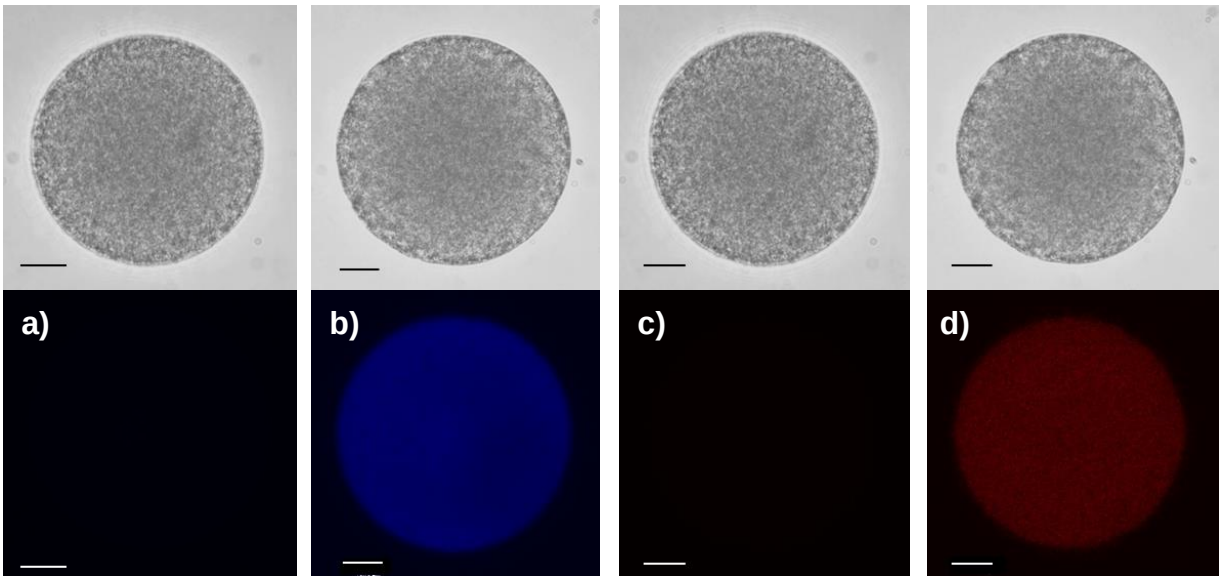

Figure 3-12 CLSM images of a) control and b) PMAA grafted Toyopearl bound with Cy5 tagged lysozyme, c) control and d) P2VP grafted Toyopearl bound with Texas red tagged BSA. Top images are the same supports analysed using a light microscope. Scale bar represents 20 μm.

3.2.3 Functional test

The static protein binding as a function of pH was studied to explore pH-responsive behaviour of both P2VP and PMAA brush modified supports. Different model proteins, based on their pI, were selected for testing. The zeta potential of proteins was measured as a function of pH to obtain pI (Appendix7.7). The pIs of proteins and net charge in different pH were summarised in Table 3.1.

Table 3-1 Net charge of model proteins from zeta potential measurements, used in the protein binding studies.

Protein	pI	Net charge at						
		pH 3.5	pH 4	pH 5	pH 6	pH 7	pH 8	pH 9
Pepsin	3.0	-ve	-ve	-ve	-ve	-ve	-ve	-ve
Amyloglucosidase	3.5	neutral	-ve	-ve	-ve	-ve	-ve	-ve
BSA	4.8	+ve	+ve	-ve	-ve	-ve	-ve	-ve
Myoglobin	5.5	+ve	+ve	+ve	-ve	-ve	-ve	-ve
RNase	9.0	+ve	+ve	+ve	+ve	+ve	+ve	neutral
Lysozyme	11.5	+ve	+ve	+ve	+ve	+ve	+ve	+ve

Three acidic proteins, pepsin, amyloglucosidase, and BSA, were used in binding studies with P2VP modified support. In addition, lysozyme was employed to investigate interaction of AEX brush with oppositely charged protein. On another hand, two basic proteins, RNase and Lysozyme, and one acidic protein, pepsin, were used for PMAA binding. Both PMAA and P2VP brushes bound with myoglobin were conducted to determine the interaction with neutral protein. To comprehend purely and effectively pH-responsive behaviour, low salt buffers were employed in all studies to explore only effect of pH in the 'osmotic regime'.

The P2VP brush should be protonated at pH below 6.7 (Houbenov *et al.*, 2003), so it was able to bind with pepsin, amyloglucosidase, and BSA, as expected (Figure 3-13). Pepsin was the highest bound among other proteins, where the highest points were observed from pH 2.5 to pH 5. At pH 6, the number began to drop and continuously reduce to almost zero at pH 7.5. This same kind of binding could also be found in amyloglucosidase, except at pH 3.5 where amyloglucosidase was neutral (Table 3-1) and very low binding was observed. Low binding of pepsin and amyloglucosidase at pH 6 and beyond in the P2VP grafted support was likely a result from the P2VP brush started to collapse, which agreed with the thickness of P2VP brush on the flat substrate using ellipsometer and AFM force measurement, reported by Drechsler *et*

al. (2010). In case of BSA, the high binding was found from pH 5 to pH 7. This might explain by effect of electrostatic interaction from oppositely charged proteins and P2VP brush in this pH range, including the pH close to the pI of BSA (Burkert *et al.*, 2009). In contrast, very low non-specific binding was observed from lysozyme amongst the studied pH. Due to positively charged lysozyme in these pHs, charge repulsion with positively charged P2VP brush and no interaction with collapsed brush were probably occurred. It indicates good selectivity of AEX brush modified support.

According to the study of PMAA brushes grafted on silicon surface (Santonicola *et al.*, 2010), the pKa of the PMAA brush was approximately 6.4. Therefore, the brush was swollen and ionised at pH above 6.4. This correlates with the results from lysozyme and RNase binding. High lysozyme and RNase bound were obtained at pH ranged from 7 to 9 (Figure 3-13), where charge interaction between the brush and proteins was expected. This correlated with the study of PMAA brush grafted substrate binding with lysozyme, showing the highest lysozyme bound at pH 7 and low binding at pH 4 (Lei *et al.*, 2014). Only low binding was found from pH below 7, except the binding of RNase at pH 6. The possible explanation for this is structure of RNase which possesses positive charges inside the pocket and not expose to outside (Beintema *et al.*, 1997; Scheraga *et al.*, 2001), so the interaction might come from hydrophobic interaction with unionised PMAA brush. The acidic protein, pepsin, was additionally studied with the PMAA brush. The results showed very low binding of pepsin throughout the pHs because of charge repulsion, which was inversely observed in P2VP brush with basic protein. It showed a good selectivity of protein binding.

Apart from acidic and basic proteins, a neutral protein, myoglobin, was also selected to perform binding studies with both P2VP- and PMAA-grafted supports. Since the pIs of myoglobin and both polymer brushes were close, it is understood that no charge interaction was occurred. Only

small amount of myoglobin bound with both P2VP and PMAA brushes at pH 6 (Figure3-13), where the brushes were expectedly less charged. This may a result from slightly hydrophobic interaction. The interaction was stronger in case of PMAA brush, which likely contains more hydrophobic backbones. This reflects in higher binding of myoglobin for PMAA brush comparing to P2VP brush.

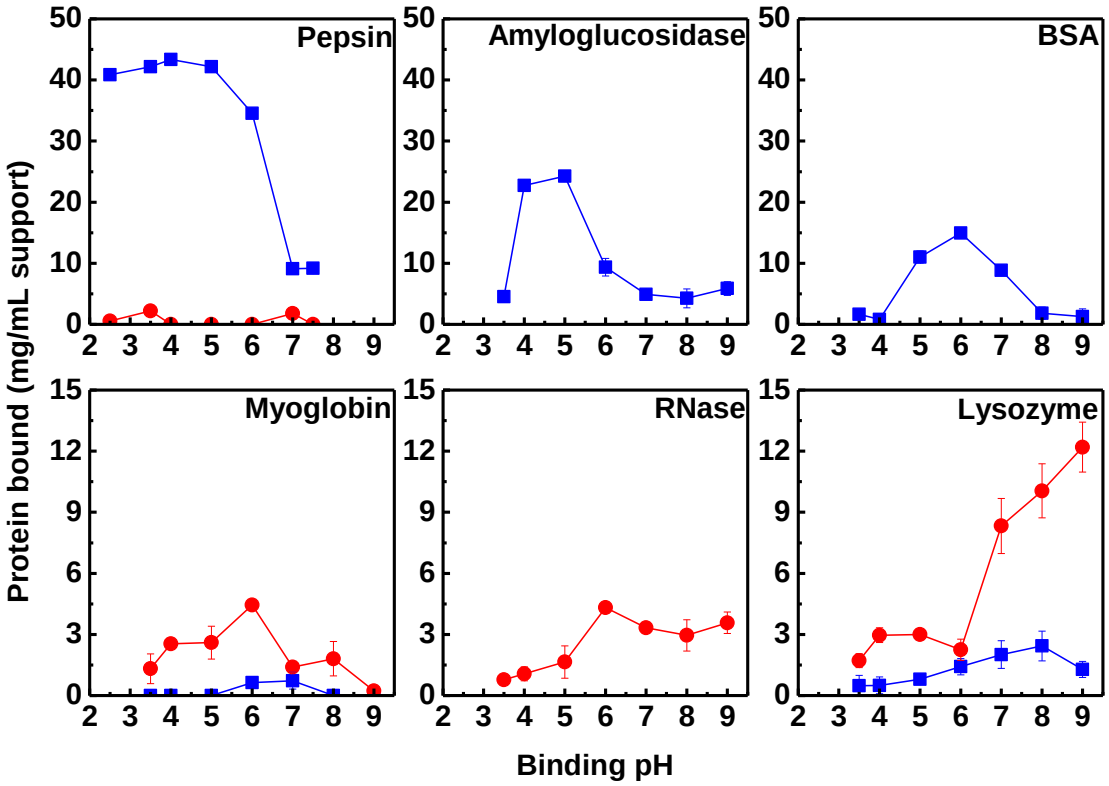

Figure 3-13 Static protein binding studies of P2VP grafted support (blue squares) and PMAA grafted support (red circles).

From these proteins binding studies, the P2VP and PMAA modified supports displayed pH-responsive protein adsorption behaviour, which relates to previous studies on flat surfaces (Uhlmann *et al.*, 2007) and non-porous magnetic adsorbent (Willett, 2009). To understand more about smart pH-switchable functions, protein desorption studies has been performed as a function of pH. The proteins that got the highest binding for each brush were selected for this study. Pepsin was bound with P2VP brush at pH 4, whereas lysozyme was bound with PMAA

brush at pH 8. Myoglobin was only tested in PMAA brush at binding pH of 6. After binding, the pHs were subsequently shifted by 1 to 3 pH units toward where the brushes would be collapsed. The results showed that the more the pH shifted, the higher the elution percentages in all cases (Figure 3-14). The elution of pepsin from P2VP brush was raised to 100% when shifting pH from 4 to 7, while shifting pH from 8 to 5 for PMAA brush, the 100% of lysozyme elution was also observed. This suggests that by switching pH, the brushes were collapsed and uncharged leading to release of bound proteins (Santonicola *et al.*, 2010). As regards myoglobin, more elution from PMAA brush was also found when lower pH. However, it was not increased to 100%. This could be attributed to hydrophobic interaction. These results from protein elution studies demonstrated pH-responsive behaviour tightly corresponding to the results from protein binding studies.

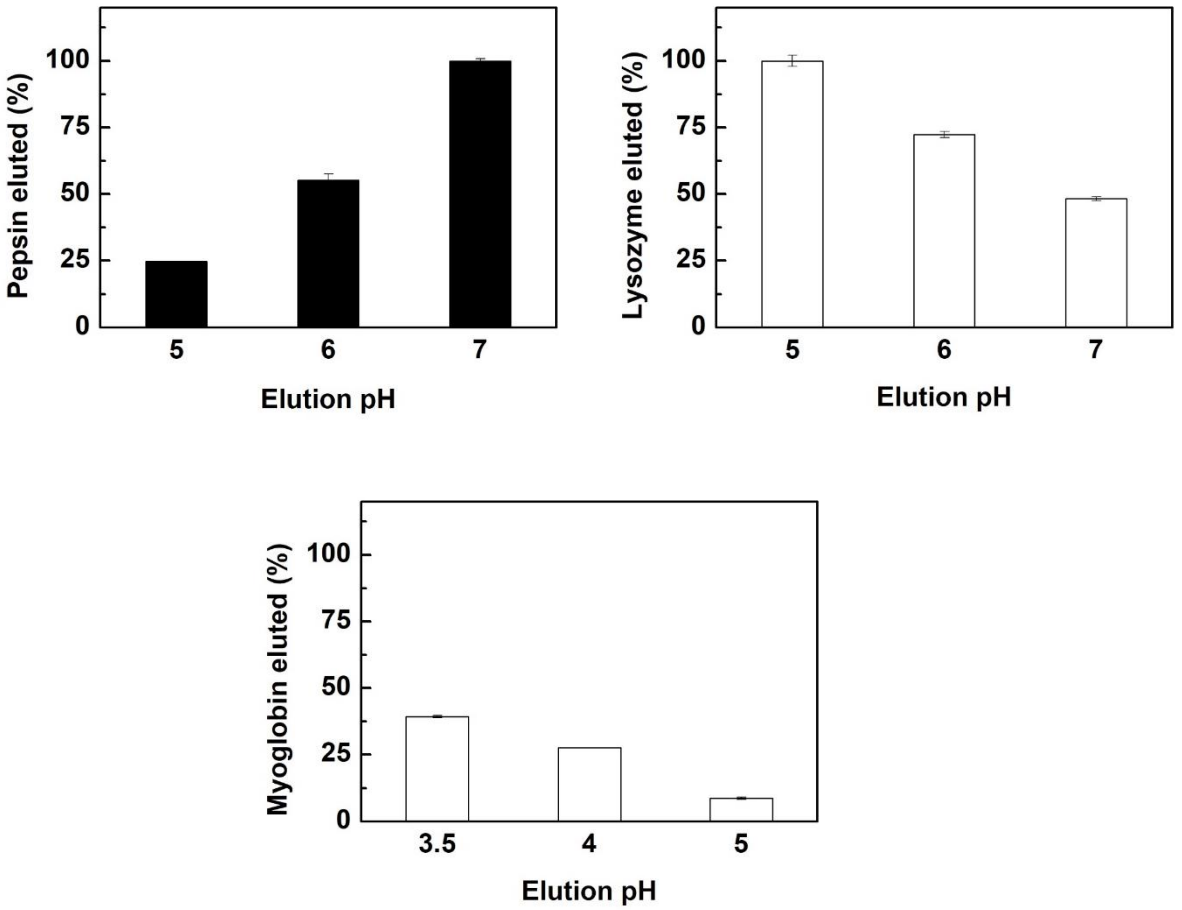

Figure 3-14 pH mediated elution of pepsin from P2VP grafted supports (top left), lysozyme from PMAA grafted supports, and myoglobin from PMAA grafted supports.

3.3 Conclusion

PEL brush is one of the smart polymers that have a potential application in separation process, especially in a chromatography matrix. With pH-responsive properties, this can provide more efficient recovery with a greener solution and no requirement of modifying equipment. Homo PEL brush modified supports was first fabricated using 'grafting to' method, which has been widely used and offers simple and flexible process to start with. Click reaction between tresyl chloride activated Toyopearl and terminal amine polymers was chosen to covalently bond both P2VP (AEX polymer) and P*t*BMA (CEX precursor polymer) with the support. Regarding optimisation, we found that acetone was a solvent of choice for grafting P2VP and P*t*BMA. The

optimal reaction time was 48 h to obtain maximum grafting density. De-protection of P*t*BMA by 50% TFA in water at 40 °C for 24 h to liberate PMAA was tested and confirmed by FTIR. Both P2VP- and PMAA-grafted Toyopearl supports were characterised by FTIR and gravimetry. Calibration curve of PEL loading was successfully constructed to provide a framework for manufacturing mixed PEL brushes in further studies. Uniform distribution of both polymers in the support was confirmed by applying fluorophore-conjugated proteins and fluorescence images were detected by CLSM.

The protein adsorption/desorption studies as a function of pH demonstrated pH-dependent behaviour of P2VP- and PMAA-grafted adsorbents, as agreed with the previous research. Acidic protein binding with P2VP chains was noticed at pH below 7, where the brush was swollen and protonated. While basic protein binding with PMAA brush was occurred at pH above 6, where PMAA chains were extended and ionised. No or low binding of the basic protein with the P2VP support and the acidic protein with the PMAA one. Neutral protein, myoglobin, only bound to PMAA support, albeit at low capacity and peaking at pH 6. Further, we found that pH-mediated elution studies showed correspondent results to the binding studies. With farther shifting pH from the binding pH, the elution percentages were larger. The highest (100%) recoveries were found in both P2VP and PMAA supports when shifting 3 pH units toward where the brush collapsed. These studies provide fundamental framework for fabricating mixed PEL modified chromatography support.

Chapter 4 Fabrication of mixed PEL brush modified Toyopearl and its application in column chromatography

4.1 Introduction

Ion exchange chromatography has been commonly used in protein separation because of its high capacity and simple process in binding and elution. However, with a conventional ion exchange, either an anion or cation exchange technique can be operated in one chromatography matrix at a time. Additionally, to achieve high protein recovery, high salt is required for elution (Levy *et al.*, 2016; Faraji *et al.*, 2017; Großhans *et al.*, 2018). The mixed PEL brush grafted porous support has a potential to overcome these problems from a conventional ion exchange chromatography. The mixed PEL brush support, containing both weak cationic polymer (P2VP) and weak anionic polymer (PMAA), can express anion or cation exchange depending on environmental pH. At acidic pH, the P2VP chains are protonated and stretched out, creating positively charged surface, which can act as an anion exchange chromatography. At basic pH, the PMAA chains are ionised and dominant, forming negatively charged surface, which can behave as a cation exchange chromatography (Figure 4-1).

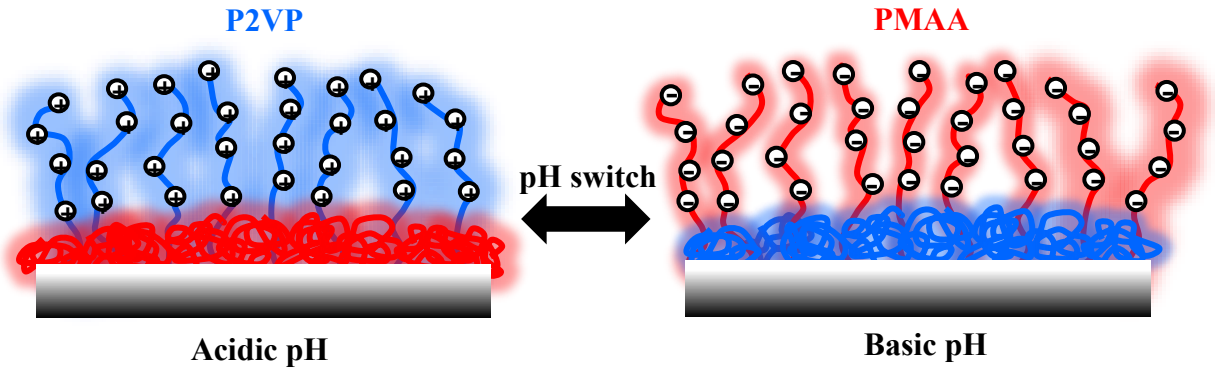

Figure 4-1 Schematic of switching charge behaviour of a mixed P2VP/PMAA brush

According to the fundamental work of homo PEL brush modified supports in Chapter 3, two different polymers, PMAA and P2VP, can be grafted on the surface by two steps via 'graft to' approach. First, one polymer species with limited amount of chains will be anchored with target of occupied roughly half of active sites. A second polymer chains will subsequently be grafted

on the remaining active sites. To prevent two oppositely charged polymers from charge-induced tangling, PMAA, with *tertiary* butyl protective groups, poly(*t*-butyl methacrylate) (P*t*BMA), will be first grafted. After grafting both polymer chains, de-protection process will be followed to liberate PMAA. This de-protection approach has been successfully applied for grafting mixed PEL brush on both flat surface (Houbenov, 2005) and non-porous adsorbent (Willett, 2009). After successful fabrication and rigorously testing of mixed PEL brush supports, the supports can be examined for their application in a column chromatography.

The protein adsorption/desorption in the column chromatography as a function of pH can be explored by employing model proteins with varied pI. Thus, the binding and elution can be tested in both ways. The list of model proteins, used in Chapter3, is provided in Table 4-1.

Table 4-1 List of model proteins with their properties

Protein	pI	MW (kDa)	Reference
Pepsin	3.0	34.6	(Sepulveda *et al.*, 1975)
Amyloglucosidase	3.5	68	(Amaral-Fonseca *et al.*, 2018)
BSA	4.8	66.3	(Kinsella and Whitehead, 1989)
Myoglobin	5.5	17	(Graf and Wätzig, 2004)
RNase	9.0	13.7	(Hirs *et al.*, 1956)
Lysozyme	11.0	14.4	(Price *et al.*, 1999)

Protein loading into a column chromatography can be tracked in a real-time from an in-line UV detector. Protein can be commonly detected by measurement of UV absorbance at 280 nm. The protein content in each fraction from the column can also be later analysed by the BCA assay, which was previously applied in Chapter3.

Gel electrophoresis is a suitable technique for analysing a mixture of proteins. This technique involves protein loading onto a polyacrylamide gel, where electrical current is passed. Before loading protein, protein is treated with sodium dodecyl sulphate (SDS) or lithium dodecyl sulphate (LDS) and a reducing agent to denature the protein structure. SDS or LDS provides protein with negatively intrinsic charge proportional to its mass. This leads to different moving distance of proteins towards the anode depending on their molecular weight. Therefore, proteins with varied sizes can be separated and identified, based on the known molecular weight proteins that travel through a gel at around the same rate. Subsequently, the proteins can be visualised by staining with a specific dye that bind with proteins.

In this chapter, we fabricate mixed PEL modified supports by two-step grafting, first with PMAA and followed by P2VP, with various compositions. The supports are properly characterised and perform pH-responsive static protein adsorption/desorption. Thereafter, the mixed PEL brush modified Toyopearl, containing the best composition of P2VP and PMAA and displaying great performances, was packed into the column before loading with the selected model proteins, including pepsin, myoglobin, and lysozyme, which represents an acidic, a neutral, and a basic protein, respectively. These proteins offer different pI and molecular weight and are, thus, useful in testing brush performance and for LDS-PAGE analysis. We explored pH-switchable protein adsorption/desorption of the support by operating in two conditions. One is loading proteins at acidic pH before elution at basic pH and another one is loading proteins at basic pH before elution at acidic pH. The fractions from the chromatography were analysed for the total protein content by the BCA assay and the protein in the mixture, associated with the peak of UV absorbance at 280 nm, were identified by SDS-PAGE. These provide qualitative and quantitative information about the performance of the mixed PEL brush modified support.

4.2 Results and discussion

4.2.1 Manufacture of mixed PEL brush modified supports

Mixed PEL brush modified Toyopearl supports were fabricated by first grafting P*t*BMA and P2VP was subsequently grafted onto the supports. This sequence was preferable because smaller P2VP is likely able to penetrate between larger P*t*BMA chains. P2VP also has the high affinity to the substrate (Houbenov, 2005), so the inverse order might prevent grafting P*t*BMA as second chains. The concentration of supplied P*t*BMA was carefully selected from the calibration curve in Figure 3-10 and 3-11. The 37.5 mg/mL support of P*t*BMA supplied was first employed to assumingly occupy half of active sites and allow the remained sites for grafting P2VP. Different concentrations of P2VP solution were subsequently grafted to observe influence of second grafting on the mixed PEL brush. The detail for each mixed PEL modified support assembling was presented in Table 4-2.

Table 4-2 List of mixed PEL modified supports with varied supply of second grafted polymer, P2VP.

Support	PEL presented (µmol/mL support)		PEL grafted (µmol/mL support)		Mol%	
	PMAA	**P2VP**	**PMAA**	**P2VP**	**PMAA**	**P2VP**
P2VP	-	7.6	-	2.1	-	100
PMAA	2.6	-	0.6	-	100	-
Mix 1	1.3	3.8	0.5	0.4	65	35
Mix 2	1.3	5.7	0.5	0.9	45	55
Mix 3	1.3	7.6	0.5	1.2	39	61
Mix 4	1.3	9.5	0.5	0.6	58	42
Mix 5	0.9	7.6	0.3	1.5	22	78
Mix 6	2.6	7.6	0.6	0.5	67	33

Mixed PEL brush supports were analysed by gravimetric approach and liquid FTIR of polymer solution to obtain each brush component grafted in the supports. The percentages of mol

(mol%) was based on each monomer content, calculated from the degree of polymerisation of 204 and 126 for PMAA and P2VP, respectively, shown in Table 4-2. When concentration of supplied P2VP was increased, more P2VP chains were grafted on the support as shown in Mix 1 to Mix 3. It appears to be that shorter chains, P2VP, were able to penetrate into the space between larger chains, PMAA, and were better grafted which was shown from more than 50 mol% of grafted P2VP in the mixed PEL support despite of low supply of P2VP. According to these data, it can infer that P2VP, supplied with high concentration, can be accessed to the active surface, although higher PMAA chains are already grafted. A possible explanation is that large chains of PMAA blocked themselves from accessing the active sites leading to limited maximum grafting densities (as shown in Figure 3-10). In contrast, with smaller size and higher affinity to the surface, P2VP is likely to pass through and attach to the surface. However, if the P2VP concentration was too high, it might have a negative effect on grafting as shown in 'Mix 4'. Since turbidity was observed from the P2VP solution supplying for Mix 4, undissolved P2VP may have caused blockage in support pores during the grafting step, decreasing the available surface area for dissolved chains to graft to the support surface, which could have resulted in the decrease in grafted P2VP. Therefore, the maximum supply of P2VP of 7.6 μmol/mL support was selected for the further experiments.

The effect of the first polymer grafting on the second polymer grafting was investigated by varying the supply of PMAA and following with the constant supply of P2VP. As higher PMAA chains were grafted, the grafted P2VP was reduced according to Mix 5 and Mix 6 (Table 4-2). P2VP chains could be grafted on the surface even though the surface was occupied by the possible maximum chains of PMAA. It indicates that there was enough gap and active sites between PMAA chains that allowed P2VP to graft on.

In order to confirm that P2VP was successfully integrated into mixed PEL modified support, solid FTIR was used. The spectrum of mixed PEL support (Figure 4-2) illustrated the peaks of first grafted PMAA, identified at 1450 and 1358 cm^{-1}, corresponding to methylene $–CH_2-$ and methyl $–CH_3$, respectively, with the uniquely additional peaks of second grafted P2VP, observed at 877 cm^{-1} for aromatic C-C bonds, also 1450 and 1600 cm^{-1}, corresponding to aromatic C-H bonds. The rise of peak heights at 752 and 697 cm^{-1} was detected from increasing in methylene $–(CH_2)_n-$ from the polymers backbone.

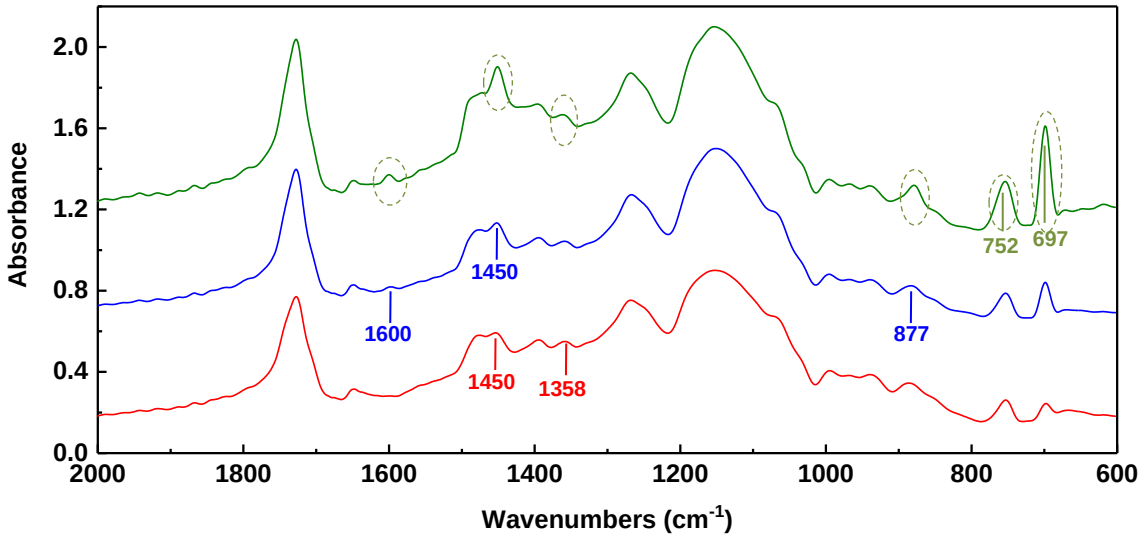

Figure 4-2 FTIR spectrum of a) PMAA, b) P2VP, and c) mixed PEL modified supports.

To understand configuration of the polymer chains on the support, grafting density was calculated by the following equation;

$$\sigma = \frac{A.N_A}{S} \qquad (4\text{-}1)$$

where σ is grafting density (chains/nm^2), A is amount of grafted polymer (mol), N_A is Avogrado's number, and S is surface area of the support (nm).

The inter-grafting space, D, (nm) was calculated by the following equation;

$$D = \frac{1}{\sqrt{\sigma}} \quad (4\text{-}2)$$

Additionally, radius of gyration (R_g) can be calculated as the following equation;

$$R_g \approx A_m . L^v \quad (4\text{-}3)$$

where A_m is the monomer size (0.33 nm for PMAA and 0.67 nm for P2VP), L is monomer units in the polymer, and v is the Flory exponent, which is dependent on the polymer-solvent interaction. Under good solvent conditions (PMAA at high pH, P2VP at low pH) where swollen chains are presented a Flory exponent of 3/5 was used (Unsworth *et al.*, 2005; Kato and Wadati, 2007). Under poor solvent conditions (low and neutral pH for PMAA and neutral and high pH for P2VP), when chains are presented in collapsed form, a Flory exponent of 1/3 was used (Cordeiro, 1999). In case of mixed PEL brushes, two different monomers were presented which leading to more than one A_m values. Therefore, an average R_g value was applied during the characterisation of the mixed PEL brushes, which was calculated with the following equations depending on the pH (Willett, 2009; Israelachvili, 2011);

$$R_{g,Mix,\ pH\ 2} = (R_{g,PMAA,\ collapsed}).N_{PMAA} + (R_{g,\ P2VP\ swollen}).N_{P2VP} \quad (4\text{-}4)$$

$$R_{g,Mix,\ neutral\ pH} = (R_{g,PMAA,collapsed}).N_{PMAA} + (R_{g,P2VP,\ collapsed}).N_{P2VP} \quad (4\text{-}5)$$

$$R_{g,Mix,\ pH\ 10} = (R_{g,\ PMAA\ swollen}).N_{PMAA} + (R_{g,P2VP,\ collapsed}).N_{P2VP} \quad (4\text{-}6)$$

Table 4-3 List of homo and mixed PEL modified brush supports with their brush characteristics.

Support	Grafting density, σ (chains/nm^2)	Inter-grafting, D (nm)	R_g			$D/2R_g$		
			pH 2	neutral	pH 10	pH 2	neutral	pH 10
P2VP	0.16	2.49	12.17	3.35	3.35	0.10	0.37	0.37
PMAA	0.05	4.62	1.94	1.94	8.02	1.19	1.19	0.29
Mix 1	0.07	3.83	6.66	2.59	5.87	0.29	0.74	0.33
Mix 2	0.11	3.01	8.75	2.88	4.92	0.17	0.52	0.31
Mix 3	0.13	2.79	9.24	2.95	4.69	0.15	0.47	0.30
Mix 4	0.08	3.52	7.51	2.71	5.48	0.23	0.65	0.32
Mix 5	0.14	2.69	10.68	3.15	4.04	0.13	0.43	0.33
Mix 6	0.08	3.46	6.44	2.56	5.97	0.27	0.67	0.29

Polymer configuration can be predicted by the value of $D/2R_g$. If $D/2R_g > 1$, polymer is in non-overlapping mushroom configuration. If $D/2R_g = 0.5 – 1$, weak overlapping is occurred. If $D/2R_g < 0.5$, brush regime is formed (Zhu *et al.*, 2007). According to $D/2R_g$ values of homo and mixed PEL supports in Table 4-3, P2VP and Mix 5 were in brush configuration at all pHs. PMAA was in mushroom regime at acidic and neutral pHs, while PMAA brush was observed at basic pH where the PMAA chains could be ionised and stretched away from the surface. In case of Mix 6, the brush regime was performed at acidic and basic pHs, where charged P2VP and PMAA chains dominated the surface, respectively. However, at neutral pH, only weak overlapping was occurred because of less grafting density comparing to Mix 5.

4.2.2 Physicochemical properties of mixed PEL brush modified support

Zeta potential measurement was adopted to understand how the brush component affects properties. The zeta potential values were measured as a function of pH, ranging from 3.5 to 9. The zeta potential curves of homo P2VP, PMAA and one of the mixed PEL (Mix 6) modified supports were shown in Figure4-3.

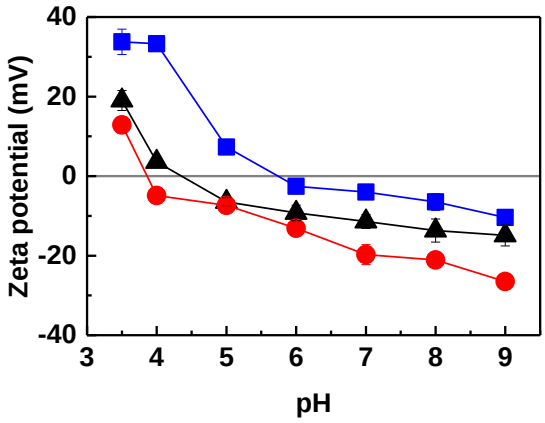

Figure 4-3 Zeta potential measurements of P2VP (blue squares), PMAA (red circles), and Mix 6 (black triangles) PEL brush supports as a function of pH.

The plot illustrated that homo PMAA brush possessed negative values almost throughout the tested pH, except at pH 3.5, indicating negatively charged surface, while the P2VP brush displayed positive values at pH below around 6, indicating positively charged surface at acidic pHs. These correlated with the previously reported curves (Houbenov *et al.*, 2003). In case of the mixed PEL support, after P2VP chains were subsequently grafted, the zeta potential numbers were shifted towards positive side, especially at acidic pHs. At pH 3.5 and 4, the zeta potentials of mixed PEL brush supports were positive and higher than ones of homo PMAA brush. It indicates that P2VP chains were successfully integrated into the PMAA-grafted supports creating mixed PEL modified supports with pH-responsive behaviour as shown as change of surface charges in the zeta potential plot. These also closely correlated with the previous study of mixed PAA-P2VP brush grafted surface (Houbenov *et al.*, 2003; Drechsler *et al.*, 2010).

From the zeta potential curve, isoelectric points (pI) or point of zero charge (PZC) of the mixed PEL supports can be estimated. The results demonstrated that the more the P2VP grafted in mixed PEL support, the higher the PZC because P2VP provided positively charges at acidic pH and consequently increased the PZC of mixed PEL support (Figure4-4). In another way, high

content of PMAA reduce the PZC of the mixed PEL modified supports. It suggested that composition of P2VP and PMAA plays an important role in surface charges in the response of pH.

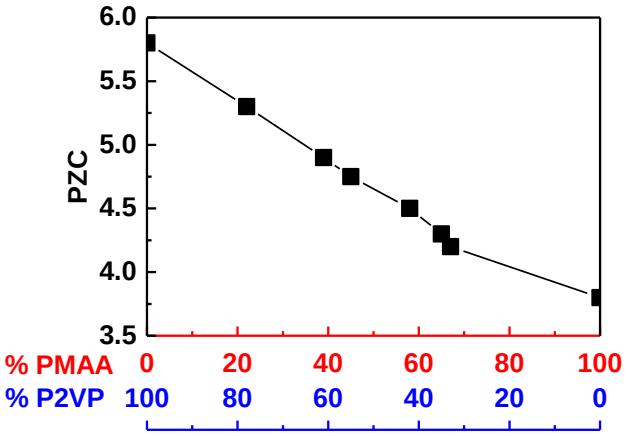

Figure 4-4 Influence of brush composition on the point of zero charge (PZC) obtained from zeta potential curve.

Zeta potential of the mixed PEL modified adsorbents had been also measured in alternating steps of acidic and basic pH to determine pH-responsive behaviour and charge reversibility. Switching pH from 3.5 and 8.5 was first applied to investigate effect of changing between extreme pH. Then, the pH was switched to 4 before measurements were carried out in intermediate pH between 4 and 7 to examine the brush behaviour in smaller pH changing range that is suitable for protein separation by chromatography. The supports were first rinsed with the desired pH buffer and were then equilibrated in the buffers for 30 minutes before measurements. Figure 4-5 shows that the mixed PEL modified support reversibly switched its zeta potential in response to changes in pH. The zeta charges also closely tracked with the original zeta potential curve of the mixed PEL support. According to Houbenov *et al.* (2003), the magnitude of zeta potential is strongly linked to brush height. This suggests signs of full reversibility without irreversible knotting or tangling of the mixed PEL brush chains and the

PEL brush functionalised supports have a potential for AEX-CEX chromatography applications, possibly for multiple cycles of adsorption and elution. The switch in surface charge may provide pH-mediated elution with an additional 'push' by electrostatic repulsion forces, increasing elution efficiency and decreasing the number of washing steps required, thus reducing waste generation.

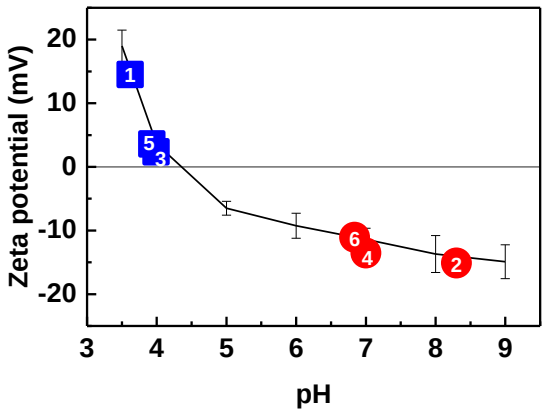

Figure 4-5 Brush reversibility determined by zeta potential measurements. The original zeta potential curve of the mixed PEL brush modified support (Mix 6) shown in black line. Change of zeta potential values after shifting pH by the following number order 1-6.

There is a strong correlation between zeta potential (surface charges) and sedimentation rate (Kinyua *et al.*, 2016). Particles are likely to suspend in solution if they possess high zeta potential, in another word, positive or negative charges, which will prevent them to agglomerate together and sediment. Thus, sedimentation rates of mixed PEL support was measured in different pH buffer and UV-Vis absorbance was measured at 400 nm wavelength for detecting light scattering of particles. The sedimentation curve was plotted between Log [A/A_0] and time (Vikesland *et al.*, 2016). The gradient of slopes related to the settling rate as shown in Figure 4-6 left. From the time of 100 seconds onward, the gradients can be distinguished in three groups, including the steepest group (pH 5 and 6), the shallowest group (pH 3.5 and 4), and the middle group (pH 7, 8, and 9). The normalised absorbance at 400 nm at the time of 180 seconds (Figure 4-6 right) also showed the similar trend to the sedimentation curve. These results

correlated with the previous zeta potential measurements (Figure 4-5). The positively charged supports (at pH 3.5 and 4) and negatively charged supports (at pH 7, 8, and 9) displayed slower sedimentation rates than the ones of less or zero charged supports (at pH 5 and 6). This behaviour may relate to the wettability of the supports as investigated by advancing contact angle measurements (Ionov *et al.*, 2004). At intermediate pH values the brush layer was collapsed and a dry hydrophobic PMAA-P2VP complex was formed (Mikhaylova *et al.*, 2007; Hinrichs *et al.*, 2009), which may result in increased aggregation of support beads and thus faster settling.

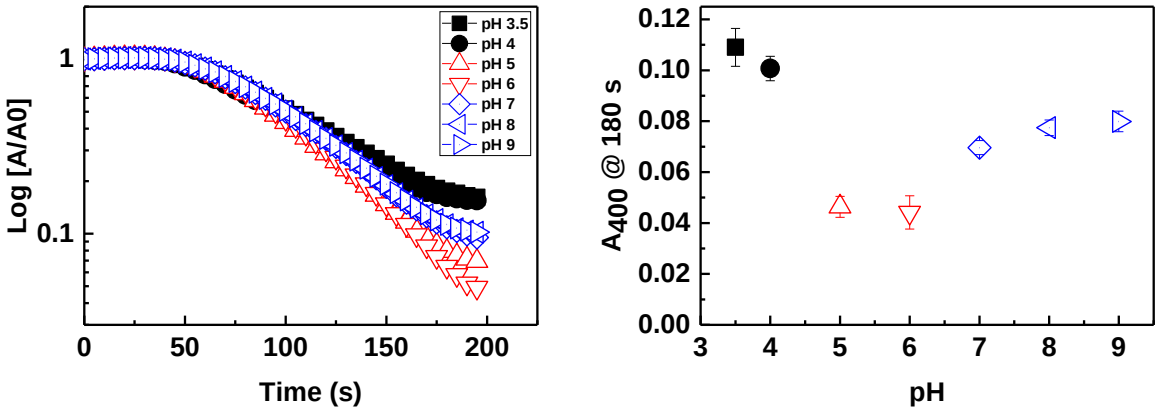

Figure 4-6 Sedimentation rate curve of mixed PEL brush modified support (Mix 6) in different pH buffers (left). Normalised absorbance at 400 nm (A_{400}) at 180 second as a function of pH.

4.2.3 Protein adsorption and desorption as a function of pH

'Mix 5' and 'Mix 6' were selected to perform batch protein binding and elution studies to investigate influence of the brush composition on their performances. Mix 5 (22% PMAA: 78% P2VP) represents the mixed PEL brush with high ratio of P2VP, while Mix 6 (67% PMAA: 33% P2VP) represents the one with high proportion of PMAA. Pepsin, myoglobin, and lysozyme were chosen as model acidic, neutral, and basic proteins, respectively, because of good binding and elution profiles shown in the homo PEL brush supports.

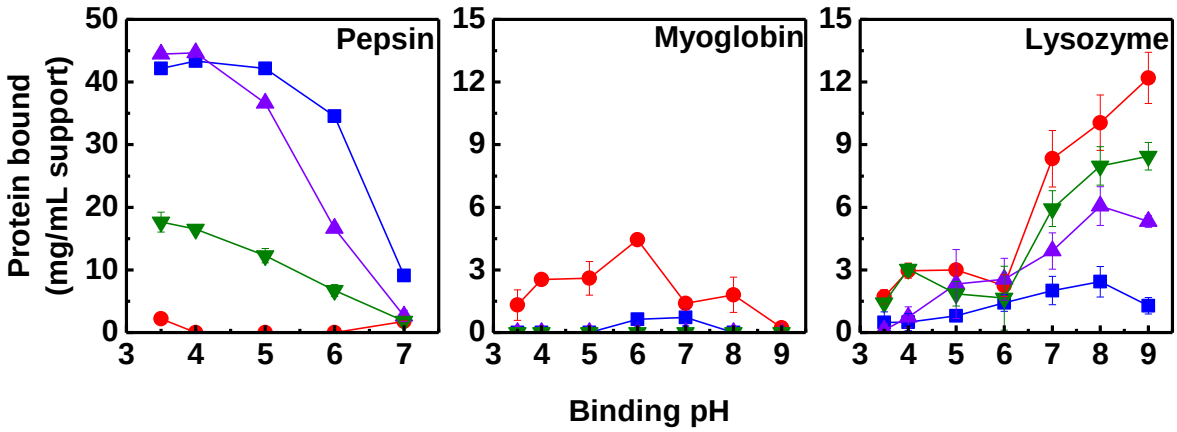

Figure 4-7 Static protein binding of P2VP (blue squares), PMAA (red circles), Mix 5 (violet up triangles), and Mix 6 (green down triangles) Toyopearl supports as a function of pH.

The results demonstrated that protein binding strongly correlated with the brush composition (Figure 4-7). According to pepsin binding, Mix 5 had higher binding than Mix 6 as expected because higher amount of P2VP chains were observed in Mix 5. It is noted that pepsin bound of Mix 5 was close to the homo P2VP support, especially at pH 3.5 and pH 4, even the grafted P2VP chains in both supports were different. This might be explained by that the brush surfaces were saturated with pepsin at low pH, where the P2VP chains were fully protonated. Thus, small difference in brush density had no effect in pepsin bound. However, when considering at pH 5 and 6, lower pepsin bound was observed in Mix 5 comparing to the homo P2VP one since less degree of protonation could be expected and the grafting density would be more prominent. With high number of P2VP chains, more charges can possibly be obtained, which leads to high pepsin bound.

In case of lysozyme binding, Mix 6 had higher lysozyme bound than Mix 5 as Mix 6 possessed higher grafted PMAA chains than Mix 5. Lysozyme bound of Mix 6 was, however, lower than the homo PMAA supports, although amount of grafted PMAA in both supports was similar. This might result from interference from another polymer, P2VP chains, in the mixed brush,

which has been observed in the PAA-P2VP mixed brush (Drechsler *et al.*, 2018). Additionally, since the numbers of grafted chains between PMAA and P2VP were close (Table 4-2), P2VP chains likely had quite an impact on the PMAA behaviour and lysozyme binding.

The binding with a neutral protein, myoglobin, was also performed for mixed PEL modified supports. However, no or very less binding was observed amongst tested pHs. The explanation for this might be that the PZC of myoglobin and mixed PEL adsorbents were quite close. Thus, there is possibly no or less attractive force from charge interaction at acidic or basic pH as well as hydrophobic interaction at around neutral pH.

One of interesting findings was that the mixed PEL modified Toyopearl supports displayed pH-responsive protein adsorption for both acidic and basic proteins. It could also perform as either an anion exchanger or a cation exchanger, which was different from the homo polymer grafted supports.

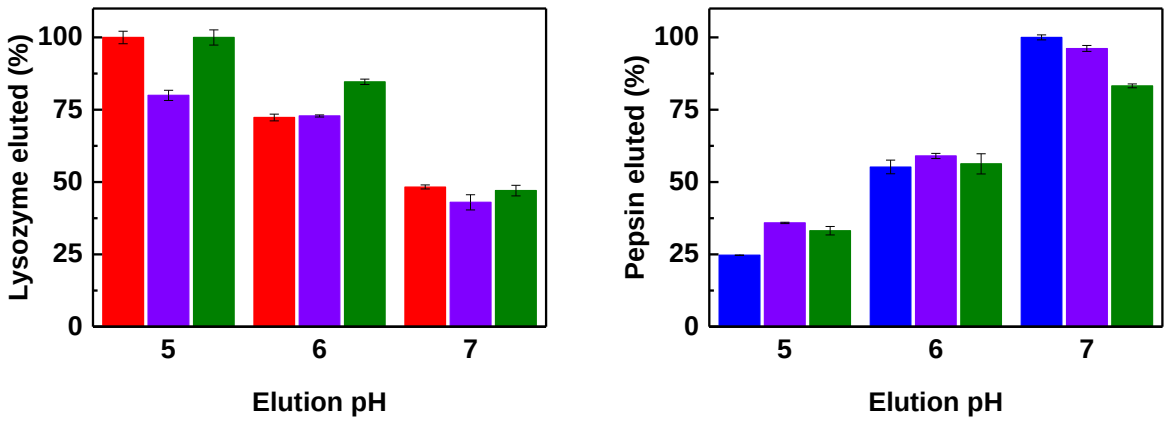

Figure 4-8 pH mediated lysozyme elution (left) and pepsin elution (right) of homo PEL and mixed PEL brush supports. Key: homo P2VP (blue); homo PMAA (red), Mix 5 (violet); and Mix 6 (green).

Mix 5 and Mix 6 performed pH mediated elution to investigate protein desorption behaviour. Pepsin binding was performed at pH 4 before shifting pH from 1 to 3 units, whereas lysozyme

binding was conducted at pH 8 and then the pH was lowered from 1 to 3 units. The elution was shown in percentages of bound protein and was compared with that from both homo PEL brush supports (Figure 4-8). Lysozyme elution was increased for both homo PMAA and mixed PEL adsorbents when shifting to higher pHs, whereas, pepsin elution for both homo P2VP and mixed PEL adsorbents were increased with decrease in pH. Mix 6, containing high PMAA ratio, displayed higher lysozyme elution percentages than Mix 5, containing lower PMAA ratio, while Mix 5 with higher P2VP content showed higher pepsin elution percentages than Mix 6. This suggests that high PMAA content in the support encourages high lysozyme elution as well as high P2VP content promotes high pepsin elution. It is noticeable that pepsin elution from Mix 5 was superior to the P2VP support at 1 and 2 pH units above the binding pH, whereas lysozyme elution from mix 6 was superior to PMAA at 1 and 2 pH units below the binding pH. This behaviour of mixed PEL supports shows a great potential over the homo brush supports when performing dynamic protein adsorption/desorption in a column chromatography. Since pH gradient will be operated for elution step, efficient protein recovery might be achieved by just changing 1 or 2 pH units from the binding pH.

4.2.4 Effect of higher degree of tresyl activation

The mixed PEL modified Toyopearl support was successfully fabricated with bi-functional and pH-responsive protein adsorption/desorption. However, there was a slight lack of balance between anion exchanger and cation exchanger performances. Low binding of lysozyme was observed comparing to pepsin binding due to less PMAA chains were grafted on the support. Therefore, increasing the grafting density of PMAA chains can improve protein binding on the cation exchanger side. One way to accomplish this is increasing the degree of tresyl activation. According to TNBS assay after amination of the surface, the extent of tresyl activation was 10.56 $\pm$ 0.38 μmol/mL support for all the Toyopearl supports used in the previous studies. The

PEL modified supports using this batch of Toyopearl will be stated with 'A' in the name from this point. Another batch of Toyopearl has higher degree of tresylation of 19.24 ± 0.02 μmol/mL support, which was used in making PEL brush modified Toyopearl supports in the experiments onward. This batch will be stated as 'B' in the name. Regarding to the values of tresyl activation, Batch B had around twice higher the active sites than Batch A, which can improve the grafting density of polymers on the Toyopearl support.

First, the mixed PEL modified supports made from 'Batch B' Toyoperal were fabricated supplying with different amount of PMAA to thoroughly investigate effect of the first grafting on the second grafting and to find the suitable brush composition that provide the balance performance. The supplied P2VP of 7.6 μmol/mL support was applied based on the previous results. List of the mixed PEL brush modified Toyopearl supports were shown along with the homo PEL modified supports in Table 4-4.

Table 4-4 List of mixed PEL modified Toyopearl (Batch B) supports with varied supply of first grafted polymer, PMAA.

Support	PEL presented (μmol/mL support)		PEL grafted (μmol/mL support)		Mol%	
	PMAA	**P2VP**	**PMAA**	**P2VP**	**PMAA**	**P2VP**
B-P2VP	-	7.6	-	3.0	-	100
B-PMAA	2.6	-	0.9	-	100	-
B-Mix 7	0.4	7.6	0.4	2.3	22	78
B-Mix 8	0.9	7.6	0.7	2.2	33	67
B-Mix 9	1.7	7.6	0.8	2.1	38	62
B-Mix 10	2.6	7.6	0.9	1.9	44	56

The result demonstrated that higher grafted PMAA decreased amount of grafted P2VP (Figure4-9), which agreed with the previous results (Table 4-2). This might be due to blocking

access of P2VP chains from dense grafted PMAA chains. However, even at maximum grafted PMAA, P2VP was still quite highly grafted on the support because P2VP chains are smaller in size and possibly passed through to the active sites and attached to the supports. With maximum grafted PMAA and followed by maximum supply of P2VP (B-Mix 10), it provided more balance compositions of PMAA and P2VP in the mixed PEL support and might also lead to balance in protein adsorption/desorption behaviour.

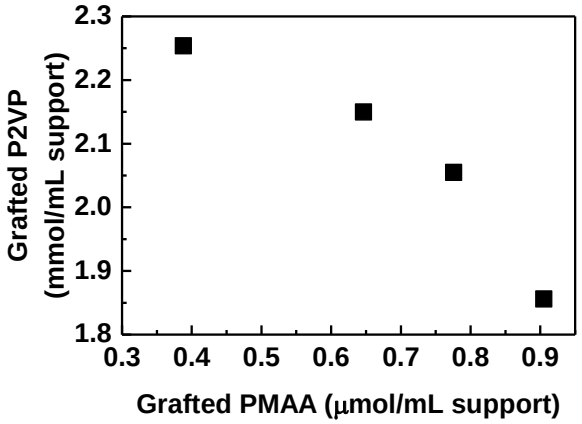

Figure 4-9 Influence of first grafting, PMAA, to second grafting, P2VP in the mixed PEL Toyopearl (Batch B) supports.

The parameters used to determine the configurations of homo and mixed PEL chains modified supports were presented in Table 4-5.

Table 4-5 List of mixed PEL modified Toyopearl (Batch B) supports with their brush characteristics.

Support	Grafting density, σ (chains/nm^2)	Inter-grafting, D (nm)	R_g			$D/2R_g$		
			pH 2	neutral	pH 10	pH 2	neutral	pH 10
B-P2VP	0.24	3.76	12.17	3.35	3.35	0.08	0.31	0.31
B-PMAA	0.07	2.06	1.94	1.94	8.02	0.97	0.97	0.23
B-Mix 7	0.21	2.21	10.67	3.15	4.04	0.10	0.35	0.27
B-Mix 8	0.22	2.15	9.81	3.03	4.43	0.11	0.35	0.24
B-Mix 9	0.22	2.13	9.37	2.97	4.63	0.11	0.36	0.23
B-Mix 10	0.21	2.16	8.82	2.89	4.88	0.12	0.37	0.22

Polymer configuration can be predicted by the value of $D/2R_g$. If $D/2R_g > 1$, polymer is in non-overlapping mushroom configuration. If $D/2R_g = 0.5 – 1$, week overlapping is occurred. If $D/2R_g < 0.5$, brush regime is formed (Zhu *et al.*, 2007). According to $D/2R_g$ values of B-Mix 7-10 in Table 3-6, B-Mix 7-10 were in brush configuration at all pHs. The homo P2VP grafted support, B-P2VP, also performed the brush regime, while the PMAA grafted support, B-PMAA, displayed the brush regime only at basic pH. The chain densities in these 'Batch B' supports were higher than the ones in 'Batch A'. This suggests that higher degree of tresylation could increase the grafted chains and brush density. To confirm this assumption, protein binding study was conducted.

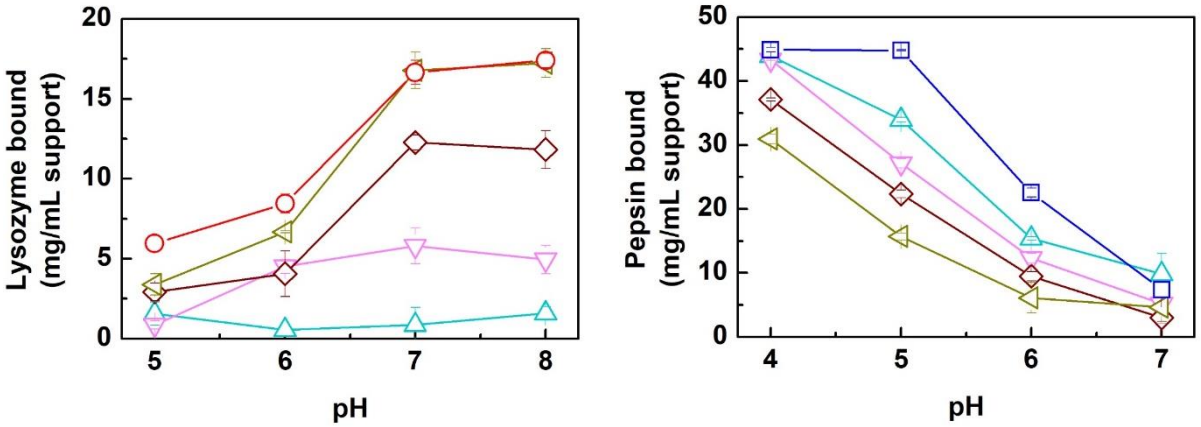

Figure 4-10 Static lysozyme binding (left) and pepsin binding (right) of homo PEL and mixed PEL supports as a function of pH. Key: B-PMAA (red circles); B-P2VP (blue squares); B-Mix 7 (light blue up triangles), B-Mix 8 (pink down triangles), B-Mix 9 (dark red diamonds), B-Mix 10 (dark yellow left triangles).

Static protein binding studies of mixed PEL modified adsorbents with different PMAA/P2VP ratios were examined comparing with the homo PEL grafted supports. Pepsin and lysozyme were employed at intermediate pH range where pH-responsive binding of each protein can be observed. Figure 4-10 (left) shows lysozyme binding of mixed PEL supports with different compositions at pH 5 to 8. It was demonstrated that lysozyme bound was reflected by the ratio of PMAA chains in the mixed PEL. At pH 7 and 8, where the PMAA brush was expected to be ionised, the supports bound lysozyme at maximum level and B-Mix 10, containing the highest amount of PMAA chains, expressed the highest binding of around 17.5 mg/mL support and the numbers were very close to the ones from homo PMAA brush adsorbents. Low or no lysozyme binding was seen in B-Mix 7 because the PMAA chains in this support may be too low and was probably blocked by dominant P2VP chains. The similar correlation between polymer composition and protein binding also applied to P2VP chains and pepsin binding (Figure 4-10 right). B-Mix 7, with the highest ratio of P2VP chains, exhibited the highest pepsin bound from pH 4 to 7, which was a bit less than the ones from homo P2VP brush adsorbents. At pH 4, pepsin was adsorbed with all supports at the highest level of approximately 45 mg/mL support

because the P2VP chains were fully protonated and interacted with negatively charged pepsin. When pH was shifted to more basic, the pepsin binding was gradually reduced due to collapse of the P2VP brush and possibly rise of oppositely charged PMAA chains. Pepsin adsorption on B-Mix 10 was the lowest number of around 30 mg/mL support. However, this amount was quite high comparing to the highest lysozyme binding that can be obtained. Therefore, B-Mix 10 looks promising in term of balance in performance and composition of both PMAA and P2VP. Overall, the protein binding of the PEL modified 'Batch B' supports was higher than the 'Batch A', which well agreed with the grafted amount data. To focus more on the effect of extent of tresylation on protein adsorption, the homo and mixed PEL modified Toyopearl supports made from Batch A and B with similar polymer supply were compared (Figure 4-11).

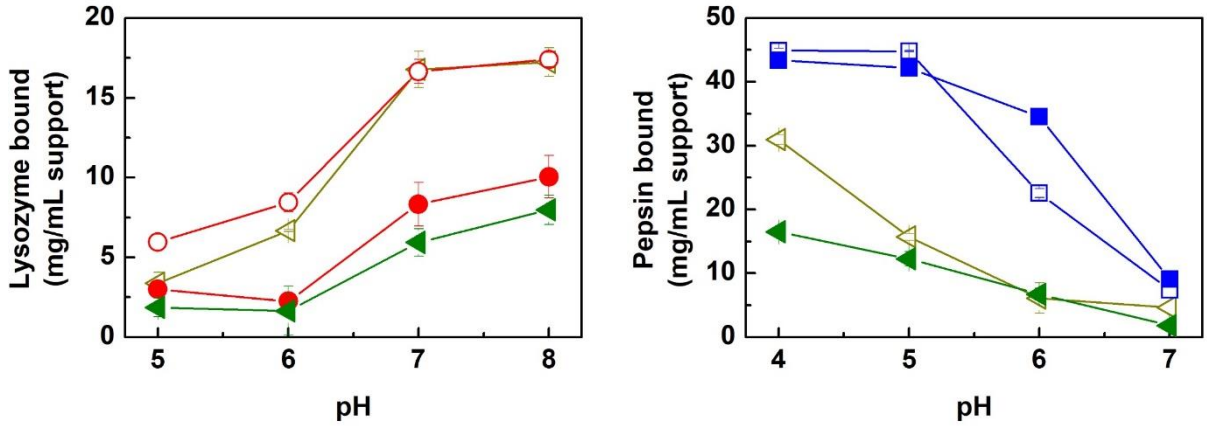

Figure 4-11 Static lysozyme binding (left) and pepsin binding (right) of A-PMAA (close red circles), B-PMAA (open red circles), A-Mix 6 (green left triangles), B-Mix 10 (dark yellow left triangles), A-P2VP (close blue squares), and B-P2VP (open blue squares). Key: close symbols represent 'Batch A' and open symbols represent 'Batch B'.

The lysozyme binding of the homo PEL support, B-PMAA, was approximately twice higher than that of A-PMAA. This was also observed in case of the mixed PEL Toyopearl supports, B-Mix 10 over A-Mix 6. This higher binding reflected higher grafting densities of polymer chains resulted from higher degree of tresyl activation. In case of pepsin binding, influence of high extent of tresylation also showed in B-Mix 10 as higher pepsin bound was obtained

comparing to A-Mix 6. However, there was only slightly different in pepsin binding between B-P2VP and A-P2VP. The possible explanation is that the pepsin bound with the P2VP grafted support surface was saturated at around 45 mg/mL support. Thus, increasing the grafted P2VP chains on the surface had no effect on the pepsin bound. It is noted that at pH 6, the pepsin bound of A-P2VP was higher than that of B-P2VP even though B-P2VP had higher grafting density of P2VP chains than A-P2VP. This infers that pH-responsive behaviour was more highlighted in higher grafting density brush as the P2VP brush was expected to partly collapse at pH 6 and pepsin bound should be lower than at pH 4 and 5. To explore pH-responsive performance, pH-mediated protein elution was conducted. B-Mix 10 was chosen to perform the protein elution because it contained a balance composition of PMAA and P2VP (44%:56%) and displayed a good protein binding profile. The lysozyme elution of B-Mix 10 was compared with A-PMAA and A-Mix6, which performed high lysozyme elution. Regarding the pepsin elution, it was compared with A-P2VP and A-Mix-5, which showed high pepsin elution (Figure 4-12).

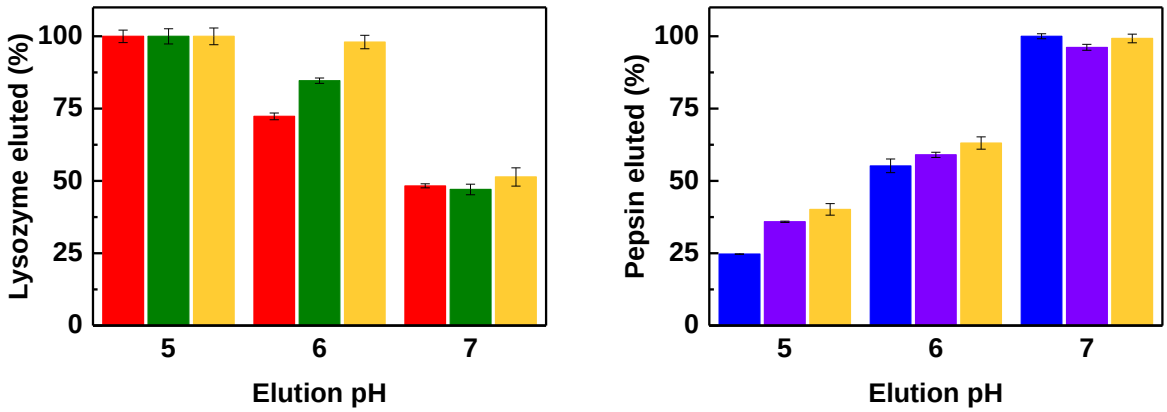

Figure 4-12 pH mediated lysozyme elution (left) and pepsin elution (right) of homo PEL and mixed PEL brush Toyopearl supports. Key: A-P2VP (red); A-P2VP (blue); A-Mix-6 (green); A-Mix 5 (violet); B-Mix-10 (yellow).

According to the result, B-Mix 10 exhibited better pH lysozyme and pepsin elution than A-Mix 6 and A-Mix 5, respectively. Additionally, it showed as good as or better pH elution comparing to both homo PEL modified supports. This indicates that increasing the grafting density by raising degree of tresylation can improve pH-responsive protein recovery.

This section has shown that high degree of tresyl activation influenced the high grafted amount of polymer chains on the Toyopearl support. This consequently improved the pH-responsive protein adsorption and desorption.

4.2.5 Application of mixed PEL brush modified Toyopearl in column chromatography

In order to investigate pH-responsive behaviour of the mixed PEL brush modified matrix in a column chromatography, it had been operated in two conditions. One is loading proteins at pH 4 to explore the anion exchange side from P2VP chains and proteins were then eluted by shifting pH to 7. Finally, the column was regenerated by diluted NaOH. Another condition is inversely loading proteins at pH 7 for the cation exchange binding from PMAA chains and pH was then shifted to 4 for elution. The regeneration was performed by diluted citric acid. All buffers used in this study, including regeneration solutions, were low ionic strength to investigate PEL brush performance in 'osmotic regime' with only pH effect. The regeneration was also operated low ionic strength acid or base to obtain extremely acidic or basic pH. In these pHs, the brush was expected to fully ionised and stretched out to kick any protein out from the adsorbent. High salt buffer, used in a conventional ion exchange matrix, might cause complex brush behaviour and brush shrink as previous reported in a flat surface (Drechsler *et al.*, 2010, 2018; Elmahdy *et al.*, 2016).

The model proteins used in this column chromatography were pepsin, myoglobin, and lysozyme, which represent an acidic, neutral, and basic proteins, respectively. From previous static binding studies, these proteins performed a good adsorption to mixed PEL supports and reflected an electrostatic interaction as a function of pH. These proteins can, however, not be mixed together and loaded in the column at the same time because pepsin will break down another two proteins and intense charge interaction between pepsin and lysozyme might lead to aggregation. Therefore, pepsin was separately loaded in the column, while the mixture of lysozyme and myoglobin was loaded together. However, the chromatography was operated in the similar conditions and the time (or volume) was synchronised to emulate a pararell runing of three proteins.

For the pepsin loading at pH 4 (Figure 4-13 a-d), the flowthrough fractions were expected to come out approximately at 1.5 mL (0.5 mL sample loop + ~1 mL column volume). UV absorbance trace at 280 nm (commonly used for protein detection), from the chromatogram show that pepsin was not found in flowthrough when it was loaded into the column at pH 4 before 10 CV. This suggested all pepsin bound with the support. The elution step was then conducted by step changing to 100% gradient of pH 7 buffer. The large peak was observed when pH shifting up. At 20 mL, the regeneration buffer, 10 mM NaOH, was initially fed to the column leading to gradually increase in pH gradient. Therefore, the pepsin peak was not completely dropped to the baseline and the small peak at 27 mL started to appear when pH reached around 7.2. This small peak continued until 31 mL when pH was 7.4, just before pH shooting because of diluted NaOH. This chromatogram strongly correlated with the protein contents in the fractions (Table 4-6). No protein was observed in the flowtroough fractions. Most pepsin was found in the first elution peak and some was observed in the second elution peak, which was just before the regeneration step. From the mass balance, it suggests that all

loaded protein bound to the column and subsequently it was completely eluted when pH was increased to 7.4.

When the mixture of lysozyme and myoglobin was fed into the column at pH 4, only flowthrough peak was shown (Figure 4-13 b). No peak was obtained by changing pH to 7 or higher. This indicates both proteins came off in the flowthrough. It was confirmed by the LDS-PAGE (Figure 4-13 d), Two bands represented lysozyme and myoglobin were found in the first two flowthrough fractions (F2 and 3). Elution and regeneration fractions were also analysed, but no band was shown the gel. Furthermore, The mass balance from the protein content analysis pointed out to the similar result. Loaded protein content was equal to the total content of the flowthrough fractions (Table 4-6).

This column chromatography demonstrated that mixed PEL brush modified support displayed pH-resposive behaviour of dynamic protein adsorption/desorption, which was similar to the previous static protein binding study. The volume of loaded protein was 125 μL. However, the flowthrough of lysozyme and myoglobin needed approximately 8 mL of washing buffer to bring protein out. This delay suggested that both proteins have some weak interaction with the mixed PEL brush or protein-protein interaction might affect this. It is noted that the pH curve of pepsin binding was slightly decreased after 9 mL, which was different from the pH curve of other proteins (Figure 4-13 b), and of only buffer (Figure 4-13 c). This might explain by bound pepsin replacing counter ions in the support. Consequently, the ions were released into the low ionic strength buffer causing a drop in pH.

When the proteins were loaded at pH 7 (Figure 4-13 e-h), pepsin was completely obtained in the flowthrough fraction, while no peak of UV 280 nm was observed in the elution and regeneration fractions, where the pH gradient was changed to pH 4 and pH 2.8, respectively.

The pH gradient after loading with pepsin was performed in the similar way as the one without protein loading (Figure 4-13 g). The protein content in the fractions, analysed by BCA assay, was matched with the peaks in chromatogram (Table 4-6). The total protein in the flowthrough fraction was 0.5 mg, which was equal the pepsin loaded in the column, whereas no protein was found in other fractions.

Loading the mixture of lysozyme and myoglobin at pH 7 resulted in two different peaks in different areas (Figure 4-13 f). One was in the flowthrough and another one was in the elution when shifting pH. According to the LDS-PAGE, the flowthrough was identified as myoglobin, whereas the elution contained lysozyme (Figure 4-13 h). Two proteins were completely separated as expected. Myoglobin did not bind with the ionised PMAA brush in the support and came out straight in the flowthrough, while lysozyme bound to the brush and was later eluted because of collapsed PMAA brush when changing pH from 7 to 4. No protein was found in the regeneration (at pH 2.8) fraction as observed from chromatogram and LDS-PAGE. The protein content also agreed with both analyses. The values from the flowthrough and elution fraction were 0.49 and 0.51 mg, respectively. The mass balance showed that no protein left in the column after the elution step. This suggested that pH shifting elution was efficient.

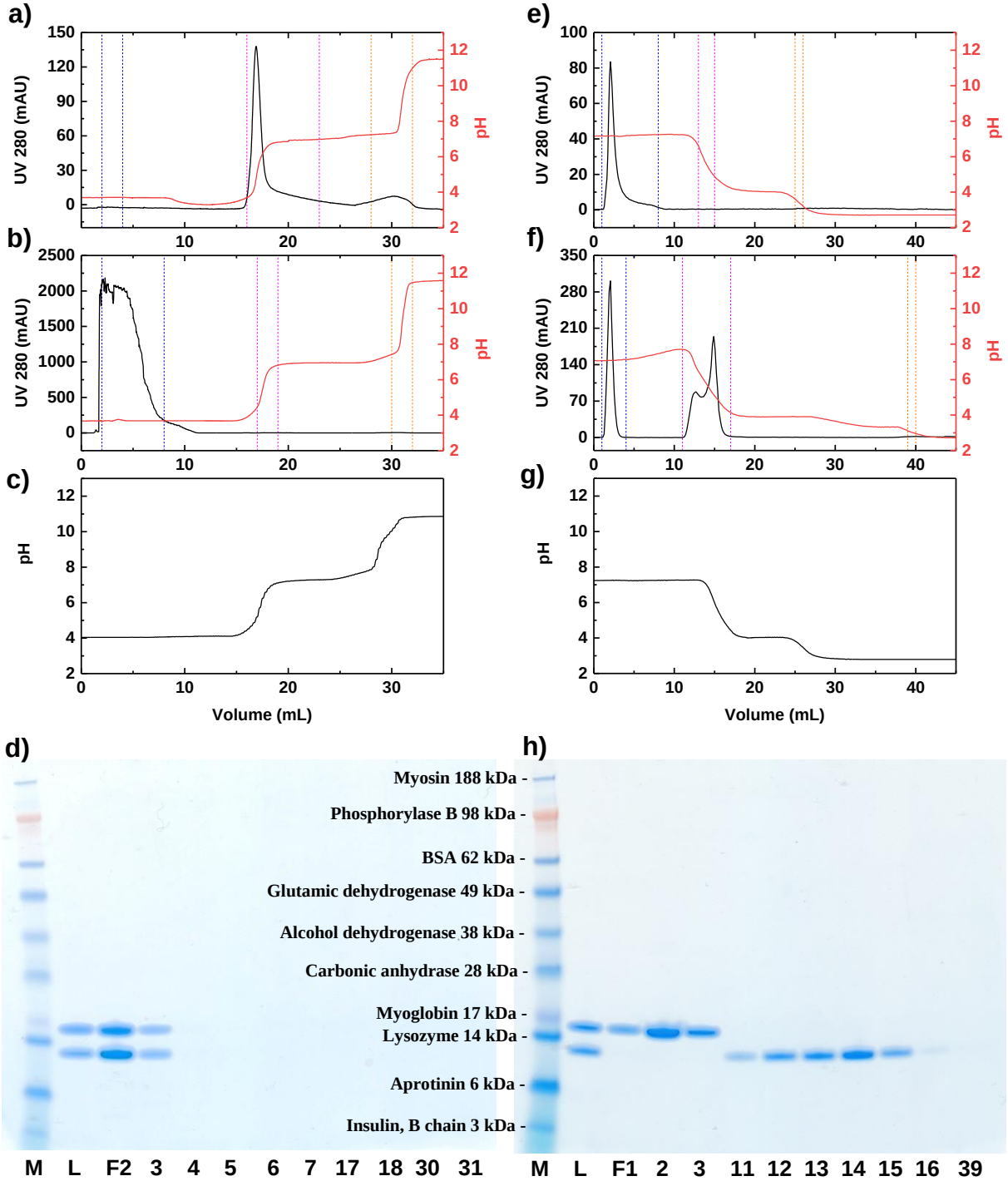

Figure 4-13 Chromatograms of mixed PEL brush modified Toyopearl with different loading proteins at pH 4: a) pepsin; b) lysozyme and myoglobin; c) only buffer; and at pH 7: e) pepsin; f) lysozyme and myoglobin; g) only buffer. SDS-PAGE of fractions collected from chromatography of lysozyme and myoglobin loading at d) pH 4 and h) pH 7. (M: marker, L: loading proteins, and F: fraction numbers related with the volume in the chromatograms, each fraction is 1 mL).

The pH gradient curve when loading lysozyme and myoglobin at pH 7 (Figure 4-13 f) was different from the ones without protein loading (Figure 4-13 g). This can be explained in the same way as it happened when loading pepsin at pH 4. At pH 7, lysozyme bound with the PMAA brush, so the ions were replaced and released from the support leading to slightly higher in pH at around 6 mL (Figure 4-13 f). This might also explain when the lysozyme elution happened and caused gradually decrease pH from 30 mL onward. Since the buffer used in the study was low ionic strength, slightly shifting in pH can occur from protein adsorption/desorption.

There is a difference between the flowthrough peaks of pepsin and myoglobin (Figure 4-13 e and f). Myoglobin came off straight from the column with a sharp peak, while pepsin had a bit of tail at the end of the peak. It suggested there is some weak interaction between pepsin and the brush causing delay of pepsin to pass through the column.

Table 4-6 Mass balance of protein content analysed from the fractions of chromatography.

Loading protein	**Loading pH**	**Loading content (mg)**	**Protein content in combined fractions (mg)**			**Mass balance (%)**
			Flowthrough	**Elution**	**Regeneration**	
Pepsin	4	0.5	0	0.414	0.085	99.8
Lysozyme& Myoglobin	4	1.0	1.018	0	0	101.8
Pepsin	7	0.5	0.538	0	0	107.6
Lysozyme& Myoglobin	7	1.0	0.493	0.522	0	101.5

4.3 Conclusion

Mixed PEL brush modified supports, consisting of PMAA and P2VP, have been fabricated by first grafting PMAA chains, and subsequently grafting P2VP. The effect of supplied P2VP concentration was investigated by applying the constant supply of PMAA. The maximum supply of P2VP (7.6 μmol/mL support) was observed as the best for fabricating mixed PEL supports. The mixed PEL modified Toyopearl support displayed pH-switchable behaviour according to zeta potential and sedimentation rate measurements. The full reversibility of mixed PEL brush was also obtained by changing between acidic and basic pH in both extreme (between 3.5 and 9) and intermediated (between 4 and 7) pH ranges. The PEL modified supports made from higher degree of tresylation Toyopearl demonstrated better characterisatics and performances. The effect of first grafting to second grafting steps was then determined by varying supply concentration of PMAA. With the highest supply of PMAA and P2VP created the best combination support, 'B-Mix 10'. This support provided balance amount of both polymers, 44: 56 mol% of PMAA: P2VP. pH mediated elution was examined after protein binding and B-Mix 10 demonstrated promising pH elution result. In conclusion, B-Mix 10 showed balanced compositions of PMAA and P2VP, which reflected in acidic and basic proteins binding, and showed sign of full reversibility when shifting pH, which reflected in pH mediated elution. Therefore, B-Mix 10 has a great potential and was selected for a further column chromatography study.

The first application of the mixed PEL brush modified adsorbent, manufactured by 'grafting to' method, in a column chromatography has been investigated. The chromatography was operated in low ionic strength buffers, where the mixed PEL brush was in 'osmotic regime' and can be fully affected by only pH alteration. When proteins were loaded at pH 4, pepsin was completely adsorbed to the support and was subsequently effectively eluted by shifting to pH 7.4, while the

mixture of lysozyme and myoglobin was passed straight through the column. Inversely, at pH 7, 0.5 mg of lysozyme was bound to the support and was later eluted at pH 4, whereas pepsin and myoglobin came out from the column at pH 7. These demonstrate the pH-responsive mechanism, shown in the previous studies. The extended and positively charged P2VP brush was occurred at pH 4 and was collapsed at pH 7, while the PMAA brush was extended and negatively charged at pH 7 and collapsed at pH 4. This is a proof that the mixed PEL brush modified support can be exploited in the column chromatography for protein separation based on its pI. Furthermore, the mixed PEL modified support show effective pH elution and a good recovery of protein, which bring a new aspect to a conventional ion exchange chromatography.

Chapter 5 Improvement of mixed PEL modified support

5.1 Introduction

As we demonstrated in the Chapter 2 and 3 that the mixed PEL brush modified Toyopearl had several advantages over a conventional ion exchange chromatography, including switchable anion-cation exchange performances, effective pH-responsive binding and elution, and low salt operational condition. The mixed PEL brush support did not only provide a great work in a static batch study, but it also performed well in the dynamic column chromatography. However, there is an issue about the protein binding capacity which was not high and improvement may be required to achieve better performance.

One aspect to improve this mixed PEL modified support is increasing the grafting density of cation exchange polymer, PMAA chains. The grafted PMAA chains were less dense than the grafted P2VP chains in the mixed PEL support, reflecting in the low binding of basic proteins. As the issue originated from large molecular weight of P*t*BMA (precursor of PMAA) with low solubility in the solvent, alternative polymer with higher solubility could replace P*t*BMA. Since chemical structure of P*t*BMA contains *tertiary* butyl protective groups (Figure 5-1 a), which create long side chains, it is difficult to be dissolved in a solvent. Poly (methyl methacrylate) (PMMA) has methyl protective groups (Figure 5-1 b) leading to better solubility in the solvent. With better solubility, high concentration of PMMA solution can be obtained and provide more PMAA chains to the support. Furthermore, PMMA can be hydrolysed and generate PMAA, as same as P*t*BMA (Patel *et al.*, 2006; Clarke, 2017).

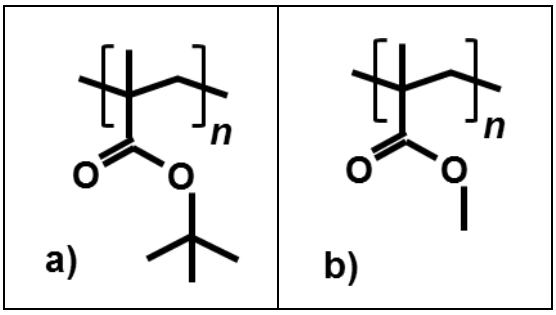

Figure 5-1 Chemical structures of a) P*t*BMA and b) PMMA.

Another way to upgrade the mixed PEL support is to improve the surface area of the base matrix. Agarose-based matrix with small particle size and narrow size distribution, such as, Praesto Pure 45®, can provide larger surface area that will allow more polymer chains to be anchored on. Also, with different based material, agarose adsorbent could offer different pore structure that might allow better access for the polymer chains. However, the agarose-based matrix need surface activation to create active sites for functionalised polymer chains. Sulphonyl chloride activation is one of the suitable approaches to establish stable covalent bond with amine or thiol-terminated groups of the polymer chains as it was conducted in the Toyopearl matrix.

As agarose matrix commonly exposes several hydroxyl groups at the surface, which can be attacked by a sulphonyl chloride group. The chlorine atom is subsequently replaced by the hydroxyl group, forming a sulphonyl ester group (Hermanson *et al.*, 1992). Pyridine was first introduced in this reaction to improve the performance in 1944 (Tipson, 1944) and since then sulphonyl chloride was widely used in organic syntheses. Adding pyridine helped to accelerate the reaction by removing generated hydrochloric acid (Hamilton *et al.*, 2001). The sulphonyl ester group, acting as a good leaving group, can be attacked by nucleophiles, including amine and thiol groups. This leads to formation of stable covalent bond (Figure 5-2).

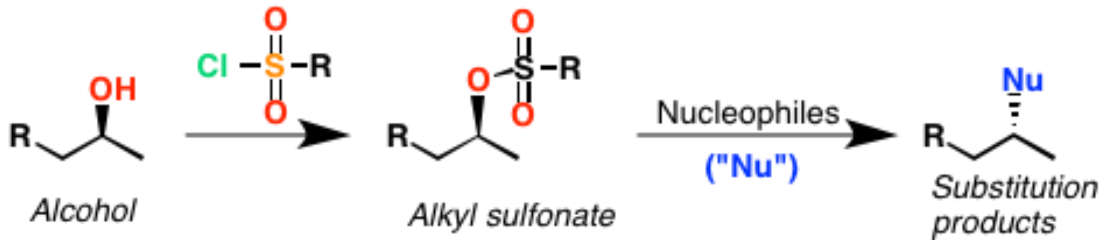

Figure 5-2 Sulphonyl chloride activation reaction and nucleophilic substitution reaction (Quintero and Meza-León, 2005).

Tresyl chloride (2,2,2-Trifluoroethanesulphonyl chloride) is one of the most extensively used sulphonyl chlorides. Tresyl chloride has been used in several studies to coupling ligands to chromatography supports bearing hydroxyl groups, such as agarose and cellulose (Nilsson and Mosbach, 1980; Scouten *et al.*, 1986; Demiroglou *et al.*, 1994). These studies have demonstrated that tresyl chloride is suitable for activating surfaces, especially in agarose-based matrix.

In this work, the result and discussion section is separated into 2 parts. In part I, we explored the feasibility of PMMA, which has smaller molecular weight and better solubility, as an alternative cation exchange polymer with improved performances. The PMMA chains were grafted on the Toyopearl before de-protection to liberate PMAA chains. Routine analysis of this de-protected PMAA grafted Toyopearl was done and compared to the one contains grafted de-protected P*t*BMA. This includes protein binding and elution studies as a function of pH. Regarding part II, the agarose-based matrix, Praesto, was introduced as an alternative matrix for grafting PEL brushes. Praesto provides larger surface area and may be different pore structure that might improve grafting density and performances. Praesto was first activated using tresyl chloride and degree of tresylation was, subsequently, analysed by ICP-OES to investigate the optimum tresylation. The activated Praesto was grafted with homo and mixed PEL chains before routine analysis and functional test.

5.2 Results and discussion

5.2.1 Part I: PMMA grafting as an alternative cation exchange brush modified support

5.2.1.1 Fabrication of PMAA brush support from PMMA

Due to the problem of large molecular weight of P*t*BMA (MW = 29000, DP = 206), the solubility of P*t*BMA in acetone was not high enough to generate high grafting density of brush on the support. The large size of grafted P*t*BMA might also block more polymer chains to access active sites on the surface. This reflected in low protein binding as previously reported in Chapter 2. From this reason, PMMA (MW = 9800, DP = 98), which is smaller in size and is also a precursor for PMAA, was chosen as an alternative polymer to improve the performance of cation exchange PEL brush support.

The grafted PMAA on the tresylated Toyopearl (Batch B) support, which displayed around twice higher in degree of tresylation than 'Batch A', was compared to the grafted P*t*BMA ones (both 'Batch A' and 'B'), which was previously done in Chapter 3. Since PMMA is more soluble in acetone than P*t*BMA, higher concentration of PMMA could be supplied to the support (Figure 5-3). The higher grafted amount of PMMA was found when increasing PMMA supply until the point of 37.50 mg/mL support (Figure 5-3 left). The maximum grafting amount of 26.25 mg/mL support was observed at the maximum supply of 187.50 mg/mL support. From the supply of 37.50 to 187.50 mg/mL support, the grafted amounts seem to be plateau. This showed the similar trend and maximum grafted amount as the grafted-P*t*BMA Toyopearl 'Batch B' supports. However, the grafted PMMA chains and monomers were higher than the P*t*BMA chains (Figure 5-3 right and Table 5-1). It suggested that PMMA can more easily access to the active sites on the surface because of its smaller size and chain length. It is noted that both P*t*BMA and PMAA chains grafted on the 'Batch B' Toyopearl were higher than the P*t*BMA

chains grafted on the 'Batch A' Toyopearl (Table 5-1). This emphasises the influence of tresyl activation on the grafted chains on the support.

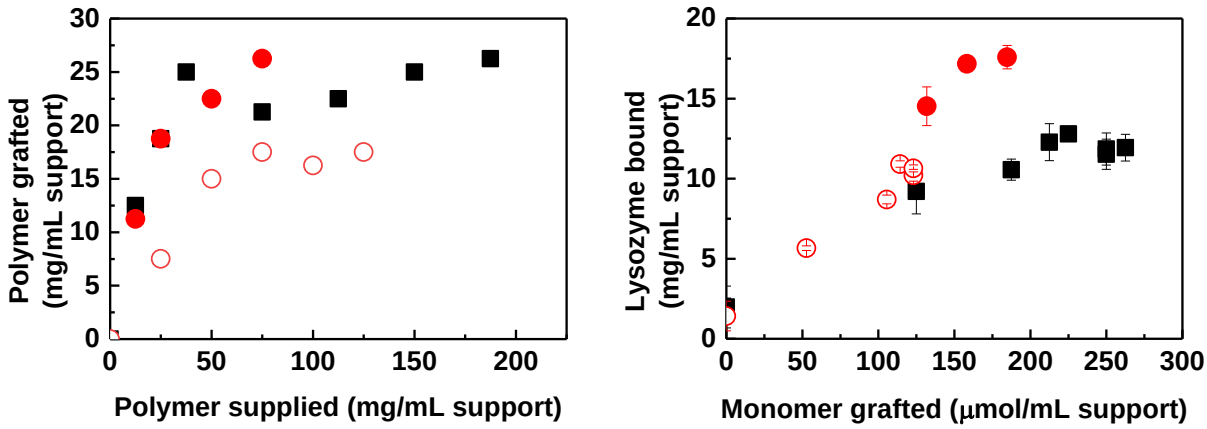

Figure 5-3 (left) Calibration curve of PEL loading for polymer-grafted supports. (right) Lysozyme bound against monomer grafted on the supports. De-protected PMMA-grafted support (close squares) and De-protected P*t*BMA-grafted Toyopearl support 'Batch A' (open red circles) and 'Batch B' (close red circles).

To investigate brush conformation, grafting density (σ**)**, inter-grafting space (D), and radius of gyration (R_g) were calculated from the mentioned equations 4-1, 4-2, and 4-3, respectively. These brush parameters were shown in Table 5-1.

Table 5-1 Brush characteristics of PMMA- and P*t*BMA-grafted support with different polymers supply.

Support	Polymer supplied (µmol/mL support	Polymer grafted (µmol/mL support	Grafting density, σ (chains/nm^2)	Inter-grafting, D (nm)	R_g (pH 10)	$D/2R_g$ (pH 10)
B-PMMA	1.28	1.28	0.10	3.18	5.17	0.31
	2.55	1.91	0.15	2.59	5.17	0.25
	3.83	2.55	0.20	2.25	5.17	0.22
	7.65	2.17	0.17	2.44	5.17	0.24
	11.48	2.30	0.18	2.37	5.17	0.23
	15.31	2.55	0.20	2.25	5.17	0.22
	19.13	2.68	0.21	2.19	5.17	0.21
B-P*t*BMA	0.43	0.39	0.03	5.76	8.02	0.36
	0.86	0.65	0.05	4.46	8.02	0.28
	1.72	0.78	0.06	4.07	8.02	0.25
	2.59	0.91	0.07	3.77	8.02	0.24
A-P*t*BMA	0.86	0.26	0.02	7.06	8.02	0.44
	1.72	0.52	0.04	4.99	8.02	0.31
	2.59	0.60	0.05	4.62	8.02	0.29
	3.45	0.56	0.04	4.79	8.02	0.30
	4.31	0.60	0.05	4.62	8.02	0.29

Higher grafting density and smaller inter-grafting space were obtained from PMMA-grafted support (Table 5-1). This leads to high possibility of brush formation as shown from $D/2R_g < 0.5$ (Zhu *et al.*, 2007). Therefore, the PMMA-grafted support could achieve higher binding capacity and could be beneficial for fabricating balance compositions of mixed PEL brush support.

The de-protected PMMA-grafted support with different grafting amount was hydrolysed to liberate PMAA brush and then bound with lysozyme at pH 9 (Figure 5-3 right). The lysozyme

binding correlated with the PMMA chains on the surface. When more PMMA chains were grafted, lysozyme binding was also higher. The plateau phase of binding reflected the plateau of PMMA grafted. It was appeared that lysozyme bound with the de-protected P*t*BMA-grafted supports were higher than the de-protected PMMA-grafted supports, even though higher grafted chains and monomers of PMMA were achieved. This indicates not all PMMA grafted monomers contributed to the lysozyme binding.

5.2.1.2 Protein binding and elution study

The lysozyme binding of de-protected PMMA brush support as a function of pH was conducted and was compared with the result from de-protected P*t*BMA brush 'Batch B' Toyopearl support (Figure 5-4 left). Low binding between lysozyme and the de-protected PMMA brush was found at low pH, while slightly higher binding was observed when pH became more basic. The highest lysozyme binding of 13.18 mg/mL support was achieved at pH 9, which was lower than the lysozyme binding of the de-protected P*t*BMA brush. The de-protected PMMA brush support did not display fully pH-responsive behaviour as shown in the de-protected P*t*BMA. At pH 7 and 8, the lysozyme binding of the P*t*BMA one was higher than the binding at pH 5 to 6, whereas the numbers from the PMMA one were slightly different. This suggests the de-protected PMMA brush was not fully ionised at mild basic pH due to likely incomplete hydrolysing PMMA chains to PMAA chains. As PMAA have a pKa of 6.4 (Santonicola *et al.*, 2010), the PMAA brush should be initially ionised from pH around 7 and bind with positively charged lysozyme. More ionised brush and higher binding can be expected with increasing pH. The hydrolysed P*t*BMA brush exhibited this PMAA brush behaviour. This indicated successful de-protection of P*t*BMA chains, which might be the issue for the PMMA brush.

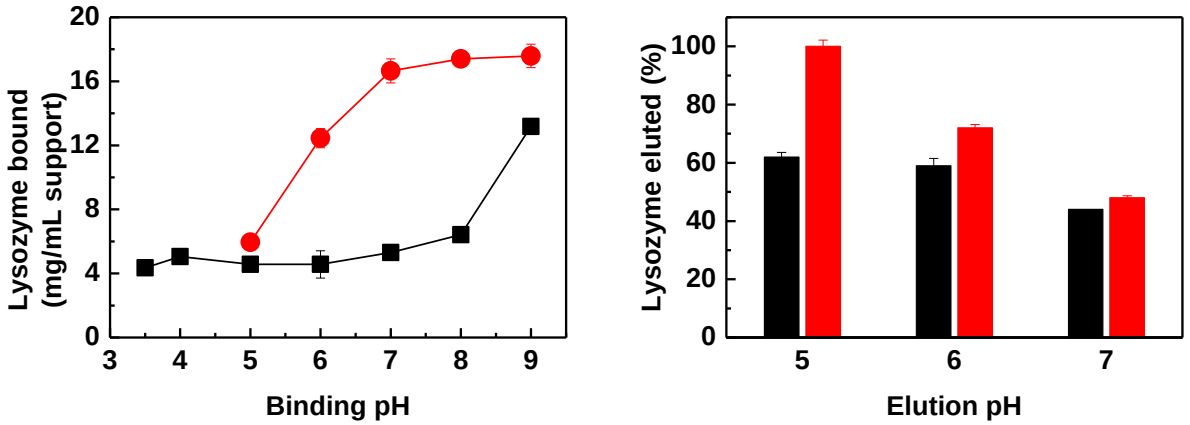

Figure 5-4 (left) Lysozyme bound of de-protected PMMA- (black squares) and P*t*BMA- (red circles) grafted Toyorearl supports as a function of pH. (right) pH mediated elution of bound lysozyme of de-protected PMMA- (black bars) and P*t*BMA- (red bars) grafted supports.

The pH shifting elution of lysozyme was performed after binding at pH 9 to explore pH-responsive desorption (Figure 5-4 right). Higher eluted lysozyme was observed in both de-protected PMMA and P*t*BMA brushes when higher pH switch range was conducted. The increase of lysozyme elution was around 40-50% when shifting each 1 pH unit for the de-protected P*t*BMA brush support, whereas, approximately 5-30% increase of lysozyme elution pH switch was observed for the de-protected PMMA brush support. This small increase when changing pH indicates low degree of ionisation. It was also supported by the maximum lysozyme elution at pH 5. 100% elution was achieved by the P*t*BMA one, while only 62% elution was obtained from the PMMA one. Therefore, the incomplete hydrolysis of PMMA might be the issue and need to be investigated.

5.2.1.3 FTIR analysis

The PMMA-grafted and de-protected PMMA-grafted brush supports were analysed by FTIR to check the hydrolysis step (Figure 5-5). The Toyopearl support is methacrylate base, and its chemical structure is quite similar to PMMA. Thus, the spectrum of base support and PMMA-grafted support were not much different. However, PMMA-grafted support showed absorption

band at 1148 cm^{-1} (ester C-O) (Yang and Dan, 2003; Zhang *et al.*, 2016). 1478 and 1255 cm^{-1} for methyl $–CH_3$ (Coates, 2006; Jiang *et al.*, 2010).

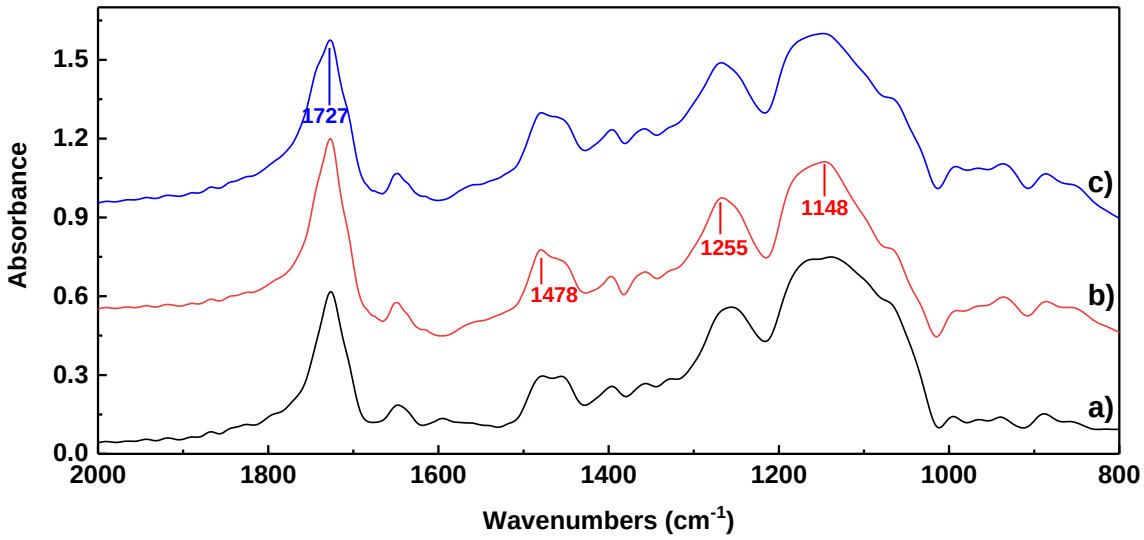

Figure 5-5 FTIR spectrum of a) Toyopearl, b) PMMA-, and c) De-protected PMMA-grafted supports.

After hydrolysis (Figure 5-5 c), the absorption peak at 1727 cm^{-1} was slight lower and broader, suggesting a change from ester carbonyl bonds to carboxyl carbonyl bonds (Zhang *et al.*, 2016). This change was subtle comparing to the one from hydrolysis of P*t*BMA (Figure 3-9). These could be due to the incomplete de-protection of PMMA. To examine this issue, the non-grafted polymers, both PMMA and P*t*BMA, were hydrolysed by the methods described before and a series of FTIR measurements were conducted along with PMAA, which is the desired polymer after complete hydrolysis.

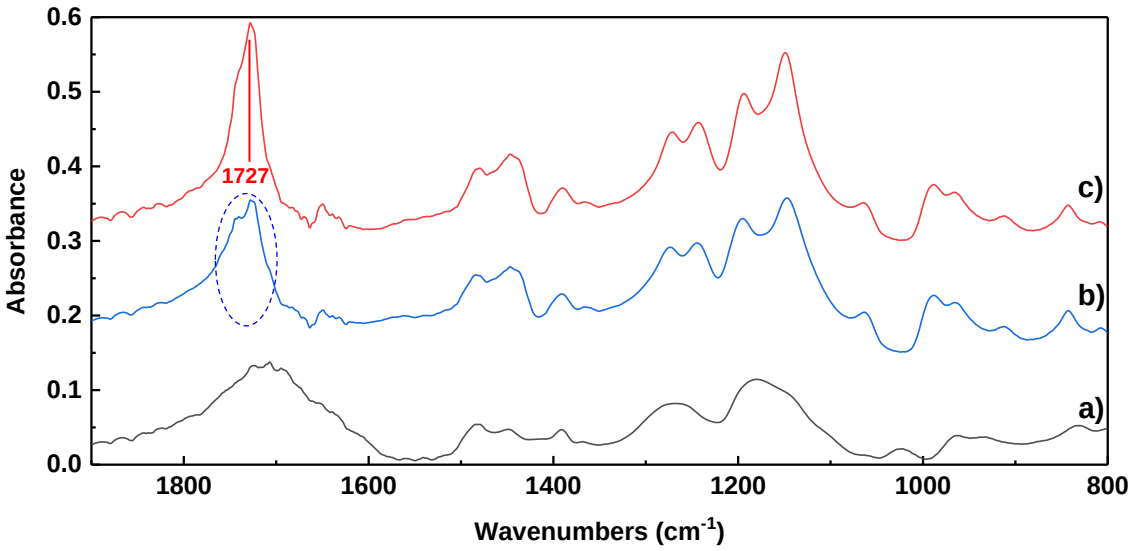

Figure 5-6 FTIR spectrum of a) PMAA b) hydrolysed PMMA, and c) PMMA.

The spectrum of PMMA and hydrolysed PMMA were shown in Figure 5-6 b) and c). They were quite similar, except the change of the peak at 1727 cm^{-1}. The broader and lower peak were observed for hydrolysed PMMA, indicating the change from the localised ester carbonyl to the delocalised carboxyl carbonyl, which was found in the PMAA spectra (Figure 5-6 a). These are likely from partial hydrolysis of PMMA. In contrast, the spectra from the hydrolysed P*t*BMA showed similarity to the one from the PMAA (figure 5-7). The complete change from the ester groups to the carboxylic groups was achieved, reflected from the similar broad peaks of the hydrolysed P*t*BMA and PMAA at 1727 cm^{-1}. Moreover, loss or reduction of the specific peaks for P*t*BMA was observed, including 1399 and 1366 cm^{-1} for the *tert*-butyl group; 849 and 1255 cm^{-1} for methyl $–CH_3$; 1147 cm^{-1} for ester C-O (Shin *et al.*, 2002).

These FTIR measurements demonstrated the incomplete de-protection of PMMA, which possibly caused low lysozyme binding of the support even though high grafting of PMMA was achieved. It is more challenging for hydrolysing PMMA and obtaining PMAA, as previously

reported (Semen and Lando, 1969; Erhardt *et al.*, 2003; Guo *et al.*, 2014). Therefore, optimisation for this is required to improve a better performance of PMMA-grafted modified support.

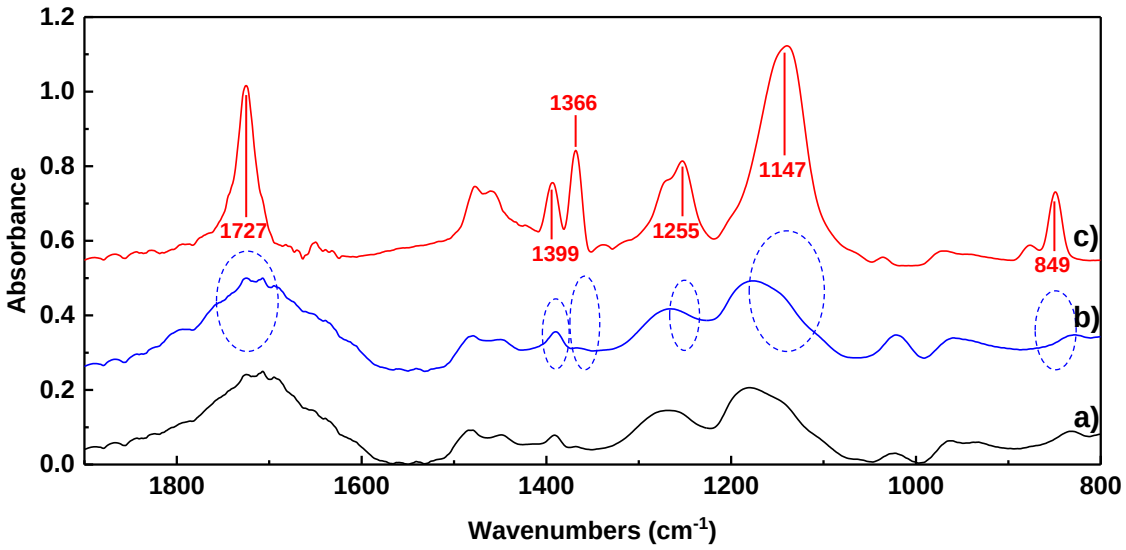

Figure 5-7 FTIR spectrum of a) PMAA, b) de-protected P*t*BMA, and c) P*t*BMA.

5.2.2 Part II: Agarose base matrix for PEL brush modified support

5.2.2.1 Tresyl chloride activation of agarose based matrix

'Graft to' approach has been also employed for PEL brush synthesis on the agarose based matrix, Praesto. A 'click-chemistry' was required to covalently bond base matrix with the polymers. Sulphonyl chloride reaction with amine or thiol groups were chosen for grafting because this conventional method has been studied for long time and proved to form a stable bond for ligand conjugation in chromatography supports. However, sulphonyl chloride activation of Praesto was required due to no pre-activated support is commercially available at the moment. Tresyl chloride was used to activate the agarose surface via hydroxyl groups. A series of tresyl chloride concentration was applied in the reaction to find an optimum concentration for the maximum activation. Sulphur content, specifically found in tresyl chloride, in the activated matrix was analysed using ICP-OES to determine degree of activation (Figure 5-8).

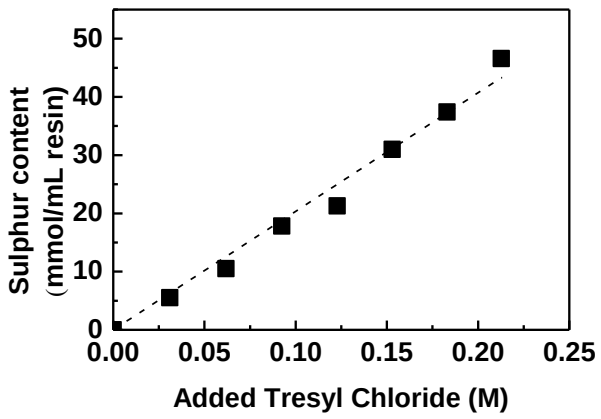

Figure 5-8 Sulphur content of tresylated Praesto against supplied concentration of tresyl chloride.

As the molar ratio between sulphur and tresyl chloride is 1:1, sulphur content in Figure 5-8 can be referred to tresyl activation of surface. This plot demonstrates that tresylation of Praesto

followed a linearly stoichiometric reaction. The maximum surface activated of 46.60 μmol/mL resin was obtained when supplying maximum tresyl chloride concentration of 0.21 M. This level of activation was fairly comparable with the number reported before from tresyl activation of Sepharose 4B (Demiroglou and Jennissen, 1990). The value from Sepharose 4B was slightly higher than the one from Praesto because Sepharose 4B was not cross-linked agarose support and had more available hydroxyl groups. Although the degree of activation could be increased beyond 46.60 μmol/mL resin, the tresyl concentration cannot exceed 0.21 M because it will lead to a destruction of the agarose matrix (Demiroglou and Jennissen, 1990). From this reason, 0.21 M of tresyl chloride has been used for all grafting studies to possibly obtain the highest active sites.

5.2.2.2 Fabrication of PEL brush on agarose based matrix

The tresylated Praesto was supplied by three different concentrations of P*t*BMA (20, 40, and 60 mg/mL support) or P2VP (20, 40, and 80 mg/mL support). These concentrations were chosen based on the previous studies in Toyopearl support (Chapter3) and the limited maximum solubility in acetone of both P*t*BMA and P2VP. The grafted amount of P2VP was increased with more P2VP supply and then reached the plateau phase at supply of 40 mg/mL support (Figure 5-9). The maximum number of 32.0 mg/mL support was achieved at 60 mg/mL support of P2VP supply. On the other side, P*t*BMA grafted amount was roughly similar for each P*t*BMA supply concentration and the maximum value of 8.4 mg/mL support was obtained from 60 mg/mL support of P*t*BMA supply. The P2VP grafted amount on the Praesto was quite similar to the one on the Toyopearl and the loading curve also show the same trend, whereas the P*t*BMA grafted amount on the Praesto was lower than the one on the Toyopearl and this grafted amount was limited since the lowest supply of P*t*BMA without much improving by increasing supply. This suggests that P*t*BMA might struggle to access to the Praesto surface.

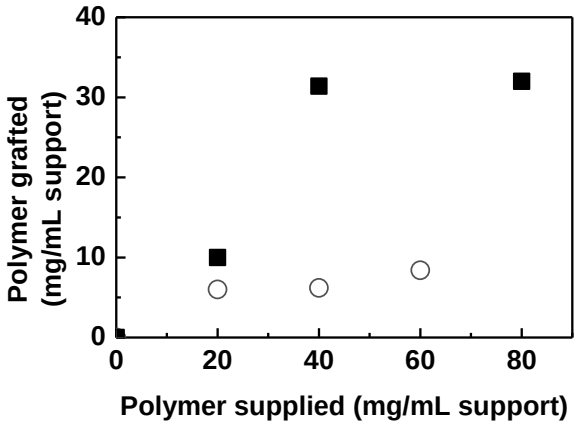

Figure 5-9 Calibration curve of PEL loading for P2VP-grafted activated Praesto (close squares), and P*t*BMA-grafted activated Praesto (open circles)

Brush characteristics were calculated, according to the equation 4-1, 4-2, and 4-3 in Chapter 2, to investigate the possibility of brush formation as previously determined in the Toyopearl support. Table 5-2 shows the brush parameters, including grafting density, inter-grafted space (D), radius of gyration (R_g), and $D/2R_g$ value, in a good solvent state to predict a conformation of the polymer chains on the Praesto support.

Table 5-2 Brush characteristics of PMAAand P2VP grafted Praesto

Support	Polymer supplied (µmol/mL support	Polymer grafted (µmol/mL support	Grafting density, σ (chains/nm^2)	Inter-graft space, D (nm)	R_g (nm)	$D/2R_g$*	
						pH 2	pH 10
PMAA	0.69	0.21	0.002	21.95	8.02	-	1.37
	1.38	0.21	0.003	21.59	8.02	-	1.35
	2.07	0.29	0.003	18.55	8.02	-	1.16
P2VP	1.52	0.76	0.008	11.47	12.17	0.47	-
	3.03	2.38	0.024	6.47	12.17	0.27	-
	6.06	2.42	0.024	6.41	12.17	0.26	-

*Calculation based on the good pH for each brush which allows them to be fully charged and extended.

The numbers show that the grafting density for both PMAAand P2VP on Praesto was smaller than the one for Toyopearl due to a larger surface area of Praesto. Although comparable amount of polymers grafted on the surface, larger surface area led to low grafting density and high inter-grafted space. From $D/2R_g$ values and the previously mentioned criteria (Zhu *et al.*, 2007), P2VP chains were likely to form a brush conformation, whereas, a mushroom regime was possibly formed from P*t*BMA chains on the Praesto support. Accessibility of the Praesto for the PMAAchains might be limited and cannot produce high grafting density for brush conformation. The PMAA- and P2VP-grafted support with the highest grafting density was employed in the further studies because of high possibility of PEL brush formation.

5.2.2.3 Characterisation of PEL modified Praesto

FTIR technique was employed to evaluate the presence of both grafted P*t*BMA and P2VP on the support. The spectrum of agarose based matrix, Praesto, P*t*BMA-, and P2VP-grafted Praesto were demonstrated in Figure 5-10. The unique absorption peaks of P*t*BMA were observed in

the spectrum of P*t*BMA-grafted support. These include the peaks at 1739 cm^{-1} for the carbonyl group (C=O), 1460 cm^{-1} for the methylene group vibration (-CH_2-), and 1374-1252 cm^{-1} for the methyl groups (-CH_3). In case of P2VP-grafted support's spectrum, the specific peaks at 1600, 1567, 1471, and 1434 cm^{-1}, corresponding to the aromatic carbon, were found. Apart from these peaks, there were also common peaks found in both spectrum, including the secondary amine peaks (N-H) at 1663-1642 cm^{-1} and C-N peaks at 1180-1179 cm^{-1}. These absorption peaks were obtained as a consequence of amine-terminated polymers coupling with tresyl activated Praesto. This finding confirms the success of P*t*BMA and P2VP grafting.

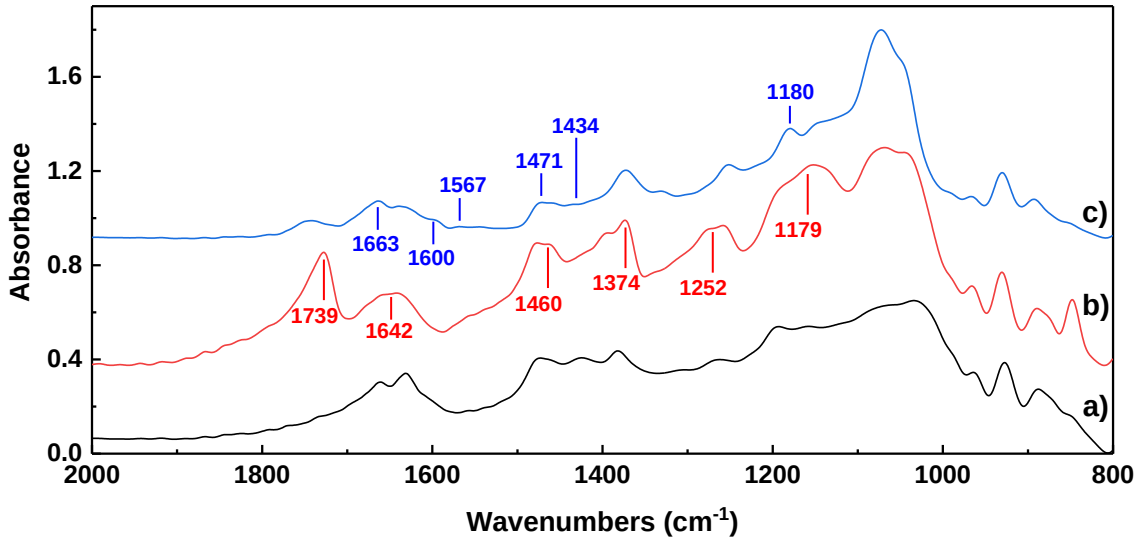

Figure 5-10 FTIR spectrum of a) agarose base matrix, Praesto, b) P*t*BMA-grafted, and c) P2VP-grafted Praesto.

The FTIR spectrum of de-protected P*t*BMA grafted Praesto was obtained and compared to the P*t*BMA-grafted Praesto to check hydrolysis process (Figure 5-11). Change from the ester carbonyl groups to the carboxyl carbonyl groups was achieved, reflecting from lower and broader peak at 1727 cm^{-1}. Loss or reduction of the P*t*BMA's peaks was observed, including 1399 and 1366 cm^{-1} for the *tert*-butyl group; 849 and 1255 cm^{-1} for methyl –CH_3; 1147 cm^{-1}

for ester C-O (Shin *et al.*, 2002). This suggests the good conversion from P*t*BMA to PMAA brush.

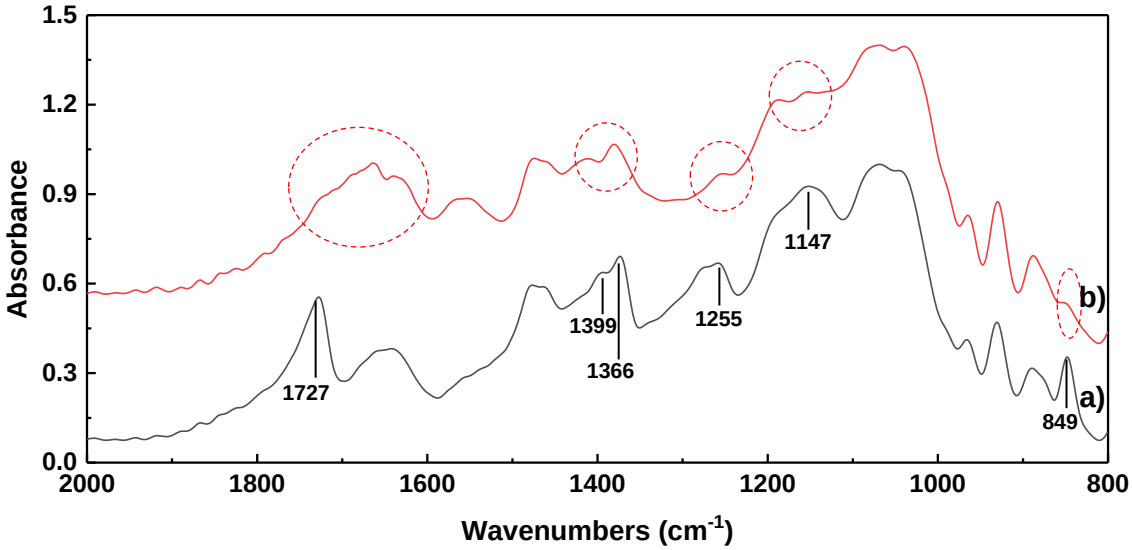

Figure 5-11 FTIR spectrum of a) P*t*BMA- and b) de-protected P*t*BMA-grafted Praesto.

To explore the uniformity of grafted polymers on the Praesto, CLSM was used to investigate the binding between the grafted support and fluorescence-tagged proteins, which will refer to the distribution of polymers in the beads. Strong light intensity from Cy 5-tagged lysozyme was observed throughout the PMAA (de-protected P*t*BMA) grafted Praesto (Figure 5-12 b), while no signal of the tagged lysozyme on the control Praesto was observed (Figure 5-12 a). For the P2VP grafted Praesto, high intensity of signal from Texas red-tagged BSA was shown (Figure 5-12 d), whereas, the signal was unobservable on the control one (Figure 5-12 c). This finding indicates a good distribution of polymer in the Praesto matrix.

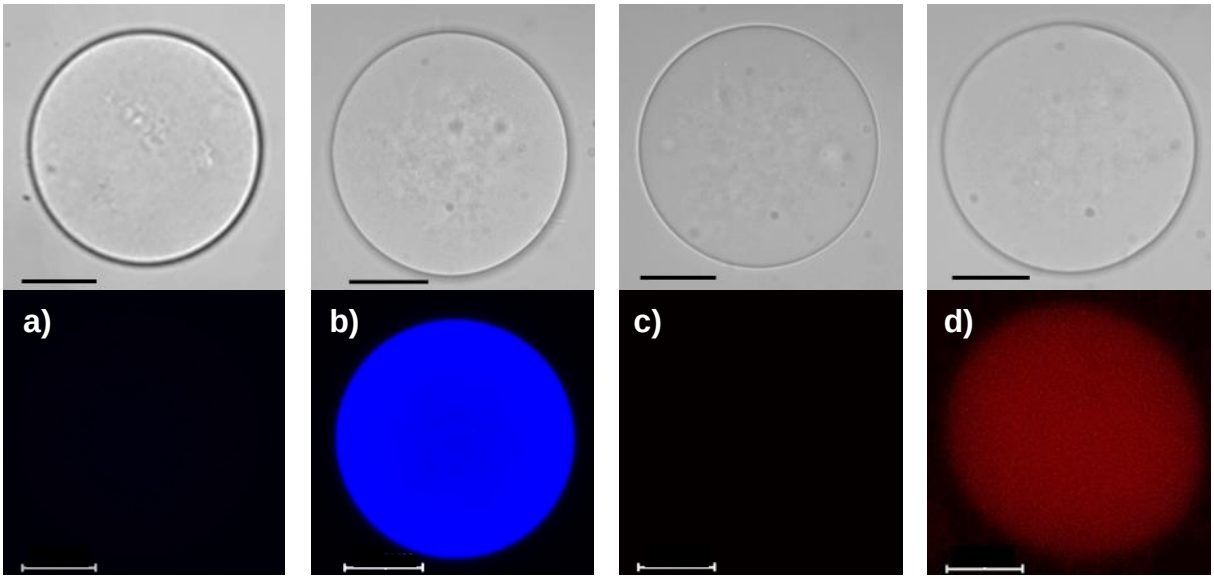

Figure 5-12 CLSM images of a) control and b) PMAA grafted Praesto bound with Cy 5-tagged lysozyme, c) control and d) P2VP grafted Praesto bound with Texas red tagged BSA. Top images are the same supports on a light microscope. Scale bar represents 20 μm**.**

Zeta potential measurement had been conducted to determine surface charges of the support after grafting with PMAA and P2VP (Figure 5-13). The Praesto base matrix demonstrated negative zeta potential values amongst the studied pHs. These negative values were comparable with the values previously reported for other agarose particles (Huang *et al.*, 2011; Ibraheem *et al.*, 2014; Li and Liu, 2018). The P2VP-grafted Praesto exhibited positive zeta potential numbers at acidic pH (3.5-5) due to protonation of P2VP and subsequent hydronium ions adsorption. In contrast, at basic pH, adsorption of hydroxyl ions resulted in negative zeta potential values (Drechsler *et al.*, 2012). These values are roughly similar to the ones published for P2VP (Burkert *et al.*, 2009; Billing *et al.*, 2016). The difference of zeta potential between the base matrix and the P2VP-grafted one confirms successful incorporation of P2VP to the surface. The PMAA-grafted Praesto, however, showed a slight difference from the base matrix in zeta potential curve. At acidic pH, the zeta potential values of the PMAA-grafted support were shifted up, which indicated PMAA-attached surface (Yu and Chow, 2004). The small changes might come from similarity of PMAA's zeta potential curves with the base matrix

(Houbenov *et al.*, 2003; Li *et al.*, 2014). Another possible explanation is that low amount of PMAA was grafted on the support as previously mentioned.

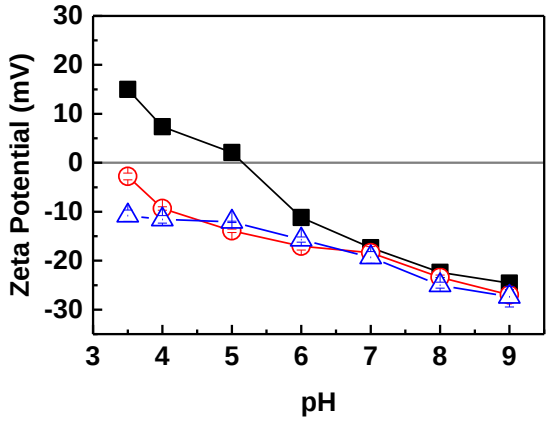

Figure 5-13 Zeta potential measurement of Praesto base matrix (open triangles), PMAA-grafted Praesto (open circles), and P2VP-grafted Praesto (close squares) as a function of pH.

5.2.2.4 Functional test by static protein binding and elution

The static protein adsorption as a function of pH was conducted by using the model proteins that previously used in the PEL modified Toyopearl in Chapter 3. List of model proteins, including pepsin, amyloglucosidase, BSA, myoglobin, RNase, and lysozyme, and their pIs were shown in Table 3-1. Briefly, acidic proteins (pepsin, amyloglucosidase, and BSA) and a neutral protein (myoglobin) were assigned to the P2VP-grafted Praesto, acting as an anion exchange adsorbent. On the other hand, basic proteins (RNase and lysozyme) and also a neutral protein (myoglobin) were applied to the PMAA-grafted Praesto, displaying a cation exchange matrix. The PMAA- and P2VP-grafted Praesto with the maximum grafting density were selected for the binding and elution studies to provide the possibly highest protein bound. As previously done in the polymer-grafted Toyopearl, the binding and elution studies for the Praesto were performed in low ionic strength buffer to investigate only pH effect on brush behaviour.

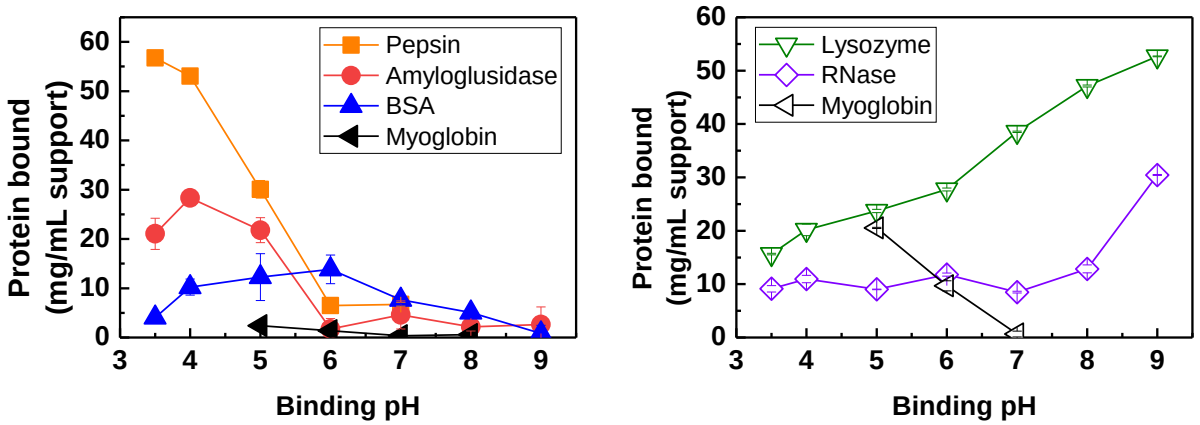

Figure 5-14 Static protein binding studies of P2VP-grafted Praesto (left), PMAA-grafted Praesto (right).

The P2VP-grafted Praesto expressed pH-responsive protein adsorption with the acidic proteins (Figure 5-14 left) as same as the P2VP-grafted Toyopearl, but higher protein binding was obtained (Figure 3-13). High binding of pepsin and amyloglucosidase was found at pH below 6 because P2VP chains were protonated at pH below 6.7 (Houbenov *et al.*, 2003) and bound with negatively charged pepsin and amyloglucosidase. Only amyloglucosidase bound at pH 3.5 was slightly dropped because it was close to amyloglucosidase's pI and it provided less charged. The BSA highly bound with the P2VP-grafted Praesto at pH 5 and 6, where BSA and P2VP chains were oppositely charged, according to BSA's pI and pK_a of P2VP. From pH 6, less protein binding was initially observed since the P2VP brush started to collapse as expected (Drechsler *et al.*, 2010). No binding of myoglobin was shown because no charge interaction was expected. Protein binding of the P2VP-grafted Praesto was higher than the one of grafted Toyopearl, which might be caused from larger surface area of Praesto provide more active sites to P2VP and also proteins for binding.

The PMAA-grafted Praesto also exhibited pH-responsive behaviour as shown in lysozyme and RNase binding (Figure 5-14 right). Since the pK_a of PMAA was approximately 6.4 (Santonicola *et al.*, 2010), rise of ionised PMAA chains can be expected when increasing pH above 6.4. This

led to increased lysozyme and RNase bound at basic pH. The lysozyme and RNase bound of the PMAA-grafted Praesto was 3 to 4 times higher than the one of grafted Toyopearl (Figure 3-13). Myoglobin binding of this PMAA-grafted Praesto showed similar trend of binding as the one from Toyopearl, but in higher numbers. In spite of larger surface area provided by Praesto support, grafted amount of PMAA was not higher than the grafted Toyopearl. It indicates that high protein binding was not directly related with high grafting density of PMAA chains in case of Praesto support. A possible explanation for these results may be the lack of brush formation from the PMAA chains grafted on the Praesto leads to a wide space between the PMAA chains. Thus, proteins can possibly penetrate through the chains and can also bind at the side of the chains or the protein can probably be trapped at the support surface. In case of the brush conformation, small inter-graft space is expected because high grafting density of polymer chains, so, proteins are unlikely to penetrate through the brush and are expected to bind at the top of the brush. To test this assumption, further studies have to be done, including protein elution and protein binding against polymer grafted.

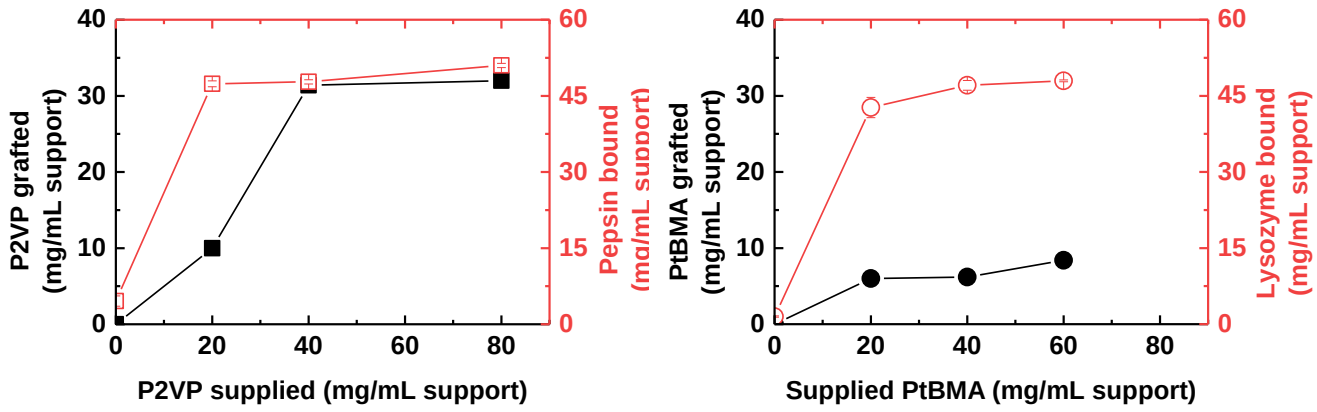

Figure 5-15 (left) Influence of P2VP supplied to P2VP grafted on Praesto (black close squares) and pepsin binding (red open squares). (right) Effect of supplied PtBMA on PtBMA grafted on Praesto (black close circles) and lysozyme binding (with de-protected P*t*BMA, PMAA) (red open circles).

The grafted amount of P2VP and pepsin binding affected by P2VP supply were demonstrated in Figure 5-15 left. Pepsin bound correlated with P2VP grafted on the surface at P2VP supply of 40 and 80 mg/mL support, where the higher grafting density was achieved comparing to the number from 20 mg/mL of P2VP supply. However, at 20 mg/mL support of P2VP supply, pepsin bound was comparable to the values from 40 and 80 mg/mL support, even though less than a half of P2VP grafted. This suggested that at low grafting density of P2VP, pepsin tended to pass through a space between the P2VP chains, which was larger than the one from high grafting density, and possibly bound to the side of the P2VP chains rather than only on the top of chains, in case of brush formation. As reported by Gtari *et al.* (2017) and Thévenot *et al.* (2017), hydrodynamic diameter of pepsin is approximately 6.0 nm. Therefore, at high grafting density, it is unlikely that pepsin can penetrate through the inter-graft space of P2VP chains because of the brush formation and the predicted inter-graft space of around 6.4 nm (Table 5-2). In contrast, the predicted inter-graft space was approximately 11.4 nm in case of low P2VP grafting density, which was around twice the size of pepsin and can likely allowed the protein to fill in the space.

For the PMAA-grafted Praesto, grafted amount of PMAA was low for all supply concentrations, which was, however, not proportionally related with high lysozyme bound (Figure 5-15 right). This was quite similar with the low grafting density of P2VP on the support and can be explained in the same way. As low grafting density was obtained from PMAA grafting, the inter-graft space was predictably around 18.5-21.9 nm, which was a lot larger than the values from the P2VP-grafted one. This infers that the proteins, with smaller size, are more likely to invade between the PMAA chains. It might also be the case for lysozyme, possessing hydrodynamic diameter of around 2.5 nm (Saha *et al.*, 2013). This finding supports the previous results of lysozyme binding as a function of pH and the reason that the PMAA-grafted Praesto

did not show a great pH-responsive behaviour and had some background binding at acidic pH might come from non-specific binding with the support and/or the non-brushed PMAA chains.

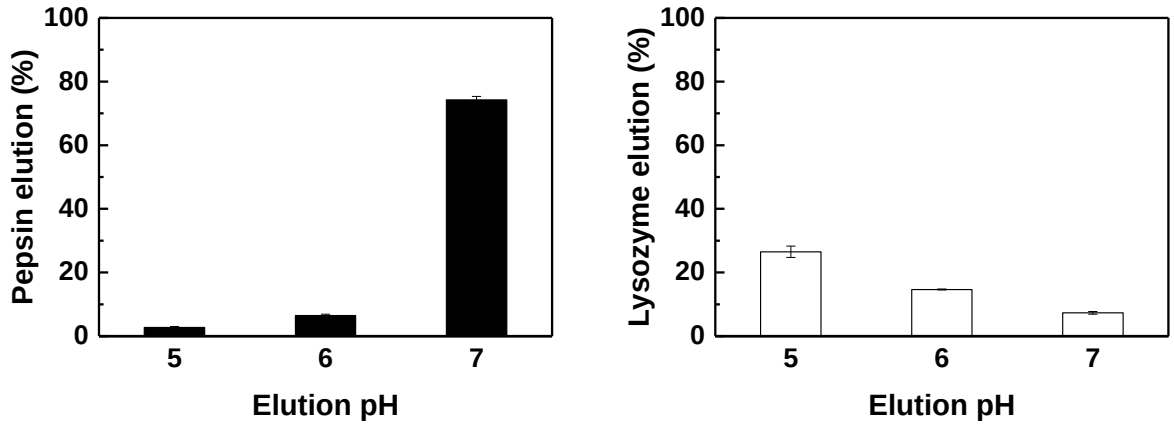

Figure 5-16 pH mediated elution of pepsin from P2VP grafted Praesto after binding at pH 4 (left) and lysozyme from PMAA grafted Praesto after binding at pH 9 (right).

The pH-mediated elution was performed after the maximum P2VP- and PMAA-grafted Praesto was adsorbed with pepsin and lysozyme at pH 4 and 9, respectively. The pH was shifted 1 to 4 pH units from the binding pH and elution was reported as eluted percentage from protein bound. As expected, the further pH from the binding pH, the higher the eluted percentage (Figure 5-16). Since both pepsin and lysozyme still displayed as similar charges as in binding pH, the elution was occurred due to the polymer chains collapse when shifting to these elution pHs. The elution trend was quite similar to the P2VP- and PMAA-grafted Toyopearl, but it showed lower numbers. The highest pepsin elution of around 70% from the P2VP-grafted Praesto was achieved when changing pH from 4 to 7. The percentage of elution was smaller than the one from the grafted Toyopearl, which was 100%. A possible explanation is that dense P2VP brush, with small inter-chain space, was successfully grafted on the Toyopearl, whereas, looser P2VP brush was observed on the Praesto and the inter-chain space was close to the hydrodynamic size of pepsin. There might be a chance that some pepsin molecules passed through the brush and bound at the side of the P2VP chains or the support surface, which could be subsequently

trapped during brush collapse in pH elution step. It is also noted that pH-responsive desorption of pepsin from the P2VP-grafted Praesto was not as spontaneous as from the grafted Toyopearl because not much pepsin elution was obtained when shifting pH to 5 or 6 and larger pH shift was required to elute pepsin. This correlates with the previous discovery that low grafting density of P2VP brush on the flat surface was less sensitive to pH and ionic strength (Elmahdy *et al.*, 2016).

The PMAA-grafted Praesto exhibited pH-responsive elution of lysozyme, although the values were around 4 times less than the grafted Toyopearl (Figure 5-16 right). Since very low grafting of PMAA chains was attached on the Praesto, most of lysozyme might pass through the PMAA chains and bind at the side of the chain and/or at the support surface. Consequently, during pH elution, the PMAA chains were collapsed and could trap lysozyme at the surface causing low lysozyme elution. This elution profile also supports the assumption that the PMAA brush was not formed and agreed with all protein binding results.

5.2.2.5 Fabrication of mixed PEL brush modified Praesto

Mixed PEL brush Praesto supports were manufactured by two different grafting sequences to explore the effect of first polymer on grafting density and its performance. The tresylated Praesto was first grafted with P*t*BMA chains by using the highest supply concentration to achieve the possibly highest grafting density of P*t*BMA. As previously shown in the mixed PEL grafted Toyopearl, the maximum P*t*BMA-grafted support still allowed P2VP chains penetrate to the active sites and were grafted. The P*t*BMA-grafted support was subsequently supplied with the highest P2VP concentration. Another different grafting sequence was done by first grafting with P2VP chains before P*t*BMA chains. The P2VP supply concentration used in the first step was 20 mg/mL support to obtain approximately a half of grafted P2VP, which allowed more space for the larger P*t*BMA chains to access the support surface. The supports were de-

protected to liberate PMAA. Both mixed PEL modified Praesto were listed in Table 5-3 with their compositions and brush characteristics.

Table 5-3 Brush characteristics of mixed PEL brush modified Praesto.

Support	Polymer grafted (µmol/mL support	Monomer contents (mol%)	Grafting density, σ (chains/nm^2)	Inter-graft space, D (nm)	D/2R_g		
					pH 2	Neutral	pH 10
PMAA	0.29	20	0.003	18.55	-	-	-
P2VP	1.91	80	0.019	7.21	-	-	-
Mix-PM*	2.20	-	0.022	6.72	0.31	1.06	0.85
P2VP	0.76	73	0.008	11.47	-	-	-
PMAA	0.17	27	0.002	24.04	-	-	-
Mix-PV*	0.93	-	0.009	10.35	0.50	1.67	1.23

*__Mix-PM__ represents mixed brush first grafted with PMAA and __Mix-PV__ represents mixed brush first grafted with P2VP.

The result shows that Mix-PM achieved higher grafting density of PEL brush than Mix-PV. This correlated with the previous studies in Toyopearl and also in the flat surfaces (Houbenov, 2005). There was a large gap between the P*t*BMA chains that allow smaller P2VP chains to pass through and access the active sites. By contrast, P*t*BMA chains were limited to access the surface after P2VP was grafted, even though less than a half of the maximum grafted P2VP was previously grafted. Due to high affinity of P2VP chains with the surface and its smaller size, P2VP was grafted at higher grafting density causing smaller inter-graft space that prevented the P*t*BMA chains to pass through.

According to the D/2R_g from Table 5-3 and the criteria previously published by Zhu *et al.*, 2007, Mix-PM was likely to form brush at pH 2, form mushroom at neutral pH, and form weak-

overlap at pH 10, while, Mix-PV possibly exhibited brush at pH 2 and formed mushroom at neutral and pH 10. As Mix-PM had higher grafting density of polymer chains than Mix-PV, the brush regime was more likely to happen in Mix-PM. However, brushes were only formed at pH 2 in both supports because only P2VP chains were grafted highly enough and could be ionised and extended at such pH. The protein binding and elution was further conducted to test the prediction of polymer chains conformation.

5.2.2.6 Protein adsorption/desorption of mixed PEL modified Praesto

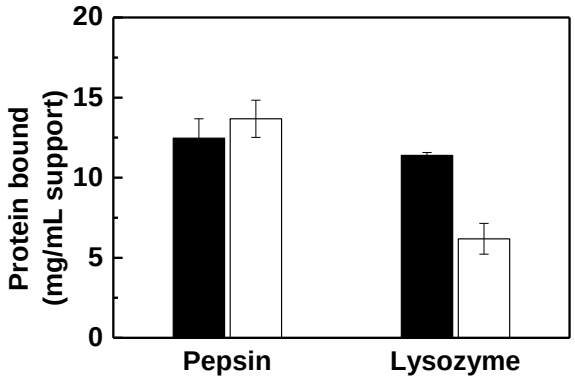

Figure 5-17 Static protein binding of Mix-PM (black bars) and Mix-PV (white bars), binding with pepsin at pH 4 and lysozyme at pH 9.

For binding study, pepsin and lysozyme were selected as model proteins to investigate anion and cation exchange properties of mixed PEL brush modified Praesto. Both Mix-PM and Mix-PV were able to bind pepsin at pH 4 and lysozyme at pH 9 (Figure 5-17). It indicates that both P2VP and PMAA could be incorporated in the mixed PEL support. The pepsin bound for both supports was very close and the values were around 3 to 4 times less than the one from the homo-P2VP grafted Praesto. This was due to the P2VP grafted on the mixed supports were lower, which allow grafting PMAA on the support. The PMAA chains could also interfere with the pepsin bound in the mixed brush, even though it was not fully ionised. For this reason, Mix-PM had slightly lower pepsin bound than Mix-PV because it contained higher amount of grafted

PMAA chains. For lysozyme binding, both Mix-PM and Mix-PV also showed 3 to 5 times less lysozyme bound than the homo PMAA grafted Praesto since lower grafting density of PMAA chains in the mixed brush one. Mix-PM had higher numbers than Mix-PV because of its higher grafting density of PMAA chains. The binding result well agrees with the polymer chains conformation as previously predicted. The pepsin bound for both supports was from protonated P2VP brush, while the weak-overlap regime of PMAA chains influenced higher lysozyme bound than the mushroom conformation of PMAA chains. According to this binding study, both mixed supports displayed bi-functional protein adsorption (anion and cation exchange). Mix-PM, however, demonstrated more balance in acidic and basic protein binding as higher grafting density of both P2VP and PMAA was obtained.

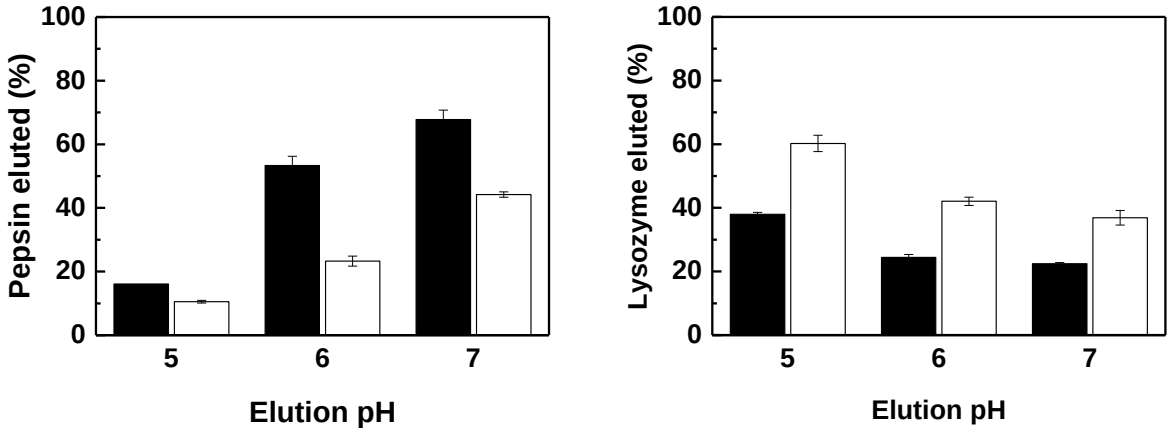

Figure 5-18 pH mediated elution of pepsin (left) and lysozyme (right) from Mix-PM (black bars) and Mix-PV (white bars) after binding at pH 4 for pepsin and at pH 9 for lysozyme.

The elution profiles for both mixed PEL Praesto supports displayed pH-responsive behaviour as the more the pH shift, the higher the protein recovery (Figure 5-18). It is noted that the percentage of elution from both mixed PEL supports in both proteins was improved from both homo PEL supports (Figure 5-16). These mixed PEL supports also showed more sensitive to the pH changing as illustrated in a fairly linear elution as a function of pH shifting. Moreover,

with small pH shift (1-2 pH units) from the binding pH, higher protein eluted was observed comparing to the one of the homo PEL Praesto. It indicates that mixed PEL supports promoted pH-responsive protein desorption. This might result from higher grafting density was achieved after introducing another polymer chains to fill an inter-graft space. Apart from increasing grafting density, this oppositely charged polymer chains could effectively push the bound proteins out from the support when changing pH. This effect demonstrated in pepsin elution from Mix-PM. Since Mix-PM contained higher amount of PMAA chains than Mix-PV, negatively charged PMAA can create repulsion force with similar charged pepsin leading to higher elution. However, this behaviour was not found in lysozyme elution, even Mix-PM had high P2VP chains. Mix-PV exhibited higher lysozyme elution than Mix-PM probably because lysozyme loosely bound to low amount of PMAA chains. Additionally, PMAA brush was unlikely formed in the mixed PEL Praesto. Thus, pH-responsive was less effective as shown in the homo PEL PMAA support. In order to improve the pH-responsive behaviour in protein adsorption and desorption, higher grafting density of polymer chains are required, especially cation exchange chains, PMAA.

5.2.2.7 Summary of protein binding and elution of homo and mixed PEL modified Praesto

The results described in this Part II indicate protein binding and elution on homo and mixed PEL Praesto was influenced by the polymer chains conformation on the surface and the inter-graft space between the chains. The conformation of attached polymer chains was dependant to the grafting density of chain and can be roughly predicted by $D/2R_g$ value, which is calculated by mentioned equations in Chapter 4. Three possible conformations of grafted polymer chains, including mushroom, weak-overlap, and brush, were described by Zhu *et al.*, 2007 and the schematic is shown in Figure 5-19.

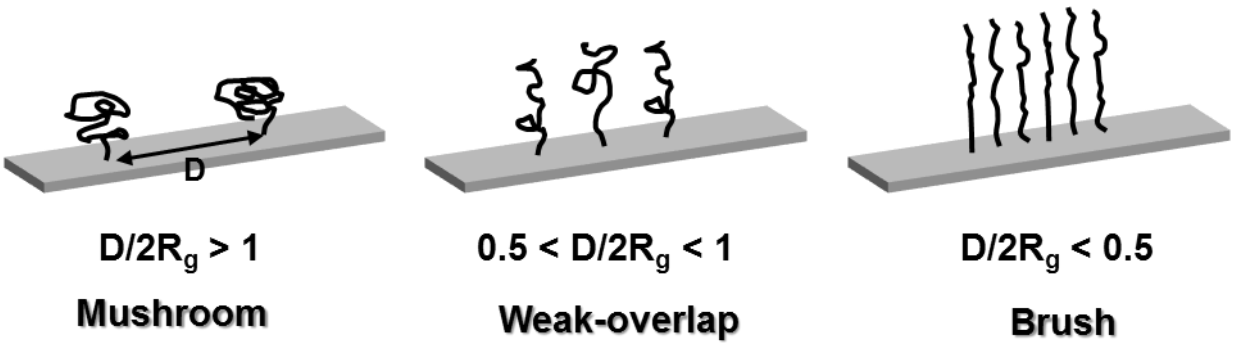

Figure 5-19 Different configurations of attached polymer chains determined by $D/2R_g$ value (adapted from Zhu *et al.*, 2007).

According to the protein binding and elution results of homo P2VP and PMAA grafted Praesto, schematic of proteins binding with the homo PEL Praesto was introduced in Figure 5-20. The P2VP brush was generated after grafting on the Praesto and bound with pepsin at acidic pH, where P2VP brush was protonated and stretched out from the surface and pepsin possessed negative charges. If high grafting density was achieved, P2VP dense brush could be obtained with a small inter-graft space. Thus, pepsin could hardly penetrate into the space and mostly bound at the top of the brush. In the case of low grafting density, the inter-graft space was larger, so pepsin could pass through the brush and bound at the side of the brush. This is possibly the reason why low grafting density of P2VP showed almost the same pepsin bound as the high grafting density one (Figure 5-15 left). As regards PMAA-grafted Praesto, only mushroom regime was formed because of very low grafting density of PMAA chains. With this regime, the gap between the PMAA chains was even larger than of the P2VP chains with low grafting density. Therefore, lysozyme could fill the gap and bound with the PMAA chains at the side at basic pH, where the PMAA chains were ionised and lysozyme had positive charges. The mushroom regime allowed some spaces for lysozyme binding under the PMAA chains. Hence, it could likely trap lysozyme at the surface when shifting pH and subsequently PMAA chain

collapse. This might also happen in the loose P2VP brush as reflected in the pH elution profile (Figure 5-16).

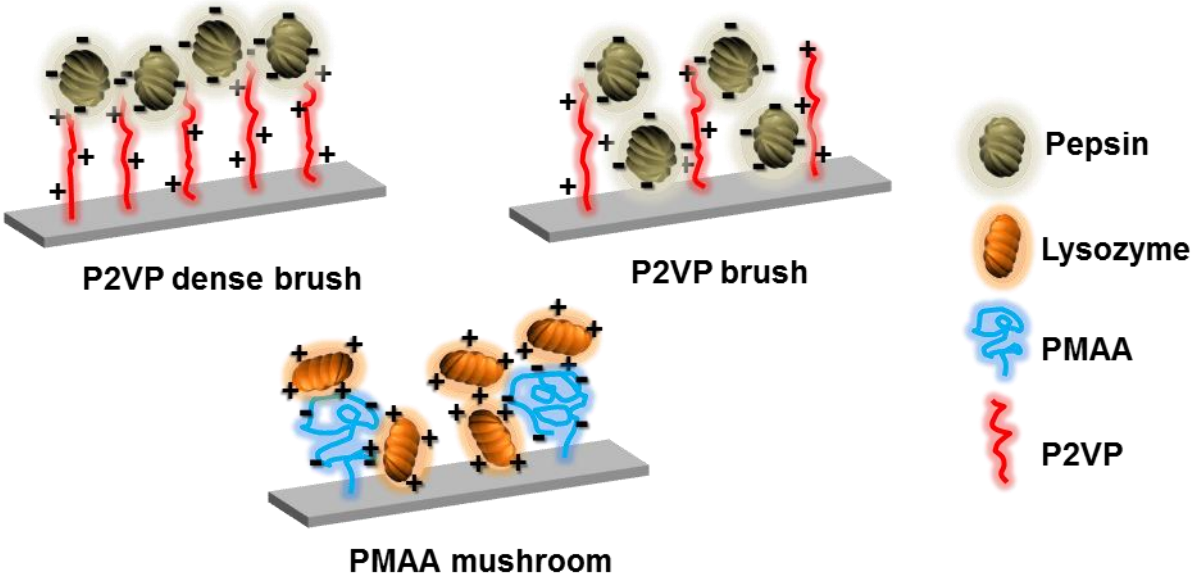

Figure 5-20 Schematic of homo P2VP and PMAA grafted Praesto bind with oppositely charged proteins, pepsin and lysozyme, respectively.

For the mixed PEL modified Praesto, schematic of proteins binding and elution was shown in Figure 5-21, where Mix-PM was selected as an example. The lysozyme and pepsin binding were decreased comparing to the numbers from the homo PEL grafted Praesto because another polymer chain were introduced on the surface and interfere proteins bound. Additionally, the polymer chains were also reduced to allow another polymer chain to graft on the surface. However, pH elution was improved in the mixed PEL Praesto as another oppositely charged polymer chains could repulse the similarly charged proteins out from the layer when changing to elution pH. Having another polymer chain on the surface might also prevent the proteins to interact with the surface. This improved elution reflected in more sensitive to pH shifting as previously mentioned.

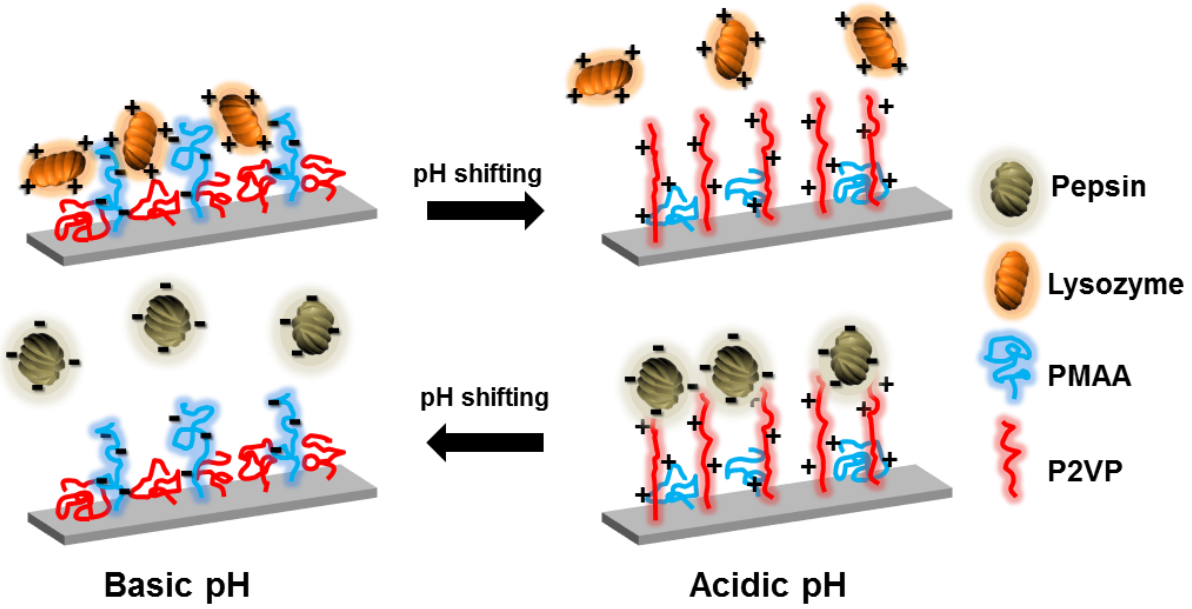

Figure 5-21 Diagram illustrates pH-responsive protein adsorption/desorption of mixed PEL modified Praesto (Mix-PM).

The protein adsorption and desorption study of mixed PEL modified Praesto demonstrates pH-responsive behaviour, which has a great potential to develop to bi-functional chromatography matrix. The Praesto agarose-based support provides large surface area for anchoring polymer, which encourages high binding capacity. However, polymers could not be densely grafted on the surface leading to form loose brush or non-brush configurations. Consequently, protein recovery was not as high as expected. A possible explanation for this might be that the structure of agarose matrix was mainly consisted of water and the grafting reaction was performed in dry acetone that could cause shrinking of agarose structure. Thus, it might prevent polymer chains to pass through the pore and access the active sites.

5.3 Conclusion

In part I, PMMA was selected as an alternative polymer for P*t*BMA, which was previously utilised and was likely to have an issue about low solubility, leading to limited accessibility to the support surface. PMMA with smaller molecular weight (MW = 9800) had higher solubility

and was grafted on the tresylated Toyopearl support with the same method used in grafting P*t*BMA. Grafting 2.68 μmol/mL support of PMMA chains was achieved and this was higher than the number from grafting P*t*BMA chains. With this high grafting density of PMMA chains, the calculated brush parameters show PMMA brush formation with smaller inter-graft space than P*t*BMA grafted support. However, after de-protection of PMMA, lysozyme binding was not higher than the one from P*t*BMA. The lysozyme adsorption and desorption of de-protected PMMA grafted support as a function of pH were also performed and it demonstrated that the support did not display pH-responsive behaviour in lysozyme binding and elution as expected from the PMAA brush, liberated from complete hydrolysing P*t*BMA or PMMA. This could be the de-protection of PMMA was incomplete and the brush cannot be fully ionised.

FTIR analysis has been carried out to investigate the root cause of this issue. The spectrum show that ester groups were slightly converted to carboxylic groups in the de-protected PMMA grafted support. Hydrolysis of non-grafted PMMA and P*t*BMA was performed and analysed by FTIR. The spectrum of the de-protected PMMA shows incomplete hydrolysis, whereas, the de-protected P*t*BMA's spectrum was identical to the one of PMAA, indicating complete hydrolysis. In conclusion, PMMA has a potential for grafting mixed PEL brush modified support with high grafting density. However, de-protection of PMMA need optimisation to achieve a better performance.

Part II described fabrication homo and mixed PEL grafted Praesto, which is an agarose base matrix possessing larger surface area than Toyopearl. P2VP and PMAA chains was successfully grafted on the Praesto using "graft to" approach, which previously used in Toyopearl. The presence of polymers was confirmed by FTIR analysis and zeta potential measurement. The uniform distribution of polymer chains in the support was observed by fluorescence images

from CLSM. The maximum grafted P2VP was 2.42 μmol/mL support, whereas 0.29 μmol/mL of support was the highest grafted PMAA. Lower grafting density of PMAA chains resulted from its larger size. With higher grafting density, P2VP brush was likely formed, while, mushroom regime was possibly obtained from grafted PMAA chains. However, the highest protein binding for both polymer chains was closely similar, approximately 45 mg/mL support, because a larger inter-chain space between PMAA chains allowed protein to fill the gap and bind at the side of the chains. This impacted on low protein elution from PMAA chains since the protein could be trapped when the chain collapsed during pH elution. However, both P2VP- and PMAA-grafted Praesto displayed pH-responsive protein binding and elution.

In the case of mixed PEL Praesto, the high grafting density was achieved by first grafting P*t*BMA and subsequently grafting P2VP. This grafting order provided PEL brush conformation leading to bi-functional protein binding with more balance between anion and cation exchange functions. Apart from the protein binding, the mixed PEL modified Praesto offered pH-responsive protein elution with more sensitive to pH shift than the homo PEL support. These performances are promising for manufacture of mixed PEL brush modified support. Nevertheless, improvement of grafting density is required to achieve better Protein adsorption and desorption in term of capacity, selectivity, and sensitivity.

Chapter 6 Conclusions and Future work

6.1 Conclusions

The work described in this thesis responds to the need for greater innovation in chromatography to mitigate perceived sustainability failings of currently practiced adsorption chromatography (Prazeres *et al.*, 1999; Przybycien *et al.*, 2004; Farid, 2008; Jagschies, 2008; Maharjan *et al.*, 2008; Maharjan *et al.*, 2009; Müller *et al.*, 2013; Cao *et al.*, 2015; De Palma, 2017), and ion exchange chromatography in particular. Ion exchange processes invariably employ copious amounts of salt for desorption, which must be removed, recycled or disposed of, in additional operations. Smart polymer modified supports employing changes in temperature (Pankaj Maharjan *et al.*, 2008; Maharjan *et al.*, 2009; Müller *et al.*, 2013; Cao *et al.*, 2015) or pH (Willett, 2009) for desorption, provide obvious ways of minimising salt use and associated recycle/disposal issues. Matrices embellished with pH tunable polymers have the advantage that they are compatible with standard bioprocess chromatography equipment, whereas thermos-responsive media are not (Müller *et al.*, 2013; Cao *et al.*, 2015). Hence, the aims of this study were to: (i) employ oppositely charged weak polyelectrolyte chains to fabricate a new class of porous ion exchange adsorbent with reversible pH switchable AEX – CEX binding and elution behaviour; and subsequently (ii) test the concept using zeta potential measurements, and bind-elute studies employing model acidic, neutral and basic proteins in batch and chromatographic modes.

Previously Willett (2009) employed ‘grafting from’ and ‘grafting to’ approaches to modify the surfaces of non-porous magnetic beads (M-PVA, a cross-linked poly(vinyl alcohol) impregnated with magnetite) with mixed PELs of P2VP and PMAA. Though much higher polymer loadings and protein capacities were obtained using sequential Cerium (IV) initiated ‘graft from’ polymerisation, sequential ‘grafting to’ was selected for modification of meso-macroporous chromatography beads for reasons of simplicity, control, ease of characterisation,

and perceived concerns, that unless properly controlled, 'graft from' polymerisation of monomers could lead to closing down of pores, especially those at the surface and of smaller mesopores,[1] leading to non-uniform polymer distribution throughout the support. Within limits (discussed below) the sequential 'grafting to' approach adopted did indeed provide precise control of the compositional make-up of mixed PEL brush adsorbents from both starting materials (tresyl activated Toyopearl HW65 and Praesto 45). Systematic optimisation of the homo PEL grafting reactions for each polymer chain type was fundamental in guiding the manufacture of mixed PEL adsorbents and informing understanding of brush characteristics and performance. Uniform distribution, pH reversible charging, protein binding and elution behaviour were all demonstrated, and the crowning success of the chromatographic pH elution studies (i.e. ~100% recovery in both directions) validated the pH switchable IEX separation concept.

Despite all of the above, two issues prevented fabrication of densely grafted mixed PELs possessing high lysozyme binding capacities, namely: (i) the poorer grafting efficiency of the protected precursors[2] of PMAA *cf.* P2VP on both Toyopearl HW65 and Praesto 45 media; and (ii) in the case of PMMA, incomplete removal of the protecting group. While using the shorter more soluble amine-terminated PMMA (DP = 98) raised the chain grafting density ~2.5–fold and increased the PMMA monomer loading by ~35%, the resulting lysozyme binding capacity following deprotection dropped. FTIR analysis work highlighted the need for rigorous optimisation of this step in future.

[1] According to IUPAC nomenclature mesopores have diameters between 2 and 50 nm. Pores smaller than 2 nm are classified as micropores and those bigger than 50 nm are macropores (Mays, 2007).

[2] For Toyopearl HW65 based PEL adsorbents >2 and ~1.5 fold lower for P*t*BMA and PMMA respectively (calculated on a monomer basis).

6.2 Future work

Commercial polymer grafted ion exchange media prepared from a single type of chain are made by 'grafting to' and 'grafting from' methods (Müller, 1990; Brooks Lenhoff, 2011; Zhao *et al.*, 2019. Classical commercial representatives of the 'graft to' and 'graft from' type are respectively: GE Healthcare's Sepharose XL ion exchangers, which feature flexible dextran extenders that are subsequently coupled with quaternary amine (Q) or sulphopropyl (SP) functions; and Merck's Fractogel® EMD series of ion exchange matrices prepared Ce(IV) initiated polymerisation of functionalised monomers (Müller, 1990; Willett, 2009; Brown *et al.*, 2013). 'Grafting from' schemes tend to be much more complex and expensive than 'grafting to', but they generally result in higher grafting densities and more ordered layers (Minko, 2008; Hansson *et al.*, 2013; W. Chan *et al.*, 2016; Ming Zhao *et al.*, 2019). Using identical strong cation exchange PELs synthesised in solution from 3-sulphopropyl methacrylate (SPM) and then covalently grafted and on support by atom transfer radical polymerisation (ATRP) of the same SPM monomer Zhao and coworkers (2019) showed that at equivalent PEL loadings very different architecture were formed. 'Grafting from' gave more regular ligand distribution, denser chain packing, smaller layer depths and less pore closure *cf.* 'grafting to', which resulted in significantly enhanced dynamic binding capacities for lysozyme (~2 fold) and especially the much larger γ-globulin (~7 fold). For the future development of highly performing AEC–CEX chromatographic media the use of 'grafting from' polymerisation with controlled monomer addition (Rubio *et al.*, 2017) should be investigated. Increased PEL grafting density will likely bring concomitant improvements in protein binding capacity (Meng *et al.*, 2012) and also perhaps stimuli-dependent response (Elmahdy *et al.*, 2016) *cf.* the 'grafting to' procedure employed in this study, and should therefore be investigated. The base starting materials used in this work have similar pore size distributions to the bulk of base matrices used for

commercially available PELs. However, with the growing interest in increasingly larger and more complex therapeutic proteins (e.g. monoclonal antibodies, antibody drug conjugates) and other entities perhaps the use of chromatography media or alternative formats with larger accessible pores, e.g. monoliths (Simone *et al.*, 2017) or membranes (Fan *et al.*, 2017), or non-porous fibres (Schwellenbach *et al.*, 2016; Jiang and Marcus, 2017; Trang *et al.*, 2019) that can be packed in columns, might prove more suitable for the manufacture of AEX–CEX media.

The preliminary column chromatography studies performed in this study should be extended in rigorous fashion. Particular focus should be placed on breakthrough curve analysis as functions of pH and flowrate with acidic, neutral and basic proteins, and especially on developing and applying pH gradients of appropriate shape to explore whether AEX–CEX chromatography exhibits promise for use in polishing applications. Additionally, applying mixture of acidic, neutral, and basic proteins in column chromatography studies should be investigated. Such studies should be augmented with: (i) measurements of pore-size distribution analysis by using inverse size-exclusion chromatography (ISEC), which would add understanding concerning brush architecture and behaviour during pH alteration (Yao and Lenhoff, 2006; Bhambure *et al.*, 2016; Wang *et al.*, 2016), and (ii) modelling and simulation to provide a comprehensive understanding of protein adsorption mechanisms on the mixed PEL-grafted porous matrices (Basconi *et al.*, 2015; Zhu *et al.*, 2018).

Finally, all batch binding and elution and chromatography studies were done in the ‘osmotic brush regime’ (low ionic strength) and the study focused on the balance of AEX – CEX character, reversibility of charge and the electrostatic interactions thought to drive protein binding and elution. However, charge compensation between two oppositely charged PEL chains, P2VP and PAA, has been observed at around neutral pH, resulting in the

hydrophobic/complex mixed mode (Mikhaylova *et al.*, 2007; Hinrichs *et al.*, 2009).[3] Given that hydrophobic interactions increase with ionic strength driving higher binding capacity, the examination of protein adsorption – desorption to mixed PEL adsorbents in the 'salted brush' regime (Elmahdy *et al.*, 2016; Yu *et al.*, 2016; Drechsler *et al.*, 2018) is merited, although clearly it doesn't provide a 'green 'solution to reduced salt use!

[3] The mixed PELs described herein exhibited very low binding to all proteins at pHs 6 and 7.

Chapter 7 Appendices

7.1 Order of blocking and hydrolysation

To investigate influence of the sequence of blocking and hydrolysation to one another, the PtBMA-grafted Toyopearl supports were prepared in two different orders. One was first blocked by 1 M ethanolamine after grafting, and subsequently hydrolysed by 50%V/V TFA. Another one was done in the reverse order with first hydrolysation and then blocking. No significant different in lysozyme binding observed from two different orders of blocking and hydrolysation (Figure 7-1).

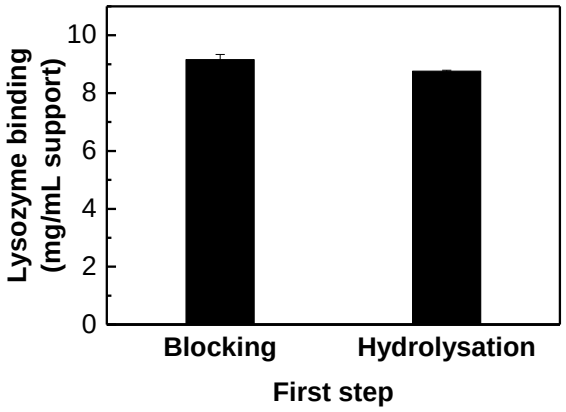

Figure 7-1 Effect of different sequence between blocking and hydrolysation on lysozyme binding

7.2 Column efficiency testing

The peak asymmetry was used to determine the quality of packing column (Bak and Thomas, 2007). Briefly, 5% (v/v) of acetone in water (10 µL) was injected to the column and the obtained peak was analysed by Unicorn 5.15 software for an asymmetry factor (A_s). A typical acceptance range is $0.8 < A_s < 1.8$. The A_s of the mixed PEL Toyoreal packed column was 0.99 which is in the acceptable range (figure 7-2).

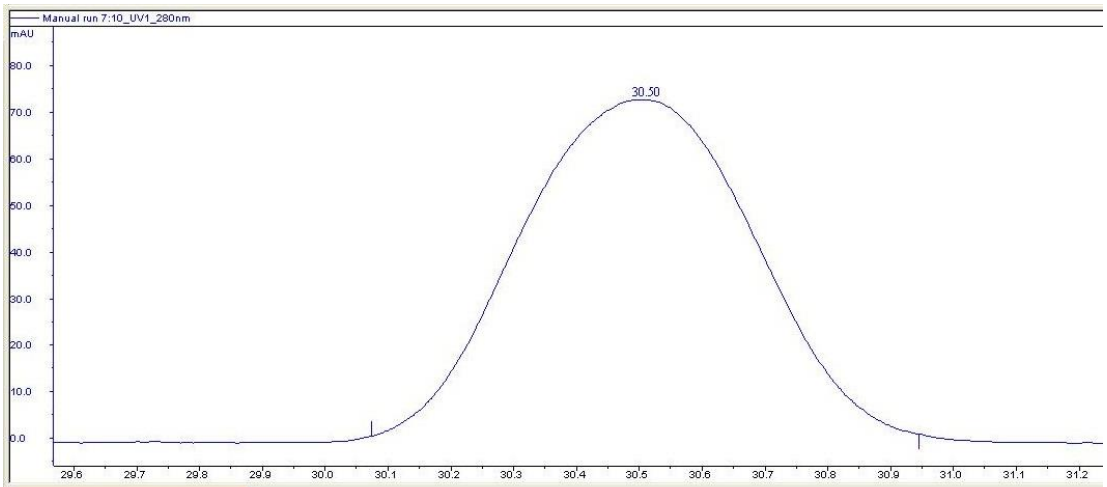

A: Manual run 7:10_UV1_280nm@01,PEAK1

No	Retention (ml)	Area (mAU*ml)	Height (mAU)	10.00% Left (ml)	10.00% Right (ml)	Asymmetry
1	30.50	32.1265	73.820	30.15	30.85	0.99
2						
3	Total number of detected peaks			176		
4	Total area (mAU*ml)			342.4193		
5	Area in evaluated peaks (mAU*ml)			32.1265		
6	Ratio peak area / total area			0.093822		
7	Total peak width (ml)			0.87		
8	Calculated from			Manual run 7:10_UV1_280nm		
9	Baseline			Manual run 7:10_UV1_280nm@01,BASEM		
10	Peak rejection on					
11	Maximum number of peaks ()			20		
12						

Figure 7-2 Screenshot from Unicorn 5.15 sofware showed an 2% acetone peak from the mixed PEL Toyopearl packed column with A_s of 0.99.

7.3 Calibration curve of picric acid in NaOH for the TNBS assay

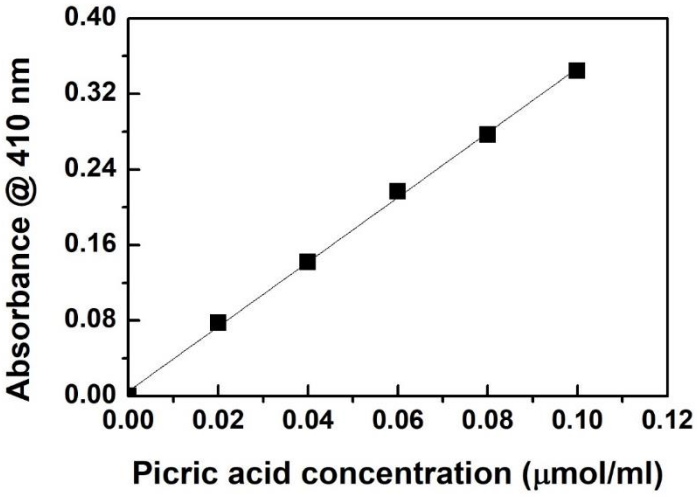

Equation	y = a + b*x
Plot	Absorbance @ 410 n
Weight	No Weighting
Intercept	cell://[Book1]FitLinear
Slope	cell://[Book1]FitLinear
Residual Sum of Squares	9.86561E-5
Pearson's r	0.9994
R-Square(COD)	0.9988
Adj. R-Square	0.9985

Figure 7-3 Calibration curve of picric acid in NaOH for the TNBS assay

7.4 Calibration curve of Orange II

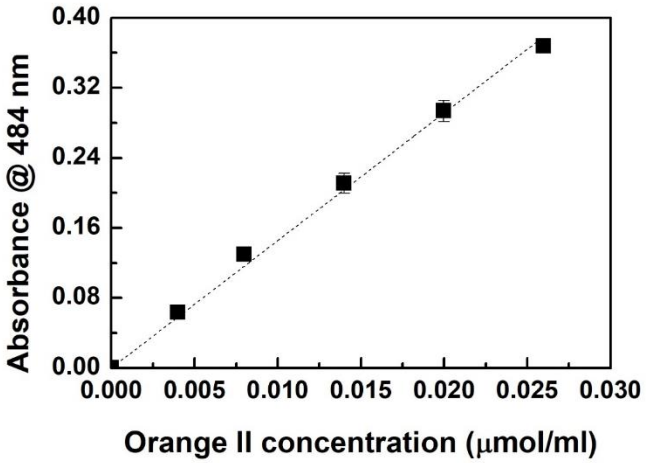

Equation	y = a + b*x
Plot	Absorbance @ 484
Weight	No Weighting
Intercept	cell://[Book1]FitLin
Slope	cell://[Book1]FitLin
Residual Sum of Squ	3.758E-4
Pearson's r	0.99934
R-Square(COD)	0.99869
Adj. R-Square	0.99843

Figure 7-4 Calibration curve of Orange II

7.5 Calibration curve of sulphur element from ICP-OES

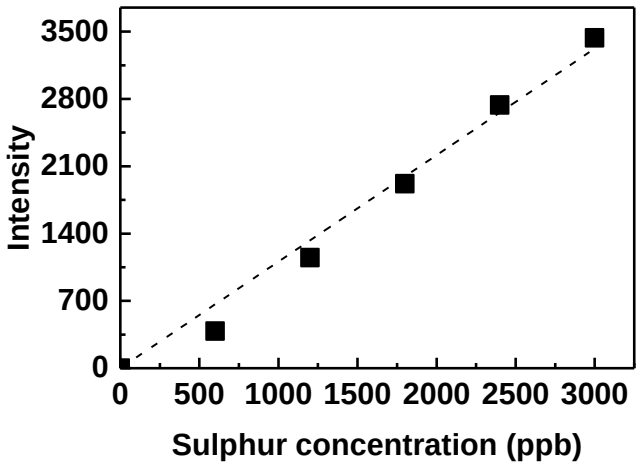

Equation	y = a + b*x
Plot	B
Weight	No Weighting
Intercept	0 ± --
Slope	1.10807 ± 0.036
Residual Sum of Squa	134305.57271
Pearson's r	0.99725
R-Square(COD)	0.99451
Adj. R-Square	0.99341

Figure 7-5 Calibration curve of sulphur from ICP-OES

7.6 Calibration curve of polymer solutions from FTIR

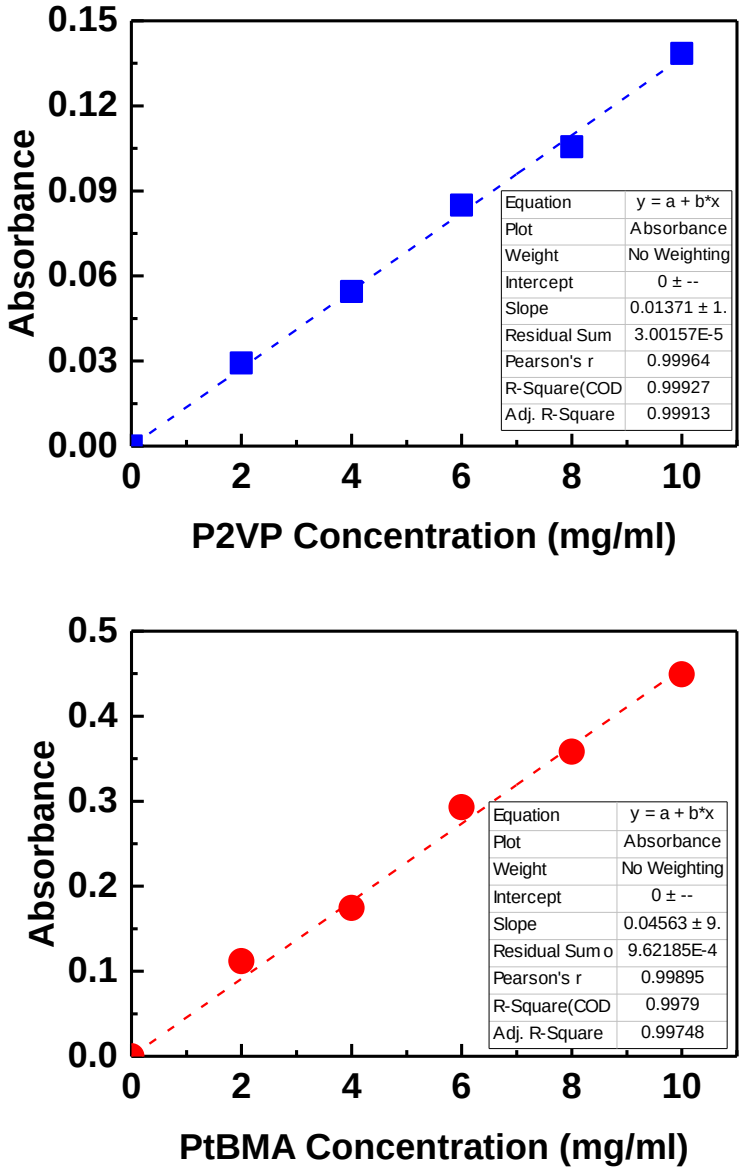

Figure 7-6 FTIR calibration curve P2VP (top) and P*t*BMA (bottom) in 1-butanol

7.7 Zeta potential measurements of model proteins as a function of pH

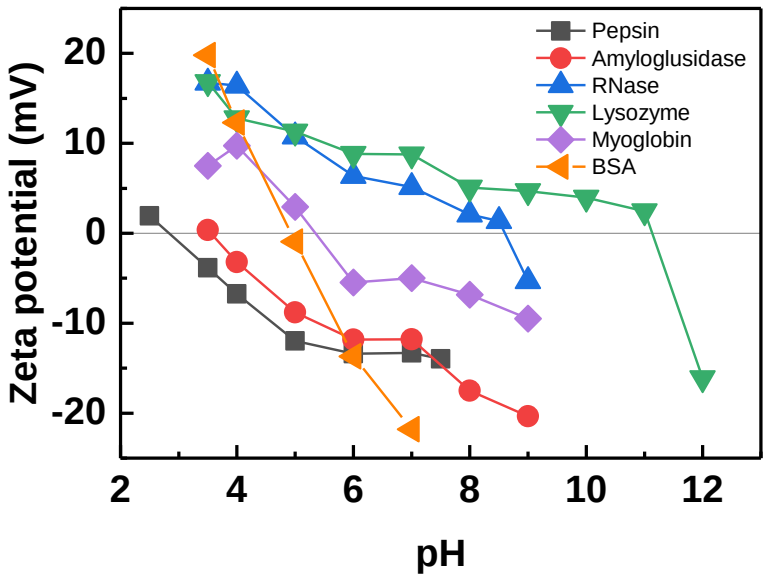

Figure 7-7 Isoelectric focussing curves of model proteins

7.8 Degree of conjugation

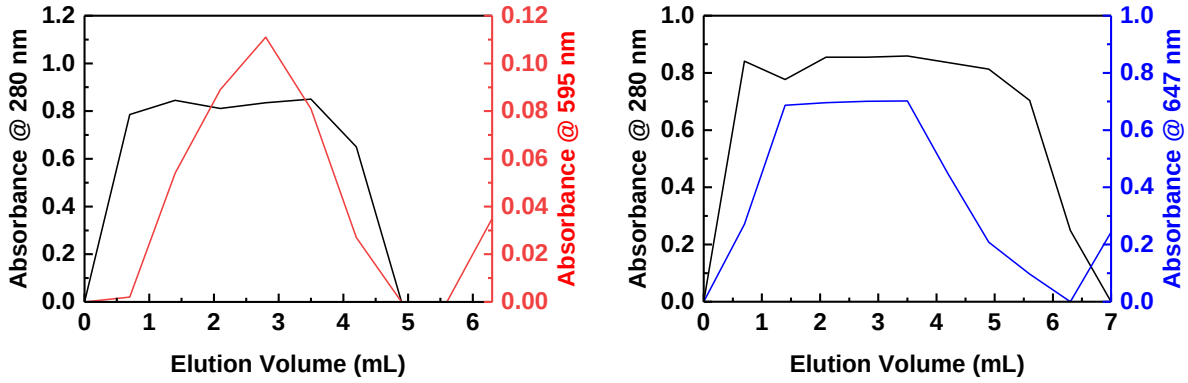

Figure 7-8 Chromatograms of Texas Red-X-tagged BSA (left) and Cy5-tagged lysozyme (right) purified by PD-10 desalting columns packed with Sephadex™ G-25 resin. Key: A_{280} for proteins (black lines); A_{595} for Texas Red-X (red line); A_{647} for Cy5 (blue line).

Degree of conjugation was calculated by the following equation;

$$DOC = \frac{A_{max} x\ MW}{[protein] x\ \varepsilon_{dye}}$$

where A_{max} is the absorbance of the protein-dye conjugate at the λ_{max} for the dye, MW is the molecular weight of protein, ε_{dye} is the extinction coefficient of the dye at its λ_{max}, and protein concentration was calculated by the following equation;

$$Protein\ concentration\ \left(\frac{mg}{mL}\right) = \frac{(A_{280} - A_{max}[CF])}{\varepsilon_{protein}} x\ MW$$

where A_{280} is the absorbance of the protein-dye conjugate at 280 nm and $\varepsilon_{protein}$ is the extinction coefficient of the protein and CF is the correction factor of the dye (www.lifetechnologies.com).

Dye	λ_{max}	ε_{dye}	CF
Texas Red®	595	80,000	0.18
Cy5®	649	250,000	0.05

Protein	MW	$\varepsilon_{protein}$ ($M^{-1}cm^{-1}$)	After conjugation	
			A_{280}	A_{max}
BSA	66,400	43,824	0.835	0.111
Lysozyme	14,400	38,940	0.859	0.702

Thus, DOC of the BSA-Texas Red conjugate is 0.14, whereas DOC of the lysozyme-Cy5 conjugate is 0.1

7.9 Calibration curve of BSA used in BCA assay

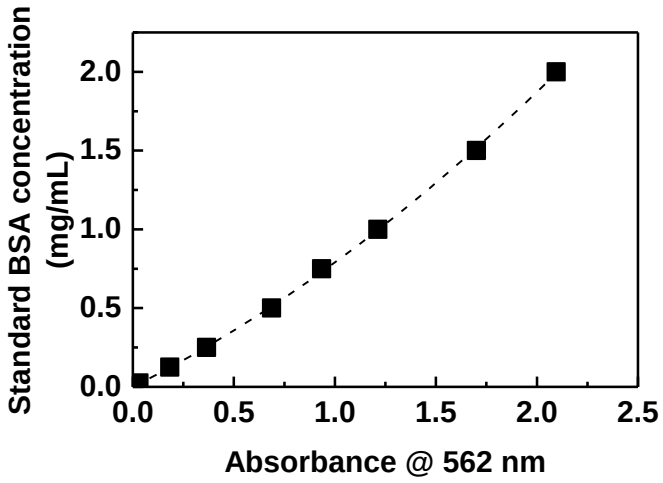

Equation	y = Intercept + B1*x^1 + B2*x^2
Plot	Standard BSA
Weight	No Weighting
Intercept	0 ± --
B1	0.64448 ± 0.01353
B2	0.14588 ± 0.00781
Residual Sum of Squares	9.98684E-4
R-Square(COD)	0.99988
Adj. R-Square	0.99984

Figure 7-9 Calibration curve of standard BSA used in BCA assay

References

Acikara, O. B., Çitoğlu, G. S., Özbilgin, S. and Ergene, B. (2013) 'Affinity chromatography and importance in drug discovery', In: Martin, D. ed. *Column Chromatography*. London: IntechOpen Limited. pp. 59-70.

Acres, R. G., Ellis, A. V., Alvino, J., Lenahan, C. E., Khodakov, D. A., Metha, G. F. and Andersson, G. G. (2012) 'Molecular structure of 3-aminopropyltriethoxysilane layers formed on silanol-terminated silicon surfaces', *Journal of Physical Chemistry C*, 116(10), pp. 6289–6297. doi: 10.1021/jp212056s.

Akkahat, P. and Hoven, V. P. (2011) 'Introducing surface-tethered poly(acrylic acid) brushes as 3D functional thin film for biosensing applications', *Colloids and Surfaces B: Biointerfaces*, 86, pp. 198–205. doi: 10.1016/j.colsurfb.2011.03.042.

Alexander, S. (1977) 'Polymer adsorption on small spheres. A scaling approach', *Journal de Physique*, 38(8), pp. 977–981. Available at: http://dx.doi.org/10.1051/jphys:01977003808097700.

Amaral-Fonseca, M., Kopp, W., Giordano, R., Fernández-Lafuente, R. and Tardioli, P. (2018) 'Preparation of Magnetic Cross-Linked Amyloglucosidase Aggregates: Solving Some Activity Problems', *Catalysts*, 8(11), p. 496. doi: 10.3390/catal8110496.

Ammar, M. R., Legeay, G., Bulou, A. and Bardeau, J.-F. (2009) 'Adhesion improvement of poly (vinyl alcohol) coating on silicon substrate', *Surface and Coatings Technology*, 203(16), pp. 2202–2206. doi: 10.1016/j.surfcoat.2009.02.015.

Arita, T., Yoshimura, T. and Adschiri, T. (2010) 'Size exclusion chromatography of quantum dots by utilizing nanoparticle repelling surface of concentrated polymer brush', *Nanoscale*, 2(8), pp. 1467–1473. doi: 10.1039/c0nr00157k.

Asenjo, J. A. and Andrews, B. A. (2009) 'Protein purification using chromatography: Selection of type, modelling and optimization of operating conditions', *Journal of Molecular Recognition*, 22(2), pp. 65–76. doi: 10.1002/jmr.898.

Azzaroni, O. (2012) 'Polymer brushes here, there, and everywhere: Recent advances in their practical applications and emerging opportunities in multiple research fields', *Journal of Polymer Science, Part A: Polymer Chemistry*, 50(16), pp. 3225–3258. doi: 10.1002/pola.26119.

Azzaroni, O., Brown, A. A. and Huck, W. T. S. (2006) 'UCST wetting transitions of polyzwitterionic brushes driven by self-association', *Angewandte Chemie - International Edition*, 45(11), pp. 1770–1774. doi: 10.1002/anie.200503264.

Azzaroni, O., Moya, S., Farhan, T. and Brown, A. A. (2005) 'Switching the Properties of Polyelectrolyte Brushes via " Hydrophobic Collapse "', *Macromolecules*, 38, pp. 10192–10199. Available at: http://pubs.acs.org/doi/abs/10.1021/ma051549r.

Bak, H. and Thomas, O. R. T. (2007) 'Evaluation of commercial chromatographic adsorbents for the direct capture of polyclonal rabbit antibodies from clarified antiserum', *Journal of Chromatography B*, 848(1), pp. 116–130. doi: 10.1016/J.JCHROMB.2006.07.003.

Ballauff, M. (2007) ‘Spherical polyelectrolyte brushes’, *Progress in Polymer Science (Oxford)*, 32(10), pp. 1135–1151. doi: 10.1016/j.progpolymsci.2007.05.002.

Ballauff, M. and Borisov, O. (2006) ‘Polyelectrolyte brushes’, *Current Opinion in Colloid and Interface Science*, 11(6), pp. 316–323. doi: 10.1016/j.cocis.2006.12.002.

Banerjee, S., Soulestin, T., Patil, Y., Ladmiral, V. and Ameduri, B. (2016) ‘Towards new strategies for the synthesis of functional vinylidene fluoride-based copolymers with tunable wettability’, *Polymer Chemistry*, 7(24), pp.4004-4015. doi: 10.1039/c6py00508j.

Bartucci, R., Pantusa, M., Marsh, D. and Sportelli, L. (2002) ‘Interaction of human serum albumin with membranes containing polymer-grafted lipids: spin-label ESR studies in the mushroom and brush regimes’, *Biochimica et Biophysica Acta (BBA) - Biomembranes*, 1564(1), pp. 237–242. doi: 10.1016/S0005-2736(02)00458-3.

Basconi, J. E., Carta, G. and Shirts, M. R. (2015) ‘Effects of polymer graft properties on protein adsorption and transport in ion exchange chromatography: A multiscale modeling study’, *Langmuir*, 31(14), pp. 4176–4187. doi: 10.1021/la504768g.

Batista-Viera, F., Janson, J.-C. and Jonsson, J. A. (2011) ‘Affinity Chromatography’, In: Janson, J.C. ed. *Methods of Biochemical Analysis : Protein Purification : Principles, High Resolution Methods, and Applications*. 3rd edn. Hoboken, NJ: John Wiley & Sons, Inc., pp. 221–258. doi: 10.1002/9780470939932.ch9.

Baum, M. and Brittain, W. J. (2002) ‘Synthesis of Polymer Brushes on Silicate Substrates via Reversible Addition Fragmentation Chain Transfer Technique’, *Macromolecules*, 35(3), pp. 610–615. doi: 10.1021/ma0112467.

Beintema, J. J., Breukelman, H. J., Carsana, A. and Furiat, A. (1997) ‘Evolution of Vertebrate Ribonucleases: Ribonuclease A Superfamily’, *Ribonucleases*, pp. 245–269. doi: 10.1016/B978-012588945-2/50009-1.

Bhambure, R., Angelo, J. M., Gillespie, C. M., Phillips, M., Graalfs, H. and Lenhoff, A. M. (2017) ‘Ionic strength-dependent changes in tentacular ion exchangers with variable ligand density. II. Functional properties’, *Journal of Chromatography A*, 1506, pp. 55–64. doi: 10.1016/J.CHROMA.2017.05.021.

Bhambure, R., Gillespie, C. M., Phillips, M., Graalfs, H. and Lenhoff, A. M. (2016) ‘Ionic strength-dependent changes in tentacular ion exchangers with variable ligand density. I. Structural properties’, *Journal of Chromatography A*, 1463, pp. 90–101. doi: 10.1016/J.CHROMA.2016.08.010.

Billing, M., Elter, J. K. and Schacher, F. H. (2016) ‘Sulfo-and carboxybetaine-containing polyampholytes based on poly(2-vinyl pyridine)s: Synthesis and solution behavior’, *Polymer*, 104, pp. 40–48. doi: 10.1016/j.polymer.2016.09.081.

Bittrich, E., Rodenhausen, K. B., Eichhorn, K.-J., Hofmann, T., Schubert, M., Stamm, M. and Uhlmann, P. (2010) ‘Protein adsorption on and swelling of polyelectrolyte brushes: A simultaneous ellipsometry-quartz crystal microbalance study’, *Biointerphases*, 5(4), pp. 159–167. doi: 10.1116/1.3530841.

Brown, G. N., Müller, C., Theodosiou, E., Franzreb, M. and Thomas, O. R. T. (2013) 'Multi-cycle recovery of lactoferrin and lactoperoxidase from crude whey using fimbriated high-capacity magnetic cation exchangers and a novel "rotor-stator" high-gradient magnetic separator', *Biotechnology and Bioengineering*, 110(6), pp. 1714–1725. doi: 10.1002/bit.24842.

Burkert, S., Bittrich, E., Kuntzsch, M., Müller, M., Eichhorn, K.-J., Bellmann, C., Uhlmann, P. and Stamm, M. (2009) 'Protein Resistance of PNIPAAm Brushes: Application to Switchable Protein Adsorption', *Langmuir*, 26(3), pp. 1786–1795. doi: 10.1021/la902505q.

Burtovyy, O., Klep, V., Chen, H., Hu, R., Lin, C. and Luzinov, I. (2007) 'Hydrophobic Modification of Polymer Surfaces via "Grafting to" Approach', *Journal of Macromolecular Science, Part B*, 46(1), pp. 137–154. doi: 10.1080/00222340601044326.

Cao, P., Müller, T. K. H., Ketterer, B., Ewert, S., Theodosiou, E., Thomas, O. R. T. and Franzreb, M. (2015) 'Integrated system for temperature-controlled fast protein liquidchromatography. II. Optimized adsorbents and "single columncontinuous operation"', *Journal of Chromatography A*, 1403, pp. 118–131. doi: 10.1016/j.chroma.2015.05.039.

Chen, Y., Sun, W., Deng, Q. and Chen, L. (2006) 'Controlled grafting from poly(vinylidene fluoride) films by surface-initiated reversible addition–fragmentation chain transfer polymerization', *Journal of Polymer Science Part A: Polymer Chemistry*, 44(9), pp. 3071–3082. doi: 10.1002/pola.21410.

Cheng, N., Azzaroni, O., Moya, S. and Huck, W. T. S. (2006) 'The Effect of [CuI]/[CuII] Ratio on the Kinetics and Conformation of Polyelectrolyte Brushes by Atom Transfer Radical Polymerization', *Macromolecular Rapid Communications*, 27(19), pp. 1632–1636. doi: 10.1002/marc.200600467.

Cheng, N., Brown, A. A., Azzaroni, O. and Huck, W. T. S. (2008) 'Thickness-dependent properties of polyzwitterionic brushes', *Macromolecules*, 41(17), pp. 6317–6321. doi: 10.1021/ma800625y.

Cheung, R. C. F., Wong, J. H. and Ng, T. B. (2012) 'Immobilized metal ion affinity chromatography: A review on its applications', *Applied Microbiology and Biotechnology*, 96(6), pp. 1411–1420. doi: 10.1007/s00253-012-4507-0.

Choi, I. S. and Langer, R. (2001) 'Surface-Initiated Polymerization of l-Lactide: Coating of Solid Substrates with a Biodegradable Polymer', *Macromolecules*, 34(16), pp. 5361–5363. doi: 10.1021/ma010148i.

Clarke, A. E. (2017) *Modification of poly (methyl methacrylate) surfaces with azobenzene groups to develop a photoresponsive surface*. MSc thesis. Ontario: Queen's University. Available at: https://qspace.library.queensu.ca/bitstream/handle/1974/23815/Clarke_Ashley_E_201712_MASc.pdf?sequence=2&isAllowed=y (Accessed: 19 March 2019).

Clayden, J., Greeves, N. and Warren, S. (2012) 'Organic Chemistry'. New York: Oxford University Press, pp. 43–80. Available at: www.oxfordtextbooks.co.uk/orc/clayden2e/ (Accessed: 21 October 2019).

Coates, J. (2006) ‘Interpretation of Infrared Spectra, A Practical Approach’, In: Meyers, R.A. ed. *Encyclopedia of Analytical Chemistry*. Chichester: John Wiley & Sons Ltd. doi: doi:10.1002/9780470027318.a5606.

Cordeiro, C. . (1999) ‘Confined polymer chains in poor solvent’, *Journal of Physics and Chemistry of Solids*, 60(10), pp. 1645–1648. doi: 10.1016/S0022-3697(99)00150-X.

Cramer, S. M. and Holstein, M. A. (2011) ‘Downstream bioprocessing: recent advances and future promise’, *Current Opinion in Chemical Engineering*, 1(1), pp. 27–37. doi: 10.1016/J.COCHE.2011.08.008.

Cuatrecasas, P. and Parikh, I. (1972) ‘Adsorbents for Affinity Chromatography. use of N-Hydroxysuccinimide Esters of Agarose’, *Biochemistry*, 11(12), pp. 2291–2299. doi: 10.1021/bi00762a013.

Cummins, P. M., Dowling, O. and O’Connor, B. F. (2011) ‘Ion-exchange chromatography: basic principles and application to the partial purification of soluble mammalian prolyl oligopeptidase.’, In: Walls D., Loughran S. eds. *Protein Chromatography. Methods in Molecular Biology (Methods and Protocols)*.vol 681, Clifton, NJ: Humana Press. pp. 215–228. doi: 10.1007/978-1-60761-913-0_12.

Das, S., Banik, M., Chen, G., Sinha, S. and Mukherjee, R. (2015) ‘Polyelectrolyte brushes: theory, modelling, synthesis and applications’, *Soft Matter*, 11(44), pp. 8550–8583. doi: 10.1039/C5SM01962A.

Demiroglou, A., Bandel-Schlesselmann, C. and Jennissen, H. P. (1994) ‘A Novel Reaction Sequence for the Coupling of Nucleophiles to Agarose with 2,2,2-Trifluoroethanesulfonyl Chloride’, *Angewandte Chemie International Edition in English*, 33(1), pp. 120–123. doi: 10.1002/anie.199401201.

Demiroglou, A. and Jennissen, H. P. (1990) ‘Synthesis and protein-binding properties of spacer-free thioalkyl agaroses’, *Journal of Chromatography A*, 521(1), pp. 1–17. doi: 10.1016/0021-9673(90)85060-9.

Desai, M. A., Rayner, M., Burns, M. and Bermingham, D. (2000) ‘Application of Chromatography in the Downstream Processing of Biomolecules’, *Downstream Processing of Proteins Methods and Protocols*, 9, pp. 73–94.

Draper, J., Luzinov, I., Minko, S., Tokarev, I. and Stamm, M. (2004) ‘Mixed Polymer Brushes by Sequential Polymer Addition: Anchoring Layer Effect’, *Langmuir*, 20(10), pp. 4064–4075. doi: 10.1021/la0361316.

Drechsler, A., Elmahdy, M. M., Uhlmann, P. and Stamm, M. (2018) ‘PH and Salt Response of Mixed Brushes Made of Oppositely Charged Polyelectrolytes Studied by in Situ AFM Force Measurements and Imaging’, *Langmuir*, 34(16), pp. 4739–4749. doi: 10.1021/acs.langmuir.8b00498.

Drechsler, A., Synytska, A., Uhlmann, P., Elmahdy, M. M., Stamm, M. and Kremer, F. (2010) ‘Interaction Forces between Microsized Silica Particles and Weak Polyelectrolyte Brushes at Varying pH and Salt Concentration’, *Langmuir*, 26(9), pp. 6400–6410. doi: 10.1021/la904103z.

Drechsler, A., Synytska, A., Uhlmann, P., Stamm, M. and Kremer, F. (2012) 'Tuning the Adhesion of Silica Microparticles to a Poly(2-vinyl pyridine) Brush: An AFM Force Measurement Study', *Langmuir*, 28(44), pp. 15555–15565. doi: 10.1021/la303131d.

Durham, R. J., Sleigh, R. W. and Hourigan, J. A. (2004) 'Pharmaceutical lactose: a new whey with no waste', *Australian journal of dairy technology*, 59(2), pp. 138–141. Available at: http://europepmc.org/abstract/AGR/IND43648069.

Ejaz, M., Yamamoto, S., Ohno, K., Tsujii, Y. and Fukuda, T. (1998) 'Controlled Graft Polymerization of Methyl Methacrylate on Silicon Substrate by the Combined Use of the Langmuir−Blodgett and Atom Transfer Radical Polymerization Techniques', *Macromolecules*, 31(17), pp. 5934–5936. doi: 10.1021/ma980240n.

Ejaz, M., Yamamoto, S., Tsujii, Y. and Fukuda, T. (2002) 'Fabrication of patterned high-density polymer graft surfaces. 1. amplification of phase-separated morphology of organosilane blend monolayer by surface-initiated atom transfer radical polymerization', *Macromolecules*, 35(4), pp. 1412–1418. doi: 10.1021/ma010371f.

Elmahdy, M. M., Drechsler, A., Uhlmann, P. and Stamm, M. (2016) 'Swelling and Surface Interactions of End-Grafted Poly(2-vinylpyridine) Layers in Acidic Solution: Influence of Grafting Density and Salt Concentration', *Langmuir*, 32(22), pp. 5451–5459. doi: 10.1021/acs.langmuir.6b00316.

Emilsson, G., Schoch, R. L., Feuz, L., Höök, F., Lim, R. Y. H. and Dahlin, A. B. (2015) 'Strongly stretched protein resistant poly(ethylene glycol) brushes prepared by grafting-to', *ACS Applied Materials and Interfaces*, 7(14), pp. 7505–7515. doi: 10.1021/acsami.5b01590.

Erhardt, R., Zhang, M., Böker, A., Zettl, H., Abetz, C., Frederik, P., Krausch, G., Abetz, V. and Müller, A. H. E. (2003) 'Amphiphilic Janus micelles with polystyrene and poly(methacrylic acid) hemispheres', *Journal of the American Chemical Society*, 125(11), pp. 3260–3267. doi: 10.1021/ja028982q.

Eriksson, K.-O. and Belew, M. (2011) 'Hydrophobic Interaction Chromatography', In: Janson, J.C. ed. *Methods of Biochemical Analysis : Protein Purification : Principles, High Resolution Methods, and Applications*. 3rd edn. Hoboken, NJ: John Wiley & Sons, Inc., pp. 165–181. doi: 10.1002/9780470939932.ch6.

Fairbanks, B. D., Gunatillake, P. A. and Meagher, L. (2015) 'Biomedical applications of polymers derived by reversible addition – fragmentation chain-transfer (RAFT)', *Advanced Drug Delivery Reviews*, 91, pp. 141–152. doi: 10.1016/J.ADDR.2015.05.016.

Fan, J., Luo, J., Song, W. and Wan, Y. (2017) 'One-step purification of α1-antitrypsin by regulating polyelectrolyte ligands on mussel-inspired membrane adsorber', *Journal of Membrane Science*, 528, pp. 155–162. doi: 10.1016/J.MEMSCI.2017.01.037.

Faraji, N., Zhang, Y. and Ray, A. (2017) 'Optimization of Lactoperoxidase and Lactoferrin Separation on an Ion-Exchange Chromatography Step', *Separations*, 4(2), p. 10. doi: 10.3390/separations4020010.

Farid, S. S. (2008) 'Economic drivers and trade-offs in antibody purification processes', *BioPharm International*, 21(3), p. 37.

Ferreira, G. N. M. (2005) ‘Chromatographic approaches in the purification of plasmid DNA for therapy and vaccination’, *Chemical Engineering and Technology*, 28(11), pp. 1285–1294. doi: 10.1002/ceat.200500158.

Fleer, G. J., Stuart, M. A. C., Scheutjens, J. M. H. M., Cosgrove, T. and Vincent, B. (1998) ‘Terminally-Attached Chains’, *Polymers at Interfaces*, pp. 372–395. doi: 10.1007/978-94-011-2130-9_8.

GE Healthcare (2012) ‘Hydrophobic Interaction and Reversed Phase Chromatography: Principles and Methods’, p. 168. doi: 10.1016/j.ymeth.2011.10.007.

GE Healthcare (2014) *GE Protein Skills Blog: An Introduction to Size Exclusion Chromatography & the next generation of Superdex 200 & Superose 6*. Available at: http://geproteinskills.blogspot.com/2014/11/an-introduction-to-size-exclusion.html (Accessed: 9 January 2020).

GEN-Genetic Engineering & Biotechnology News (2018) ‘Disruption downstream bottlenecks’, June. Available at: https://www.genengnews.com/magazine/320/disrupting-downstream-bottlenecks/.

De Gennes, P. G. (1976) ‘Scaling theory of polymer adsorption’, *Journal de Physique*, 37(12), pp. 1445–1452. doi: 10.1051/jphys:0197600370120144500ï.

Goheen, S. C. and Gibbins, B. . (2000) ‘Protein losses in ion-exchange and hydrophobic interaction high-performance liquid chromatography’, *Journal of Chromatography A*, 890(1), pp. 73–80. doi: 10.1016/S0021-9673(00)00572-0.

Graf, M. and Wätzig, H. (2004) ‘Capillary isoelectric focusing - Reproducibility and protein adsorption’, *Electrophoresis*, 25(17), pp. 2959–2964. doi: 10.1002/elps.200305978.

Großhans, S., Wang, G., Fischer, C. and Hubbuch, J. (2018) ‘An integrated precipitation and ion-exchange chromatography process for antibody manufacturing: Process development strategy and continuous chromatography exploration’, *Journal of Chromatography A*, 1533, pp. 66–76. doi: 10.1016/J.CHROMA.2017.12.013.

Gtari, W., Bey, H., Aschi, A., Bitri, L. and Othman, T. (2017) ‘Impact of macromolecular crowding on structure and properties of pepsin and trypsin’, *Materials Science and Engineering: C*, 72, pp. 98–105. doi: 10.1016/J.MSEC.2016.11.046.

Guo, L., Wang, H., Du, X., Xu, D. and Lei, J. (2014) ‘Preparation of polymethylacrylic acid standard samples for GPC applications via a precipitation fractionation-separated step hydrolysis method’, *Journal of Macromolecular Science, Part B: Physics*, 53(12), pp. 1846–1855. doi: 10.1080/00222348.2014.942214.

Hagel, L. (2011) ‘Gel Filtration: Size Exclusion Chromatography’, In: Janson, J.C. ed. *Methods of Biochemical Analysis : Protein Purification : Principles, High Resolution Methods, and Applications*. 3rd edn. Hoboken, NJ: John Wiley & Sons, Inc., pp. 51–91. doi: 10.1002/9780470939932.ch3.

Halling, P. J. and Dunnill, P. (1979) ‘Improved nonporous magnetic supports for immobilized enzymes’, *Biotechnology and Bioengineering*, 21(3), pp. 393–416. doi: 10.1002/bit.260210304.

Halperin, A., Tirrell, M. and Lodge, T. P. (1992) ‘Tethered chains in polymer microstructures’, in *Macromolecules: Synthesis, Order and Advanced Properties*, pp. 31–71. doi: 10.1007/BFb0051635.

Hamilton, G. S., Haas, J. and Huérou, Y. Le (2001) ‘p-Toluenesulfonic Acid’, In Charette, A., Bode, J., Rovis, T., Shenvi, R. eds. *Encyclopedia of Reagents for Organic Synthesis*. Chichester, UK: John Wiley & Sons, Ltd. doi: 10.1002/047084289X.rt134.pub2.

Hansson, S., Trouillet, V., Tischer, T., Goldmann, A. S., Carlmark, A., Barner-Kowollik, C. and Malmström, E. (2013) ‘Grafting efficiency of synthetic polymers onto biomaterials: A comparative study of grafting- from versus grafting- to’, *Biomacromolecules*, 14(1), pp. 64–74. doi: 10.1021/bm3013132.

He, X., Yang, W. and Pei, X. (2008) ‘Preparation , Characterization , and Tunable Wettability of Poly (ionic liquid) Brushes via Surface-Initiated Atom Transfer Radical Polymerization’, *Macromolecules*, pp. 4615–4621. doi: 10.1021/ma702389y.

Heldt, C. L., Gurgel, P. V, Jaykus, L.-A. and Carbonell, R. G. (2009) ‘Influence of peptide ligand surface density and ethylene oxide spacer arm on the capture of porcine parvovirus’, *Biotechnology progress*, 25(5), pp. 1411–1418. doi: 10.1002/btpr.236.

Hermanson, G. T., Mallia, A. K. and Smith, P. K. (1992) *Immobilized affinity ligand techniques*. 2nd edn. San Diego: Academic Press.

Hester, J. F., Olugebefola, S. C. and Mayes, A. M. (2002) ‘Preparation of pH-responsive polymer membranes by self-organization’, *Journal of Membrane Science*, 208(1–2), pp. 375–388. doi: 10.1016/S0376-7388(02)00317-4.

Hinrichs, K., Aulich, D., Ionov, L., Esser, N., Eichhorn, K. J., Motornov, M., Stamm, M. and Minko, S. (2009) ‘Chemical and structural changes in a pH-responsive mixed polyelectrolyte brush studied by infrared ellipsometry’, *Langmuir*, 25(18), pp. 10987–10991. doi: 10.1021/la901219f.

Hirs, C. H. W., Moore, S. and Stein, W. H. (1956) ‘Peptides btained by tryptic hydrolysis of performic acid-oxidized ribonuclease’, *Journal of Biological Chemistry* , 219(2), pp. 623–642. Available at: http://www.jbc.org/content/219/2/623.short.

Houbenov, N. (2005) *Adsorption and Grafting of Polyelectrolytes at Solid-Liquid Interfaces*. PhD thesis. Dresden: Technical University of Dresden.

Houbenov, N., Minko, S. and Stamm, M. (2003) ‘Mixed polyelectrolyte brush from oppositely charged polymers for switching of surface charge and composition in aqueous environment’, *Macromolecules*, 36(16), pp. 5897–5901. doi: 10.1021/ma0341869.

Huang, H. and Penn, L. S. (2005) ‘Dense Tethered Layers by the “Grafting-To” Approach’, *Macromolecules*, 38(11), pp. 4837–4843. doi: 10.1021/ma0501444.

Huang, J., Zhang, L., Chen, P., Chen, S., Wu, Y. and Tang, S. (2011) 'Transportation efficiency of insulin loaded in agarose-grafting-hyaluronan microparticle crossing Coca-2 cell monolayer', *Current Applied Physics*, 11(3), pp. 794–799. doi: 10.1016/J.CAP.2010.11.080.

Husemann, M., Mecerreyes, D., Hawker, C. J., Hedrick, J. L., Shah, R. and Abbott, N. L. (1999) 'Surface-Initiated Polymerization for Amplification of Self-Assembled Monolayers Patterned by Microcontact Printing', *Angewandte Chemie International Edition*, 38(5), pp. 647–649. doi: 10.1002/(SICI)1521-3773(19990301)38:5<647::AID-ANIE647>3.0.CO;2-0.

Husseman, M., Malmström, E. E., McNamara, M., Mate, M., Mecerreyes, D., Benoit, D. G., Hedrick, J. L., Mansky, P., Huang, E., Russell, T. P. and Hawker, C. J. (1999) 'Controlled Synthesis of Polymer Brushes by "Living" Free Radical Polymerization Techniques', *Macromolecules*, 32(5), pp. 1424–1431. doi: 10.1021/ma981290v.

Iacono, M. and Heise, A. (2015) 'Stable poly(methacrylic acid) brush decorated silica nano-particles by ARGET ATRP for bioconjugation', *Polymers*, 7(8), pp. 1427–1443. doi: 10.3390/polym7081427.

Ibraheem, D., Iqbal, M., Agusti, G., Fessi, H. and Elaissari, A. (2014) 'Effects of process parameters on the colloidal properties of polycaprolactone microparticles prepared by double emulsion like process', *Colloids and Surfaces A: Physicochemical and Engineering Aspects*, 445, pp. 79–91. doi: 10.1016/J.COLSURFA.2014.01.012.

Ionov, L., Houbenov, N., Sidorenko, A., Stamm, M., Luzinov, I. and Minko, S. (2004) 'Inverse and reversible switching gradient surfaces from mixed polyelectrolyte brushes', *Langmuir*, 20(23), pp. 9916–9919. doi: 10.1021/la048158a.

Ionov, L., Houbenov, N., Sidorenko, A., Stamm, M. and Minko, S. (2009) 'Stimuli-responsive command polymer surface for generation of protein gradients.', *Biointerphases*, 4(2), pp. FA45-9. doi: 10.1116/1.3119722.

Israelachvili, J. N. (2011) *Intermolecular and Surface Forces*. 3rd edn. Burlington, MA: Academic Press. doi: https://doi.org/10.1016/B978-0-12-391927-4.10024-6.

Iyer, K. S., Zdyrko, B., Malz, H., Pionteck, J. and Luzinov, I. (2003) 'Polystyrene Layers Grafted to Macromolecular Anchoring Layer', *Macromolecules*, 36(17), pp. 6519–6526. doi: 10.1021/ma034460z.

Jagschies, G. (2008) 'Where is biopharmaceutical manufacturing heading?', *BioPharm International*, 21(10), pp. 72–88.

Jain, P., Sun, L., Dai, J., Baker, G. L. and Bruening, M. L. (2007) 'High-capacity purification of his-tagged proteins by affinity membranes containing functionalized polymer brushes', *Biomacromolecules*, 8(10), pp. 3102–3107. doi: 10.1021/bm700515m.

Janson, J.-C. and Jonsson, J. A. (2011) 'Introduction to Chromatography', In: Janson, J.C. ed. *Methods of Biochemical Analysis : Protein Purification : Principles, High Resolution Methods, and Applications*. 3rd edn. Hoboken, NJ: John Wiley & Sons, Inc., pp. 23–50. doi: 10.1002/9780470939932.ch2.

Jiang, L. and Marcus, R. K. (2017) 'Microwave-assisted grafting polymerization modification of nylon 6 capillary-channeled polymer fibers for enhanced weak cation exchange protein separations', *Analytica Chimica Acta*, 954, pp. 129–139. doi: 10.1016/J.ACA.2016.11.065.

Jiang, W., Zhu, H., Guo, C., Li, J., Xue, Q., Feng, J. and Gong, X. (2010) 'Poly(methyl methacrylate)-coated carbonyl iron particles and their magnetorheological characteristics', *Polymer International*, 59(7), pp. 879–883. doi: 10.1002/pi.2794.

Jonas, A. M., Glinel, K., Oren, R., Nysten, B. and Huck, W. T. S. (2007) 'Thermo-Responsive Polymer Brushes with Tunable Collapse Temperatures in the Physiological Range', *Macromolecules*, 40(13), pp. 4403–4405. doi: 10.1021/ma070897l.

Jordan, R. and Ulman, A. (1998) 'Surface Initiated Living Cationic Polymerization of 2-Oxazolines', *Journal of the American Chemical Society*, 120(2), pp. 243–247. doi: 10.1021/ja973392r.

Joseph, S. (2019) *Multifunctional chromatography materials: new designs & applications*. PhD thesis. Birmingham: University of Birmingham.

Julthongpiput, D., Lin, Y.-H., Teng, J., Zubarev, E. R. and Tsukruk, V. V. (2003) 'Y-shaped amphiphilic brushes with switchable micellar surface structures.', *Journal of the American Chemical Society*, 125(51), pp. 15912–21. doi: 10.1021/ja038051u.

Jungbauer, A. and Hahn, R. (2009) 'Ion-Exchange Chromatography', In: Richard, B. R., Deutscher, M. P. eds. *Methods in Enzymology*. vol 463. San Diego: Academic Press, pp. 349–371. doi: 10.1016/S0076-6879(09)63022-6.

Kagedal, L. (2011) 'Immobilized Metal Ion Affinity Chromatography', In: Janson, J.C. ed. *Methods of Biochemical Analysis : Protein Purification : Principles, High Resolution Methods, and Applications*. 3rd edn. Hoboken, NJ: John Wiley & Sons, Inc., pp. 183–201. doi: 10.1002/9780470939932.ch7.

Karlsson, E. (2011) 'Ion Exchange Chromatography', In: Janson, J.C. ed. *Methods of Biochemical Analysis : Protein Purification : Principles, High Resolution Methods, and Applications*. 3rd edn. Hoboken, NJ: John Wiley & Sons, Inc., pp. 93–133. doi: 10.1002/9780470939932.ch4.

Karlsson, R., Rydén, L. and Brewer, J. (1989) 'Ion Exchange Chromatography', In: Janson, J.C., Ryden, L. eds. *Protein Purification–Principles, High Resolution Methods, and Applications.* 2nd edn. New York: VCH Publishers, pp. 145-206.

Kato, H. and Wadati, M. (2007) 'Density function analysis of single polymer chain', *Chaos, Solitons & Fractals*, 32(4), pp. 1250–1257. doi: 10.1016/J.CHAOS.2005.11.084.

Kim, J.-B., Huang, W., Miller, M. D., Baker, G. L. and Bruening, M. L. (2003) 'Kinetics of surface-initiated atom transfer radical polymerization', *Journal of Polymer Science Part A: Polymer Chemistry*, 41(3), pp. 386–394. doi: 10.1002/pola.10568.

Kim, J. (2009) ‘Investigation of the Formation and Structure of APTES Films on Silicon Substrates’, pp. 1–2. Available at: https://www.piketech.com/skin/fashion_mosaic_blue/application-pdfs/Investigation_Formation_Structure_APTESFilms_SiliconSubstrates.pdf.

Kinsella, J. E. and Whitehead, D. M. (1989) ‘Proteins in Whey: Chemical, Physical, and Functional Properties’, *Advances in Food and Nutrition Research*, 33(C), pp. 343–438. doi: 10.1016/S1043-4526(08)60130-8.

Kinyua, E. M., Mwangi, I. W., Wanjau, R. N. and Ngila, J. C. (2016) ‘Clarification of colloidal and suspended material in water using triethanolamine modified maize tassels’, *Environmental Science and Pollution Research*, 23(6), pp. 5214–5221. doi: 10.1007/s11356-015-5766-y.

Kobayashi, J., Kikuchi, A., Sakai, K. and Okano, T. (2001) ‘Aqueous chromatography utilizing pH-/temperature-responsive polymer stationary phases to separate ionic bioactive compounds’, *Analytical Chemistry*, 73(9), pp. 2027–2033. doi: 10.1021/ac0013507.

Kozlov, M. and McCarthy, T. J. (2004) ‘Adsorption of poly(vinyl alcohol) from water to a hydrophobic surface: effects of molecular weight, degree of hydrolysis, salt, and temperature.’, *Langmuir : the ACS journal of surfaces and colloids*, 20(21), pp. 9170–6. doi: 10.1021/la0492299.

Kroning, A., Furchner, A., Aulich, D., Bittrich, E., Rauch, S., Uhlmann, P., Eichhorn, K. J., Seeber, M., Luzinov, I., Kilbey, S. M., Lokitz, B. S., Minko, S. and Hinrichs, K. (2015) ‘In Situ Infrared Ellipsometry for Protein Adsorption Studies on Ultrathin Smart Polymer Brushes in Aqueous Environment’, *ACS Applied Materials and Interfaces*, 7(23), pp. 12430–12439. doi: 10.1021/am5075997.

Lagoutte, P., Mignon, C., Donnat, S., Stadthagen, G., Mast, J., Sodoyer, R., Lugari, A. and Werle, B. (2016) ‘Scalable chromatography-based purification of virus-like particle carrier for epitope based influenza A vaccine produced in Escherichia coli’, *Journal of Virological Methods*, 232, pp. 8–11. doi: 10.1016/J.JVIROMET.2016.02.011.

Lamprou, A., Gavriilidou, A.-F.-M., Storti, G., Soos, M. and Morbidelli, M. (2015) ‘Application of polymeric macroporous supports for temperature-responsive chromatography of pharmaceuticals’, *Journal of Chromatography A*, 1407, pp. 90–99. doi: 10.1016/J.CHROMA.2015.06.028.

Lamprou, A., Köse, I., Peña Aguirre, Z., Storti, G., Morbidelli, M. and Soos, M. (2014) ‘Macroporous polymer particles via reactive gelation under shear: Effect of primary particle properties and operating parameters’, *Langmuir*, 30(46), pp. 13970–13978. doi: 10.1021/la502153j.

Lee, M. F. X., Chan, E. S., Tam, K. C. and Tey, B. T. (2015) ‘Thermo-responsive adsorbent for size-selective protein adsorption’, *Journal of Chromatography A*, 1394, pp. 71–80. doi: 10.1016/J.CHROMA.2015.03.034.

Lei, H., Wang, M., Tang, Z., Luan, Y., Liu, W., Song, B. and Chen, H. (2014) ‘Control of lysozyme adsorption by pH on surfaces modified with polyampholyte brushes’, *Langmuir*, 30(2), pp. 501–508. doi: 10.1021/la403781s.

Lemieux, M. C., Julthongpiput, D., Bergman, K. N., Cuong, P. D., Ahn, H.-S., Lin, Y.-H. and Tsukruk, V. V (2004) 'Ultrathin binary grafted polymer layers with switchable morphology.', *Langmuir : the ACS journal of surfaces and colloids*, 20(23), pp. 10046–54. doi: 10.1021/la048496b.

Lemieux, M., Usov, D., Minko, S., Stamm, M., Shulha, H. and V. Tsukruk, V. (2003) 'Reorganization of Binary Polymer Brushes: Reversible Switching of Surface Microstructures and Nanomechanical Properties', *Macromolecules*, 36(19), pp. 7244–7255. doi: 10.1021/ma034634c.

Lenhoff, A. M. (2016) 'Ion-exchange chromatography of proteins: the inside story', *Materials Today: Proceedings*, 3(10), pp. 3559–3567. doi: 10.1016/J.MATPR.2016.10.038.

Levy, N. E., Valente, K. N., Lee, K. H. and Lenhoff, A. M. (2016) 'Host cell protein impurities in chromatographic polishing steps for monoclonal antibody purification', *Biotechnology and Bioengineering*, 113(6), pp. 1260–1272. doi: 10.1002/bit.25882.

Li, C. and Liu, C. (2018) 'Characterization of agarose microparticles prepared by water-in-water emulsification', *Particulate Science and Technology*, 36(5), pp. 592–599. doi: 10.1080/02726351.2017.1279698.

Li, N., Qi, L., Shen, Y., Li, Y. and Chen, Y. (2013) 'Thermoresponsive Oligo(ethylene glycol)-Based Polymer Brushes on Polymer Monoliths for All-Aqueous Chromatography', *ACS Applied Materials & Interfaces*, 5(23), pp. 12441–12448. doi: 10.1021/am403510g.

Li, S., Sun, Y. and Shi, Q.-H. (2015) 'Fabrication of high-capacity protein ion-exchangers with polymeric ion-exchange groups grafted onto micron-sized beads by atom transfer radical polymerization', *Biochemical Engineering Journal*, 103, pp. 122–129. doi: 10.1016/J.BEJ.2015.07.010.

Li, X., Du, P. and Liu, P. (2014) 'Layer-by-layer polyelectrolyte complex coated poly(methacrylic acid) nanogels as a drug delivery system for controlled release: Structural effects', *RSC Advances*, 4(99), pp. 56323–56331. doi: 10.1039/c4ra05066e.

Liu, T. and Liang, J. F. (2018) 'Nanostructured surfaces from high-density grafted poly (acrylic acid) with liquid-like property', *Reactive and Functional Polymers*, 127, pp. 123–128. doi: 10.1016/J.REACTFUNCTPOLYM.2018.04.007.

Lorenz, M., Vogg, S., Finkelstein, P., Storti, G. and Morbidelli, M. (2019) 'Synthesis of Strong Cation Exchange Macroporous Polymer Cluster for Convective Protein Chromatography', *Macromolecular Materials and Engineering*, 304(10), pp. 1–7. doi: 10.1002/mame.201900311.

Luzinov, I., Julthongpiput, D., Liebmann-Vinson, A., Cregger, T., Foster, M. D. and Tsukruk, V. V. (2000) 'Epoxy-Terminated Self-Assembled Monolayers: Molecular Glues for Polymer Layers', *Langmuir*, 16(2), pp. 504–516. doi: 10.1021/la990500+.

Luzinov, I. and Tsukruk, V. V. (2002) 'Ultrathin Triblock Copolymer Films on Tailored Polymer Brushes', *Macromolecules*, 35(15), pp. 5963–5973. doi: 10.1021/ma0205818.

Maharjan, P., Hearn, M. T. W., Jackson, W. R., De Silva, K. and Woonton, B. W. (2009) 'Development of a temperature-responsive agarose-based ion-exchange chromatographic resin', *Journal of Chromatography A*, 1216(50), pp. 8722–8729. doi: 10.1016/J.CHROMA.2009.04.037.

Maharjan, P., Woonton, B. W., Bennett, L. E., Smithers, G. W., DeSilva, K. and Hearn, M. T. W. (2008) 'Novel chromatographic separation - The potential of smart polymers', *Innovative Food Science and Emerging Technologies*, 9(2), pp. 232–242.

Maharjan, P., Woonton, B. W., Bennett, L. E., Smithers, G. W., DeSilva, K. and Hearn, M. T. W. (2008) 'Novel chromatographic separation — The potential of smart polymers', *Innovative Food Science & Emerging Technologies*, 9(2), pp. 232–242. doi: 10.1016/J.IFSET.2007.03.028.

March, S. C., Parikh, I. and Cuatrecasas, P. (1974) 'A simplified method for cyanogen bromide activation of agarose for affinity chromatography', *Analytical Biochemistry*, 60(1), pp. 149–152. doi: 10.1016/0003-2697(74)90139-0.

Matsuzaka, N., Nakayama, M., Takahashi, H., Yamato, M., Kikuchi, A. and Okano, T. (2013) 'Terminal-Functionality Effect of Poly(N-isopropylacrylamide) Brush Surfaces on Temperature-Controlled Cell Adhesion/Detachment', *Biomacromolecules*, 14(9), pp. 3164–3171. doi: 10.1021/bm400788p.

Matyjaszewski, K., Miller, P. J., Shukla, N., Immaraporn, B., Gelman, A., Luokala, B. B., Siclovan, T. M., Kickelbick, G., Vallant, T., Hoffmann, H. and Pakula, T. (1999) 'Polymers at Interfaces: Using Atom Transfer Radical Polymerization in the Controlled Growth of Homopolymers and Block Copolymers from Silicon Surfaces in the Absence of Untethered Sacrificial Initiator', *Macromolecules*, 32(26), pp. 8716–8724. doi: 10.1021/ma991146p.

Mays, T. J. (2007) 'A new classification of pore sizes', *Studies in Surface Science and Catalysis*, 160, pp. 57–62. doi: 10.1016/S0167-2991(07)80009-7.

Meng, X. L., Fang, Y., Wan, L. S., Huang, X. J. and Xu, Z. K. (2012) 'Glycopolymer brushes for the affinity adsorption of RCA120: Effects of thickness, grafting density, and epitope density', *Langmuir*, 28(38), pp. 13616–13623. doi: 10.1021/la302389e.

Mikhaylova, Y., Ionov, L., Rappich, J., Gensch, M., Esser, N., Minko, S., Eichhorn, K. J., Stamm, M. and Hinrichs, K. (2007) 'In situ infrared ellipsometric study of stimuli-responsive mixed polyelectrolyte brushes', *Analytical Chemistry*, 79(20), pp. 7676–7682. doi: 10.1021/ac070853a.

Miksa, D., Irish, E. R., Chen, D., Composto, R. J. and Eckmann, D. M. (2005) 'Dextran Functionalized Surfaces via Reductive Amination : Morphology , Wetting , and Adhesion', *Biomacromolecules*, 7, pp. 557–564.

Milner, S. T. (1991) 'Polymer Brushes', *Science*, 251(4996), pp. 905–914. Available at: http://science.sciencemag.org/content/251/4996/905.abstract.

Minko, S. (2006) 'Responsive polymer brushes', *Journal of Macromolecular Sciencew, Part C: Polymer Reviews*, 46, pp. 397–420. doi: 10.1080/15583720600945402.

Minko, S. (2008) ‘Grafting on Solid Surfaces: ``Grafting to’’ and ``Grafting from’’ Methods’, In: Stamm, M. ed. *Polymer Surfaces and Interfaces: Characterization, Modification and Applications*. Leipzig: Springer-Verlag Berlin Heidelberg, pp. 215–234. doi: 10.1007/978-3-540-73865-7_11.

Minko, S., Müller, M., Usov, D., Scholl, A., Froeck, C. and Stamm, M. (2002a) ‘Lateral versus Perpendicular Segregation in Mixed Polymer Brushes’, *Physical Review Letter*, 88(3), p. 35502. doi: 10.1103/PhysRevLett.88.035502.

Minko, S., Patil, S., Datsyuk, V., Simon, F., Eichhorn, K. J., Motornov, M., Usov, D., Tokarev, I. and Stamm, M. (2002b) ‘Synthesis of adaptive polymer brushes via “grafting to” approach from melt’, *Langmuir*, 18(1), pp. 289–296. doi: 10.1021/la015637q.

Mizutani, A., Kikuchi, A., Yamato, M., Kanazawa, H. and Okano, T. (2008) ‘Preparation of thermoresponsive polymer brush surfaces and their interaction with cells.’, *Biomaterials*, 29(13), pp. 2073–81. doi: 10.1016/j.biomaterials.2008.01.004.

Mizutani, A., Nagase, K., Kikuchi, A., Kanazawa, H., Akiyama, Y., Kobayashi, J., Annaka, M. and Okano, T. (2010a) ‘Effective separation of peptides using highly dense thermo-responsive polymer brush-grafted porous polystyrene beads’, *Journal of Chromatography B*, 878(24), pp. 2191–2198. doi: 10.1016/J.JCHROMB.2010.06.026.

Mizutani, A., Nagase, K., Kikuchi, A., Kanazawa, H., Akiyama, Y., Kobayashi, J., Annaka, M. and Okano, T. (2010b) ‘Thermo-responsive polymer brush-grafted porous polystyrene beads for all-aqueous chromatography’, *Journal of Chromatography A*, 1217(4), pp. 522–529. doi: 10.1016/J.CHROMA.2009.11.073.

Mól, P. C. G., Veríssimo, L. A. A., Minim, L. A., Boscolo, M., Gomes, E. and da Silva, R. (2019) ‘Production and capture of β-glucosidase from Thermoascus aurantiacus using a tailor made anionic cryogel’, *Process Biochemistry*, 82, pp. 75–83. doi: 10.1016/J.PROCBIO.2019.03.029.

Montagne, F., Polesel-Maris, J., Pugin, R. and Heinzelmann, H. (2009) ‘Poly(N-isopropylacrylamide) thin films densely grafted onto gold surface: preparation, characterization, and dynamic AFM study of temperature-induced chain conformational changes.’, *Langmuir : the ACS journal of surfaces and colloids*, 25(2), pp. 983–91. doi: 10.1021/la803729p.

Motornov, M., Sheparovych, R., Katz, E. and Minko, S. (2008) ‘Chemical gating with nanostructured responsive polymer brushes: mixed brush versus homopolymer brush.’, *ACS nano*, 2(1), pp. 41–52. doi: 10.1021/nn700214f.

Motornov, M., Sheparovych, R., Tokarev, I., Roiter, Y. and Minko, S. (2007) ‘Nonwettable Thin Films from Hybrid Polymer Brushes Can Be’, *Langmuir*, 23(3), pp. 13–19.

Müller, T. K. H., Cao, P., Ewert, S., Wohlgemuth, J., Liu, H., Willett, T. C., Theodosiou, E., Thomas, O. R. T. and Franzreb, M. (2013) ‘Integrated system for temperature-controlled fast protein liquid chromatography comprising improved copolymer modified beaded agarose adsorbents and a travelling cooling zone reactor arrangement’, *Journal of Chromatography A*, 1285, pp. 97–109. doi: 10.1016/j.chroma.2013.02.025.

Müller, W. (1990) ‘New ion exchangers for the chromatography of biopolymers’, *Journal of Chromatography A*, 510, pp. 133–140. doi: 10.1016/S0021-9673(01)93746-X.

Nagase, K., Kobayashi, J., Kikuchi, A., Akiyama, Y., Annaka, M., Kanazawa, H. and Okano, T. (2008) ‘Influence of graft interface polarity on hydration/dehydration of grafted thermoresponsive polymer brushes and steroid separation using all-aqueous chromatography’, *Langmuir*, 24(19), pp. 10981–10987. doi: 10.1021/la801949w.

Nagase, K., Kobayashi, J., Kikuchi, A., Akiyama, Y., Kanazawa, H. and Okano, T. (2007) ‘Interfacial property modulation of thermoresponsive polymer brush surfaces and their interaction with biomolecules’, *Langmuir*, 23(18), pp. 9409–9415. doi: 10.1021/la700956b.

Nagase, K., Kobayashi, J., Kikuchi, A., Akiyama, Y., Kanazawa, H. and Okano, T. (2011) ‘Thermoresponsive polymer brush on monolithic-silica-rod for the high-speed separation of bioactive compounds’, *Langmuir*, 27(17), pp. 10830–10839. doi: 10.1021/la201360p.

Nagase, K., Kumazaki, M., Kanazawa, H., Kobayashi, J., Kikuci, A., Akiyama, Y., Annaka, M. and Okano, T. (2010) ‘Thermoresponsive polymer brush surfaces with hydrophobic groups for all-aqueous chromatography’, *ACS Applied Materials and Interfaces*, 2(4), pp. 1247–1253. doi: 10.1021/am100122h.

Nestola, P., Peixoto, C., Silva, R. R. J. S., Alves, P. M., Mota, J. P. B. and Carrondo, M. J. T. (2015) ‘Improved virus purification processes for vaccines and gene therapy’, *Biotechnology and Bioengineering*, 112(5), pp. 843–857. doi: 10.1002/bit.25545.

de Neuville, B. C., Lamprou, A., Morbidelli, M. and Soos, M. (2014) ‘Perfusive ion-exchange chromatographic materials with high capacity’, *Journal of Chromatography A*, 1374, pp. 180–188. doi: 10.1016/j.chroma.2014.11.066.

Nilsson, K. and Mosbach, K. (1980) ‘p-Toluenesulfonyl chloride as an activating agent of agarose for the preparation of immobilized affinity ligands and proteins.’, *European journal of biochemistry*, 112(2), pp. 397–402. doi: 10.3891/acta.chem.scand.35b-0019.

Nilsson, K. and Mosbach, K. (1981) ‘Immobilization of enzymes and affinity ligands to various hydroxyl group carrying supports using highly reactive sulfonyl chlorides’, *Biochemical and Biophysical Research Communications*, 102(1), pp. 449–457. doi: 10.1016/0006-291X(81)91541-2.

Noel, S., Liberelle, B., Robitaille, L. and De Crescenzo, G. (2011) ‘Quantification of primary amine groups available for subsequent biofunctionalization of polymer surfaces’, *Bioconjugate Chemistry*, 22(8), pp. 1690–1699. doi: 10.1021/bc200259c.

Nowak, D., Morrison, W., Wickramasinghe, H. K., Jahng, J., Potma, E., Wan, L., Ruiz, R., Albrecht, T. R., Schmidt, K., Frommer, J., Sanders, D. P. and Park, S. (2016) ‘Nanoscale chemical imaging by photoinduced force microscopy’, *Science Advances*, 2(3), pp. e1501571. doi: 10.1126/sciadv.1501571.

Ombelli, M., Eckmann, D. M. and Composto, R. J. (2003) ‘Dextran grafted silicon substrates: preparation, characterization and biomedical applications’, *MRS Proceedings*, 774. Available at: http://journals.cambridge.org/abstract_S1946427400138515.

De Palma, A. (2017) ‘Chromatography Makes Room for Biomolecular Diversity’, *Genetic Engineering & Biotechnology News*. Mary Ann Liebert, Inc., publishers, 37(11), pp. 18–20. doi: 10.1089/gen.37.11.09.

Patel, S., Thakar, R. G., Wong, J., McLeod, S. D. and Li, S. (2006) ‘Control of cell adhesion on poly(methyl methacrylate)’, *Biomaterials*, 27(14), pp. 2890–2897. doi: 10.1016/J.BIOMATERIALS.2005.12.009.

Patten, T. E. and Matyjaszewski, K. (1998) ‘Atom Transfer Radical Polymerization and the Synthesis of Polymeric Materials’, *Advanced Materials*, 10(12), pp. 901–915. doi: 10.1002/(SICI)1521-4095(199808)10:12<901::AID-ADMA901>3.0.CO;2-B.

Penn, L. S., Hunter, T. F., Quirk, R. P. and Lee, Y. (2002) *Deactivation of Epoxide-Derivatized Surfaces*. Available at: http://pubs.acs.org/doi/abs/10.1021/ma011114d#.VxwZhHjO6TM.mendeley (Accessed: 24 April 2016).

Pettersson, S. W. (2011) ‘High-Resolution Reversed-Phase Chromatography of Proteins’, In: Janson, J.C. ed. *Methods of Biochemical Analysis : Protein Purification : Principles, High Resolution Methods, and Applications*. 3rd edn. Hoboken, NJ: John Wiley & Sons, Inc., pp. 135–164. doi: 10.1002/9780470939932.ch5.

Prazeres, D. M. F., Ferreira, G. N. M., Monteiro, G. A., Cooney, C. L. and Cabral, J. M. S. (1999) ‘Large-scale production of pharmaceutical-grade plasmid DNA for gene therapy: problems and bottlenecks’, *Trends in biotechnology*, 17(4), pp. 169–174.

Price, W. S., Tsuchiya, F. and Arata, Y. (1999) ‘Lysozyme aggregation and solution properties studied using PGSE NMR diffusion measurements’, *Journal of the American Chemical Society*, 121(49), pp. 11503–11512. doi: 10.1021/ja992265n.

Przybycien, T. M., Pujar, N. S. and Steele, L. M. (2004) ‘Alternative bioseparation operations: life beyond packed-bed chromatography’, *Current Opinion in Biotechnology*, 15(5), pp. 469–478. doi: 10.1016/J.COPBIO.2004.08.008.

Qu, J.-B., Xu, Y.-L., Liu, J.-Y., Zeng, J.-B., Chen, Y.-L., Zhou, W.-Q. and Liu, J.-G. (2016) ‘Thermo- and pH-responsive polymer brushes-grafted gigaporous polystyrene microspheres as a high-speed protein chromatography matrix’, *Journal of Chromatography A*, 1441, pp. 60–67. doi: 10.1016/J.CHROMA.2016.02.072.

Qu, Q., Si, Y., Xuan, H., Zhang, K., Chen, X., Ding, Y., Feng, S., Yu, H.-Q., Abdullah, M. A. and Alamry, K. A. (2018) ‘Dendritic core-shell silica spheres with large pore size for separation of biomolecules’, *Journal of Chromatography A*, 1540, pp. 31–37. doi: 10.1016/J.CHROMA.2018.02.002.

Quintero, L. and Meza-León, R. L. (2005) ‘*tert* -Butylsulfonyl Chloride’, In Charette, A., Bode, J., Rovis, T., Shenvi, R. eds. *Encyclopedia of Reagents for Organic Synthesis*. Chichester, UK: John Wiley & Sons, Ltd.. doi: 10.1002/047084289X.rn00565.

Roiter, Y. and Minko, S. (2005) ‘AFM single molecule experiments at the solid-liquid interface: In situ conformation of adsorbed flexible polyelectrolyte chains’, *Journal of the American Chemical Society*, 127(45), pp. 15688–15689. doi: 10.1021/ja0558239.

Rowe, L., Khoury, G. E. and Lowe, C. R. (2012) 'Affinity Chromatography: Historical and Prospective Overview', In: Subramanian, G. ed. *Biopharmaceutical Production Technology, Advances in Process Development*. 2nd edn. Weinheim, Germany: Wiley-VCH Verlag GmbH & Co. KGaA, pp. 223–282. doi: 10.1002/9783527653096.ch8.

Rubio, N., Au, H., S. Leese, H., Hu, S., J. Clancy, A. and S. P. Shaffer, M. (2017) 'Grafting from versus Grafting to Approaches for the Functionalization of Graphene Nanoplatelets with Poly(methyl methacrylate)', *Macromolecules*, 50(18), pp. 7070–7079. doi: 10.1021/acs.macromol.7b01047.

Saha, B., Saikia, J. and Das, G. (2013) 'Tuning the selective interaction of lysozyme and serum albumin on a carboxylate modified surface', *RSC Advances*, 3(21), pp. 7867–7879. doi: 10.1039/c3ra23042b.

Santonicola, M. G., Wilhelmina De Groot, G., Memesa, M., Meszy, A. and Vancso, G. J. (2010) 'Reversible pH-Controlled Switching of Poly(methacrylic acid) Grafts for Functional Biointerfaces', *Langmuir*, 26(22), pp. 17513–17519. doi: 10.1021/la1029273.

Savina, I. N., Galaev, I. Y. and Mattiasson, B. (2005) 'Anion-exchange supermacroporous monolithic matrices with grafted polymer brushes of N,N-dimethylaminoethyl-methacrylate', *Journal of Chromatography A*, 1092(2), pp. 199–205. doi: 10.1016/J.CHROMA.2005.06.094.

Scheraga, H. A., Wedemeyer, W. J. and Welker, E. (2001) 'Bovine Pancreatic Ribonuclease A: Oxidative and Conformational Folding Studies', *Methods in Enzymology*, 341, pp. 189–221. doi: 10.1016/S0076-6879(01)41153-0.

Schneider, C. A., Rasband, W. S. and Eliceiri, K. W. (2012) 'NIH Image to ImageJ: 25 years of image analysis', *Nature Methods*, 9(7), pp. 671–675. doi: 10.1038/nmeth.2089.

Schwellenbach, J., Taft, F., Villain, L. and Strube, J. (2016) 'Preparation and characterization of high capacity, strong cation-exchange fiber based adsorbents', *Journal of Chromatography A*, 1447, pp. 92–106. doi: 10.1016/J.CHROMA.2016.04.019.

Scouten, W. H., van Den Tweel, W., Delhaes, D., Kranenberg, H. and Dekker, M. (1986) 'Sulfonyl chloride activation of hydroxylic materials', *Journal of Chromatography B: Biomedical Sciences and Applications*, 376, pp. 289–298. doi: 10.1016/S0378-4347(00)80845-2.

Semen, J. and Lando, J. B. (1969) 'The Acid Hydrolysis of Isotactic and Syndiotactic Poly(methyl methacrylate)', *Macromolecules*, 2(6), pp. 570–575. doi: 10.1021/ma60012a003.

Seo, Y. S., Kim, K. S., Galambos, A., Lammertink, R. G. H., Vancso, G. J., Sokolov, J. and Rafailovich, M. (2004) 'Nanowire and mesh conformations of diblock copolymer blends at the air/water interface', *Nano Letters*, 4(3), pp. 483–486. doi: 10.1021/nl034917i.

Sepulveda, P., Marciniszyn, J., Liu, D. and Tang, J. (1975) 'Primary structure of porcine pepsin. III. Amino acid sequence of a cyanogen bromide fragment, CB2A, and the complete structure of porcine pepsin.', *Journal of Biological Chemistry* , 250(13), pp. 5082–5088. Available at: http://www.jbc.org/content/250/13/5082.abstract.

Sheparovych, R., Motornov, M. and Minko, S. (2008) 'Adapting low-adhesive thin films from mixed polymer brushes', *Langmuir*, 24(24), pp. 13828–13832. doi: 10.1021/la803117y.

Shin, H. S., Jung, Y. M., Lee, J., Chang, T., Ozaki, Y. and Kim, S. Bin (2002) 'Structural comparison of Langmuir-Blodgett and spin-coated films of poly(tert-butyl methacrylate) by external reflection FTIR spectroscopy and two-dimensional correlation analysis', *Langmuir*, 18(14), pp. 5523–5528. doi: 10.1021/la020135d.

Shusharina, N. P. and Linse, P. (2001) 'Oppositely charged polyelectrolytes grafted onto planar surface: Mean-field lattice theory', *The European Physical Journal E*, 6(2), pp. 147–155. doi: 10.1007/s101890170016.

Sidorenko, A., Minko, S., Schenk-Meuser, K., Duschner, H. and Stamm, M. (1999) 'Switching of polymer brushes', *Langmuir*, 15(24), pp. 8349–8355. doi: 10.1021/la990869z.

Silva, R. J., Pb Mota, J., Peixoto, C., Alves, P. M. and Carrondo, M. J. (2015) 'Improving the downstream processing of vaccine and gene therapy vectors with continuous chromatography', *Pharmaceutical Bioprocess*, (8), pp. 489–505. doi: 10.4155/pbp.15.29.

Simone, P., Pierri, G., Capitani, D., Ciogli, A., Angelini, G., Ursini, O., Gentile, G., Cavazzini, A., Villani, C. and Gasparrini, F. (2017) 'Capillary methacrylate-based monoliths by grafting from/to γ-ray polymerization on a tentacle-type reactive surface for the liquid chromatographic separations of small molecules and intact proteins', *Journal of Chromatography A*, 1498, pp. 46–55. doi: 10.1016/J.CHROMA.2016.11.039.

Solomons, T. W. G., Fryhle, C. B. and Snyder, S. A. (2017) *Organic chemistry*. 12th edn. Hoboken, NJ: John Wiley & Sons, Inc.

Sousa, Â., Sousa, F. and Queiroz, J. A. (2012) 'Advances in chromatographic supports for pharmaceutical-grade plasmid DNA purification', *Journal of Separation Science*, 35(22), pp. 3046–3058. doi: 10.1002/jssc.201200307.

Stenzel, M. H., Zhang, L. and Huck, W. T. S. (2006) 'Temperature-Responsive Glycopolymer Brushes Synthesized via RAFT Polymerization Using the Z-group Approach', *Macromolecular Rapid Communications*, 27(14), pp. 1121–1126. doi: 10.1002/marc.200600223.

Tan, I., Zarafshani, Z., Lutz, J. F. and Titirici, M. M. (2009) 'PEGylated chromatography: Efficient bioseparation on silica monoliths grafted with smart biocompatible polymers', *ACS Applied Materials and Interfaces*, 1(9), pp. 1869–1872. doi: 10.1021/am900461a.

Tang, W. and Matyjaszewski, K. (2006) 'Effect of Ligand Structure on Activation Rate Constants in ATRP', *Macromolecules*, 39(15), pp. 4953–4959. doi: 10.1021/ma0609634.

Tao, S.-P., Zheng, J. and Sun, Y. (2015) 'Grafting zwitterionic polymer onto cryogel surface enhances protein retention in steric exclusion chromatography on cryogel monolith', *Journal of Chromatography A*, 1389, pp. 104–111. doi: 10.1016/J.CHROMA.2015.02.051.

Taylor, W. and Jones, R. A. L. (2010) 'Producing high-density high-molecular-weight polymer brushes by a "grafting to" method from a concentrated homopolymer solution', *Langmuir*, 26(17), pp. 13954–13958. doi: 10.1021/la101881j.

Thévenot, J., Cauty, C., Legland, D., Dupont, D. and Floury, J. (2017) 'Pepsin diffusion in dairy gels depends on casein concentration and microstructure', *Food Chemistry*, 223, pp. 54–61. doi: 10.1016/J.FOODCHEM.2016.12.014.

Thömmes, J. and Etzel, M. (2007) 'Alternatives to chromatographic separations', *Biotechnology Progress*, 23(1), pp. 42–45. doi: 10.1021/bp0603661.

Tipson, R. S. (1944) 'On esters of p-toluenesulfonic acid', *Journal of Organic Chemistry*, 9(3), pp. 235–241. doi: 10.1021/jo01185a005.

Tomaz, C. T. and Queiroz, J. A. (2013) 'Hydrophobic Interaction Chromatography', *Liquid Chromatography*, pp. 121–141. doi: 10.1016/B978-0-12-415807-8.00006-7.

Trang, H. K., Jiang, L. and Marcus, R. K. (2019) 'Grafting polymerization of glycidyl methacrylate onto capillary-channeled polymer (C-CP) fibers as a ligand binding platform: Applications in immobilized metal-ion affinity chromatography (IMAC) protein separations', *Journal of Chromatography B*, 1110–1111, pp. 144–154. doi: 10.1016/J.JCHROMB.2019.02.013.

Tsujii, Y., Ejaz, M., Sato, K., Goto, A. and Fukuda, T. (2001) 'Mechanism and Kinetics of RAFT-Mediated Graft Polymerization of Styrene on a Solid Surface. 1. Experimental Evidence of Surface Radical Migration', *Macromolecules*, 34(26), pp. 8872–8878. doi: 10.1021/ma010733j.

Uhlmann, P., Houbenov, N., Brenner, N., Grundke, K., Burkert, S. and Stamm, M. (2007) 'In-situ investigation of the adsorption of globular model proteins on stimuli-responsive binary polyelectrolyte brushes', *Langmuir*, 23(1), pp. 57–64. doi: 10.1021/la061557g.

Unsworth, L. D., Tun, Z., Sheardown, H. and Brash, J. L. (2005) 'Chemisorption of thiolated poly(ethylene oxide) to gold: surface chain densities measured by ellipsometry and neutron reflectometry', *Journal of Colloid and Interface Science*, 281(1), pp. 112–121. doi: 10.1016/J.JCIS.2004.08.022.

Vikesland, P. J., Rebodos, R. L., Bottero, J. Y., Rose, J. and Masion, A. (2016) 'Aggregation and sedimentation of magnetite nanoparticle clusters', *Environmental Science: Nano*, 3(3), pp. 567–577. doi: 10.1039/c5en00155b.

De Vos, W. M., Biesheuvel, P. M., De Keizer, A., Kleijn, J. M. and Stuart, M. A. C. (2008) 'Adsorption of the protein bovine serum albumin in a planar poly(acrylic acid) brush layer as measured by optical reflectometry', *Langmuir*, 24(13), pp. 6575–6584. doi: 10.1021/la8006469.

Vyas, M. K., Schneider, K., Nandan, B. and Stamm, M. (2008) 'Switching of friction by binary polymer brushes', *Soft Matter*, 4(5), p. 1024. doi: 10.1039/b801110a.

W. Chan, J., Huang, A. and E. Uhrich, K. (2016) 'Self-Assembled Amphiphilic Macromolecule Coatings: Comparison of Grafting-From and Grafting-To Approaches for Bioactive Delivery', *Langmuir*, 32(20), pp. 5038–5047. doi: 10.1021/acs.langmuir.6b00524.

Wang, C., Shen, J., Zhu, J., Bo, C. and Wei, Y. (2018) 'Tetrazole-functionalized cation-exchange membrane adsorbers with high binding capacity and unique separation feature for protein', *Journal of Chromatography B*, 1097–1098, pp. 18–26. doi: 10.1016/j.jchromb.2018.08.035.

Wang, H.-Y., Sun, Y., Zhang, S.-L., Luo, J. and Shi, Q.-H. (2016) 'Fabrication of high-capacity cation-exchangers for protein chromatography by atom transfer radical polymerization', *Biochemical Engineering Journal*, 113, pp. 19–29. doi: 10.1016/J.BEJ.2016.05.006.

Wang, Q., Yu, L. and Sun, Y. (2016) 'Grafting glycidyl methacrylate to Sepharose gel for fabricating high-capacity protein anion exchangers', *Journal of Chromatography A*, 1443, pp. 118–125. doi: 10.1016/J.CHROMA.2016.03.033.

Wang, S., Li, X. and Sun, Y. (2019) 'Poly(N,N-dimethylaminopropyl acrylamide)-grafted Sepharose FF: A new anion exchanger of very high capacity and uptake rate for protein chromatography', *Journal of Chromatography A*, 1597, pp. 187–195. doi: 10.1016/J.CHROMA.2019.03.035.

Ward, M. A. and Georgiou, T. K. (2011) 'Thermoresponsive polymers for biomedical applications', *Polymers*, 3(3), pp. 1215–1242. doi: 10.3390/polym3031215.

Wazer, J. R. Van (1958) *Phosphorus and Its Compounds: Vol 1, Chemistry*. Interscience Publishers. Available at: https://books.google.co.uk/books?id=qF6tngEACAAJ.

Willett, T. C. (2009) *Magnetic adsorbents displaying switchable ion-exchange behaviour, School of Chemical Engineering*. PhD thesis. Birmingham: University of Birmingham. Available at: http://etheses.bham.ac.uk/507/.

Wittemann, A., Haupt, B. and Ballauff, M. (2003) 'Adsorption of proteins on spherical polyelectrolyte brushes in aqueous solution', *Physical Chemistry Chemical Physics*, 5(8), pp. 1671–1677. doi: 10.1039/b300607g.

Xue, C., Yonet-Tanyeri, N., Brouette, N., Sferrazza, M., Braun, P. V. and Leckband, D. E. (2011) 'Protein Adsorption on Poly(N-isopropylacrylamide) Brushes: Dependence on Grafting Density and Chain Collapse', *Langmuir*, 27(14), pp. 8810–8818. doi: 10.1021/la2001909.

Yang, Y. and Dan, Y. (2003) 'Preparation of PMMA/SiO2 composite particles via emulsion polymerization', *Colloid and Polymer Science*, 281(8), pp. 794–799. doi: 10.1007/s00396-002-0845-2.

Yao, Y. and Lenhoff, A. M. (2006) 'Pore size distributions of ion exchangers and relation to protein binding capacity', *Journal of Chromatography A*, 1126(1–2), pp. 107–119. doi: 10.1016/j.chroma.2006.06.057.

Yoshikawa, C., Goto, A., Tsujii, Y., Ishizuka, N., Nakanishi, K. and Fukuda, T. (2007) 'Surface interaction of well-defined, concentrated poly(2-hydroxyethyl methacrylate) brushes with proteins', *Journal of Polymer Science, Part A: Polymer Chemistry*, 45(21), pp. 4795–4803. doi: 10.1002/pola.22224.

Yu, J., Mao, J., Yuan, G., Satija, S., Jiang, Z., Chen, W. and Tirrell, M. (2016) 'Structure of Polyelectrolyte Brushes in the Presence of Multivalent Counterions', *Macromolecules*, 49(15), pp. 5609–5617. doi: 10.1021/acs.macromol.6b01064.

Yu, S. and Chow, C. M. (2004) 'Carboxyl group (-CO2H) functionalized ferrimagnetic iron oxide nanoparticles for potential bio-applications', *Journal of Materials Chemistry*, 14(18), pp. 2781–2786. doi: 10.1039/b404964k.

Yu, W. H., Kang, E. T. and Neoh, K. G. (2004) 'Functionalization of Hydrogen-Terminated Si(100) Substrate by Surface-Initiated RAFT Polymerization of 4-Vinylbenzyl Chloride and Subsequent Derivatization for Photoinduced Metallization', *Industrial & Engineering Chemistry Research*, 43(17), pp. 5194–5202. doi: 10.1021/ie049687c.

Zdyrko, B., Klep, V., Li, X., Kang, Q., Minko, S., Wen, X. and Luzinov, I. (2009) 'Polymer brushes as active nanolayers for tunable bacteria adhesion', *Materials Science and Engineering: C*, 29(3), pp. 680–684. doi: 10.1016/j.msec.2008.12.017.

Zdyrko, B., Klep, V. and Luzinov, I. (2003) 'Synthesis and Surface Morphology of High-Density Poly(ethylene glycol) Grafted Layers', *Langmuir*, 19(24), pp. 10179–10187. doi: 10.1021/la034974r.

Zhai, G., Yu, W. H., Kang, E. T., Neoh, K. G., Huang, C. C. and Liaw, D. J. (2004) 'Functionalization of Hydrogen-Terminated Silicon with Polybetaine Brushes via Surface-Initiated Reversible Addition−Fragmentation Chain-Transfer (RAFT) Polymerization', *Industrial & Engineering Chemistry Research*, 43(7), pp. 1673–1680. doi: 10.1021/ie034274h.

Zhang, Y. W., Guan, W. J., Lu, Y. M. and Zhao, J. X. (2016) 'Efficient and "green" fabrication of pH-responsive poly(methacrylic acid) nano-hydrogels in water', *RSC Advances*, 6(71), pp. 66571–66578. doi: 10.1039/c6ra07372g.

Zhao, B. and Brittain, W. (2000) 'Polymer brushes: surface-immobilized macromolecules', *Progress in Polymer Science*, 25(5), pp. 677–710. doi: 10.1016/S0079-6700(00)00012-5.

Zhao, H., Kang, X. and Liu, L. (2005) 'Comb−Coil Polymer Brushes on the Surface of Silica Nanoparticles', *Macromolecules*, 38(26), pp. 10619–10622. doi: 10.1021/ma051822p.

Zhao, Ming, Liu, R., Luo, J., Sun, Y. and Shi, Q. (2019) 'Fabrication of high-capacity cation-exchangers for protein adsorption: Comparison of grafting-from and grafting-to approaches', *Frontiers of Chemical Science and Engineering*, 13(1), pp. 120–132. doi: 10.1007/s11705-018-1730-y.

Zhao, Mochao, Vandersluis, M., Stout, J., Haupts, U., Sanders, M. and Jacquemart, R. (2019) 'Affinity chromatography for vaccines manufacturing: Finally ready for prime time?', *Vaccine*, 37(36), pp. 5491–5503. doi: 10.1016/J.VACCINE.2018.02.090.

Zhao, X.-J. and Zhang, G.-L. (2014) 'A Theoretical Investigation on the pH-induced Switching of Mixed Polyelectrolyte Brushes', *Chinese Journal of Polymer Science*, 32(5). doi: 10.1007/s10118-014-1429-6.

Zhou, F. and Huck, W. T. S. (2005) ‘Three-stage switching of surface wetting using phosphate-bearing polymer brushes.’, *Chemical communications*, (48), pp. 5999–6001. doi: 10.1039/b512106j.

Zhu, M., Fuks, P. and Carta, G. (2018) ‘Protein adsorption in anion exchange resins – effects of polymer grafting, support structure porosity, and protein size’, *Journal of Chemical Technology and Biotechnology*, 93(7), pp. 1948–1958. doi: 10.1002/jctb.5410.

Zhu, X., Yan, C., Winnik, F. M. and Leckband, D. (2007) ‘End-grafted low-melecular-weight PNIPAM does not collapse above the LCST’, *Langmuir*, 23(1), pp. 162–169. doi: 10.1021/la061577i.